STUDY OF RHO-PI SYSTEM IN GAUGE MODELS

A Thesis Submitted
In Partial Fulfilment of the Requirements
for the Degree of

DOCTOR OF PHILOSHOPHY

By

PANKAJ SHARAN

to the

DEPARTMENT OF PHYSICS

INDIAN INSTITUTE OF TECHNOLOGY KANPUR

DECEMBER, 1976

PHY– 1976 –D-SHA - STU

CERTIFICATE

Certified that the work presented in this thesis entitled, 'Study of Rho-Pi System in Gauge Models', by Pankaj Sharan has been carried out under my supervision and that this work has not been submitted elsewhere for a degree.

(H.S. Mani)
Associate Professor
Department of Physics
Indian Institute of Technology
Kanpur 208016, INDIA

December 11, 1976

ACKNOWLEDGEMENTS

It is difficult to express how deeply indebted I am to Professor Gyan Mohan for what I have learnt from him as a student, for numerous stimulating discussions and invaluable advice.

I am grateful to Dr. H.S. Mani for suggesting the present investigation and constant help and encouragement throughout the course of this work.

I am extremely grateful to Dr. M.S. Krishnamoorthy for his invaluable and timely help in carrying out the numerical calculation.

I am thankful to Dr. S.C. Agarwal for a useful discussion, and to Dr. R. Ramachandran and Dr. Tulsi Dass for much helpful advice.

I am much indebted to Dr. A.K. Kapoor and H.S. Saratchandra for many valuable discussions.

It is a great pleasure to acknowledge the invaluable assistance I have received from several friends and colleag particularly from Anurag Jaiman, Veena Joshi, K. Vijayaragh Keya Sur and Subrata Ray in finding several mistakes in the

ACKNOWLEDGMENTS

It is difficult to express how deeply indebted I am to Professor Gyan Mohan for what I have learnt from him as a student, for numerous stimulating discussions and invaluable advice.

I am grateful to Dr. H.S. Mani for suggesting the present investigation and constant help and encouragement throughout the course of this work.

I am extremely grateful to Dr. M.S. Krishnamoorthy for his invaluable and timely help in carrying out the numerical calculation.

I am thankful to Dr. S.C. Agarwal for a useful discussion, and to Dr. R. Ramachandran and Dr. Tulsi Dass for much helpful advice.

I am much indebted to Dr. A.K. Kapoor and M.S. Saratchandra for many valuable discussions.

It is a great pleasure to acknowledge the invaluable assistance I have received from several friends and colleagues particularly from Anurag Jaiman, Veena Joshi, K. Vijayaraghavan Keya Sur and Subrata Ray in finding several mistakes in the

MS and Sudhanshu Jamuar and B.N. Srivastava in getting prints of figures.

My thanks are due to Mr. J.K. Misra for typing most of the MS, to Mr. G.L. Misra for filling in the mathematical symbols and to Mr. Hrushikesh Panda for cyclostyling the thesis.

11.12.76 Pankaj Sharan

CONTENTS

LIST OF FIGURES

SYNOPSIS

Thesis entitled 'Study of $\rho\pi$ System in Gauge Models', submitted by Pankaj Sharan in partial fulfilment of the requirements of the Ph.D. degree to the Department of Physics, Indian Institute of Technology, Kanpur

November 1976

The present work is divided into two parts. In the first part we consider low energy $\rho\pi$ scattering using the N/D method and investigate the $J^P = 1^+$ channel around the A_1 mass region. In the second part we consider the high energy behaviour at fixed momentum transfer of $\rho\pi$ scattering as well as of ρ production in $\pi\pi$ scattering at the one loop level.

The thesis consists of seven chapters and five appendices.

The first chapter is an introduction to both the parts.

In the second chapter we describe a simple SU(2) gauge model with pion. The vector meson mass is obtained by breaking the symmetry spontaneously. However, a global SU(2) is still preserved. This is the Bardakci-Halpern idea, which is discussed briefly.

In Chapter three we review the experimental and theoretical status of the $J^P(I) = 1^+(1)$ mass enhancement at 1.1 GeV, which could be the axial vector meson A_1.

In the fourth chapter we calculate $J^P = 1^+$ helicity amplitudes for $\rho\pi$ scattering. They are unitarized by using the N/D formalism. The discontinuities on the left-hand cut are evaluated using the Born diagrams from two renormalizable gauge models separately. One of them being the model discussed in Chapter Two, the other, an SU(2) X SU(2) model due to Bardakci. In both the calculations we obtain neither an enhancement in the A_1 region nor the characteristic phase-shift behaviour of a resonance. Implications of this are discussed. The details of kinematics and numerical computation are delegated to appendices.

Part Two begins with Chapter Five where a review is made of the motivation and attempts to find asymptotic behaviour of Feynman diagrams in different field theories, with particular emphasis on the recent work on high energy behaviour and Reggeization of Yang-Mills theories.

In Chapter Six a formalism is discussed to evaluate the asymptotic behaviour of any general one loop Feynman diagram corresponding to scattering or one particle production. Feynman diagrams are classified according to their topological properties, and general formulas for their asymptotic behaviour at high energy and fixed momentum transfer are obtained. The technique of Mellin transforms is found to be particularly suitable and some useful formulas are quoted in

Appendix Five. Details of kinematics are given in Appendix Four.

Using the formalism of Chapter Six, the asymptotic behaviour of the processes $\rho\pi \to \rho\pi$ and $\pi\pi \to \pi\pi\rho$ is evaluated in the seventh chapter. It is found that although our calculations are done only upto one-loop level, the results are consistent with the Reggeization of Yang-Mills field theories. Discussion and comparison with recent work is done in the final section of this chapter.

CHAPTER ONE

Since their discovery as short-range forces between nucleons, strong interaction of particles has been a great challenge to the understanding of subnuclear phenomena. Most of our understanding of the strong interaction physics has been obtained through a series of hypotheses made on the basis of experimental data and happy guess-work. There is no theory as such, if one could indeed talk in terms of a theory. Therefore, strong interaction physics draws its working and workable ideas from a variety of sources, relativistic field theory and non-relativistic potential scattering among them. To take but the most prominent examples, the low-energy phenomenology of strong interactions basically exploits the idea of unitary analytic S-matrix and of current algebra both having their roots in field theory while high energy phenomenology has successfully derived models from potential scattering, like the Regge-pole model.

Therefore, it is quite natural that with the success of spontaneously broken gauge theories (i.e. theories in which a local gauge symmetry is broken spontaneously) in providing a renormalizable unified field theory of weak and electromagnetic interactions[1], attention should be directed towards strong

interactions. Several strong interaction models based on the idea of spontaneously broken gauge theories have been put forward[2]. However, it should be kept in mind that even if we have a field theory the application of perturbation theory may not make sense for strong coupling. It can, at best, be studied with a view to obtain some insight into the qualitative aspects of the nature of strong interactions.

The success of chiral SU(2) x SU(2) current algebra naturally requires that there should be an axial vector meson just as there is a vector meson. Furthermore, Weinberg's sum rule[3] requires the lowest lying axial vector meson A_1 to have a mass about $\sqrt{2}$ times the mass of ρ, the lowest lying vector meson. However, though there is indubitable evidence for an enhancement in the 1^+ channel of 3π system in diffractive pion production $\pi N \to (3\pi)N$, the resonant nature of the enhancement has not been established. On the contrary, the evidence for A_1 has been less and less convincing. If A_1 is a resonance it should be possible to obtain it as a $\rho\pi$ resonance. A gauge model including ρ as a gauge vector meson provides us with an opportunity to test this hypothesis. In the early sixties, a lot of activity in strong interaction physics consisted in fitting low energy parameters using unitarity and analyticity of the S-matrix. The understanding of ρ as a $\pi\pi$ resonant system[4] and the $\frac{3}{2}^+$ resonance in πN

scattering[5] is well known. Although in those calculations the agreement with experiment could, at best be called rough, they explained the qualitative aspect of the interaction satisfactorily in a limited energy range. We have used the old technique of N/D equations to unitarize the $\rho\pi$ scattering amplitude in the $J^P(I) = 1^+(1)$ channel with the discontinuities across the unphysical cuts obtained from lowest order amplitudes obtained from the gauge model. We donot find any resonant behaviour near A_1 mass region.

Apart from low-energy phenomenology, the high energy behaviour of amplitudes in gauge models can be a useful guide to some qualitative aspects of strong interactions. Previously, the high-energy behaviour of Feynman diagrams in field theories has been thoroughly studied with the same motivation and the same can be done with the renormalizable gauge theories. We shall review these attempts briefly in Chapter Five. It suffices to point out here that at high energy and fixed momentum transfer, Feynman diagrams in gauge models show amazing cancellations in higher order and generally the high-energy behaviour is very good. It seems very likely from recent investigations that the vector meson in these theories 'Reggeizes', i.e., the behaviour of amplitudes with vector meson exchange in the t-channel for large s and fixed t is of the form $\beta(t)\, s^{\alpha(t)}$ and $\alpha(t)$ passes through 1 for t equal to square of the vector meson mass.

We have calculated the high energy behaviour of $\rho\pi$ scattering upto one-loop level, i.e., fourth order in the gauge coupling constant g. The calculation cannot be called definitive in the sense that two and higher loop diagrams should be calculated in order to make a statement about the high-energy behaviour in general, i.e., independently of the order upto which calculation is done. We have not been able to do this because of the large number of diagrams involved with increasing order. However, our calculations are certainly consistent with the higher-order calculations done by other authors recently. We have also looked into the high energy behaviour of production amplitude $\pi\pi \to \pi\pi\rho$ upto one-loop level, i.e. order g^5. We find that for the kinematical region for which all the three final state particles have very high momentum in the centre of mass, the diagrams that contribute to the leading order are essentially the same as for $\pi\pi$ scattering, but with the produced particle ρ emitted out of the external legs. High energy behaviour, therefore, is of the same general pattern as for scattering.

The plan of the thesis is as follows.

In the next chapter, i.e., Chapter Two we discuss a simple SU(2) gauge model constructed along the lines of the Bardakci-Halpern method[6] which preserves a global SU(2) after spontaneous breaking. The method is discussed briefly.

ρ is introduced as a gauge vector meson and it couples to the pion, Higgs scalars and with itself in a manner characteristic of such theories.

In the first part of this thesis which consists of Chapters Three and Four, we consider the low-energy $\rho\pi$ scattering, specifically in the $J^P(I) = 1^+(1)$ channel. As pointed out above the enhancement in $\pi N \to (\rho\pi)N \to (3\pi)N$ with $\rho\pi$ invariant mass near 1.1 GeV, traditionally called A_1, has no clear cut resonance interpretation. The experimental and theoretical situation of A_1 is discussed briefly in Chapter Three. As mentioned there, the enhancement can be explained by mechanisms which do not assume a $\rho\pi$ resonance.

It is therefore of interest to see what behaviour does the lowest order $\rho\pi$ scattering amplitude, properly unitarized in the $J^P = 1^+$ channel show in the vicinity of the A_1 mass region. We have done this in Chapter Four. We calculate the 1^+ helicity amplitudes for $\rho\pi$ scattering and using the 'left-hand' discontinuities given by them found the unitarized amplitude by solving N/D equations. We donot find any indication of a bump or variation of amplitudes to indicate that there is a pole in the second sheet near the A_1 mass. We have done the same calculation with another gauge model due to Bardakci.[7] This model incorporates broken chiral SU(2) x SU(2); so that an axial vector meson is explicitly

assumed in the theory. Inclusion of the left-hand cut discontinuity due to A_1-exchange in the s-channel in $\rho\pi$ scattering, again, does not produce resonant behaviour.

It should perhaps be emphasized that we donot have any arbitrary parameters in the theory except the mass of Higgs scalars, and that, however, does not produce any qualitative difference.

In the second part of the thesis, which consists of Chapters Five, Six and Seven, our concern is the high-energy behaviour of scattering and production amplitudes at fixed momentum transfer. Gauge theories have interesting high energy behaviour as has become clear from the very recent activity in the field. This, and earlier work is briefly reviewed in Chapter Five.

Chapter Six is mainly formalism. Because of the frequent occurence of derivative couplings in gauge theories, it becomes difficult to determine the true asymptotic behaviour of a Feynman graph. As far as high energy behaviour at fixed momentum transfer is concerned, we have tried to analyse and classify one-loop scattering and one-particle production graphs with an arbitrary polynomial of external and loop momentum in the integral. The task becomes specially simple, though, perhaps, less rigorous, by the use of a method

analogous to the 'momentum-space technique' used by Chang and Ma in quantum electrodynamics before, and exploited very successfully by McCoy and Wu to investigate high energy behaviour of gauge theories recently.[8]

In the last chapter we have applied the formalism discussed in Chapter Six to $\rho\pi$ scattering and ρ production in $\pi\pi \to \rho\pi\pi$. The calculation gives the same qualitative behaviour at high energies for $\rho\pi \to \rho\pi$ scattering as has been found by other authors for fermion-fermion and vector-meson-vector-meson scattering in Yang-Mills theories. Only, we have not been able to carry out the calculation to diagrams of two or higher number of loops, so that our calculation can at best be called a verification of high-energy behaviour of gauge theories for the scalar-vector-meson scattering. As far as the production amplitudes are concerned, we have not found any calculation in gauge theories to compare with. Here also the results upto one-loop are interesting in the sense that they show behaviour similar to the scattering case. The leading diagrams seem to be essentially the same.

The last section of this chapter briefly mentions the directions in which the present investigation can be extended.

Five appendices towards the end of the thesis are added to give certain details not in the text.

CHAPTER TWO

In this chapter we shall discuss a simple SU(2) gauge model for $\rho\pi$ system. It is instructive, at least at a qualitative level, to study the application of gauge models to strong interactions because they are renormalizable. In Section 2.1 we shall discuss a method, due to Bardakci and Halpern[6], of constructing a gauge model of hadrons with strong interaction symmetries preserved globally. In sections 2.2 and 2.3 we give in detail a model based on this method which has SU(2) as symmetry group. In section 2.4 we fix the gauge and in 2.5 give estimates of the coupling constant, symmetry breaking parameter etc.

2.1 A SCHEME FOR GAUGE MODELS OF HADRONS

It is well known that if a Lagrangian is invariant under a continuous symmetry group, and if the symmetry is broken spontaneously; i.e., by making the vacuum non-invariant under the group, zero-mass particles make their appearance. This is the Goldstone theorem.[9,10] It was pointed out by Higgs[11-13] that in gauge theories, one can have spontaneous symmetry breaking without the Goldstone bosons appearing. At the same time, the gauge fields acquire mass.

If we apply this idea to strong interactions, we have to retain, globally, the symmetries of the strong interactions.

Let us suppose we want to retain a global U(n) invariance. Then the suggestion of Bardakci and Halpern is to start with an $U(n)^L \times U(n)^G$ group, with $U(n)^L$ a local symmetry, and $U(n)^G$ a global one. One then takes n scalar, complex fundamental representations $\phi_j^{(i)}$ of U(n) which transforms under elements L(x) and G of $U(n)^L$ and $U(n)^G$ respectively, as

$$\phi_j^{(i)} \to L(x)_{jj'} \phi_{j'}^{(i')} G^{-1}_{i'i} \tag{2.1}$$

Other fields are defined in the usual way under $U(n)^L$. Under $U(n)^G$ they donot change.

If we give $\phi_j^{(i)}$ non-zero vacuum expectation value

$$\left\langle \phi_j^{(i)} \right\rangle_0 = \eta \, \delta_{ij} \tag{2.2}$$

and shift the fields as

$$\phi_j^{(i)} \to \phi_j^{(i)'} + \eta \delta_{ij} \tag{2.3}$$

we find that the Lagrangian, originally symmetric under $U(n)^L \times U(n)^G$, now retains a global U(n) symmetry, namely the transformations for which elements of local gauge group are constant (i.e. independent of space-time) and the group parameters defining the element are the same for the local and the global group. In other words, the $U(n)^L \oplus U(n)^G$ subgroup

is still retained as symmetry group of the Lagrangian. Moreover, all the n^2 vector mesons get the same mass, determined by the symmetry breaking parameter η.

In the next sections we discuss the SU(2) version of the above formalism.

2.1 AN SU(2) GAUGE MODEL FOR ρ AND π

We consider the group $SU(2)^L \times SU(2)^G$. The elements of $SU(2)^L$ and $SU(2)^G$ will be written as L(x) and G respectively.

We introduce the pion field π^i and the vector meson field $\rho_\mu{}^i$, both triplets, and transforming under an infinitesimal transformation

$$L(x) = 1 + i\,\vec{\theta}(x).\vec{\tau} \tag{2.4}$$

of $SU(2)^L$ as,

$$\vec{\pi} \rightarrow \vec{\pi} - 2\vec{\theta}(x) \times \vec{\pi} \tag{2.5}$$

and

$$\vec{\rho}_\mu \rightarrow \vec{\rho}_\mu - 2\vec{\theta}(x) \times \vec{\rho}_\mu + \frac{1}{g}\,\partial_\mu\,\vec{\theta}(x) \tag{2.6}$$

where we have used the vector notation $\vec{\pi}$ for π^i etc.

Under $SU(2)^G$, $\vec{\pi}$ and $\vec{\rho}_\mu$ remain invariant.

According to the scheme of Bardakci and Halpern as briefly outlined in the previous section, we choose two complex doublets

$$\phi_1 = (\phi_{11}, \phi_{21})$$

and

$$\phi_2 = (\phi_{12}, \phi_{22})$$

both transforming under L(x) as

$$\phi_1 \to L(x)\, \phi_1 \tag{2.7}$$

and

$$\phi_2 \to L(x)\, \phi_2 \tag{2.8}$$

Under an element of $SU(2)^G$, the transformation mixes the two doublets:

$$\tilde{\phi}_1 \to \tilde{\phi}_1\, G^{-1} \tag{2.9}$$

$$\tilde{\phi}_2 \to \tilde{\phi}_2\, G^{-1} \tag{2.10}$$

where

$$\tilde{\phi}_1 = (\phi_{11}, \phi_{12}) \tag{2.11}$$

and

$$\tilde{\phi}_2 = (\phi_{21}, \phi_{22}) \tag{2.12}$$

We denote by ϕ the 2 x 2 matrix ϕ_{ij}, and if we parametrize it as

$$\phi = M_o + iN_o + (\vec{M} + i\vec{N}).\vec{\tau} \tag{2.13}$$

the transformation properties (2.7 - 10) can be summarised as

$$\phi \to L(x)\ \phi\ G^{-1} \tag{2.14},$$

or, in terms of M's and N's, as

$$M_o \to M_o - (\vec{\theta} - \vec{\psi}).\vec{N} \tag{2.15}$$

$$N_o \to N_o + (\vec{\theta} - \vec{\psi}).\vec{M} \tag{2.16}$$

$$\vec{M} \to \vec{M} - (\vec{\theta} - \vec{\psi})N_o - (\vec{\theta} + \vec{\psi}) \times \vec{M} \tag{2.17}$$

$$\vec{N} \to \vec{N} + (\vec{\theta} - \vec{\psi})M_o - (\vec{\theta} + \vec{\psi}) \times \vec{N} \tag{2.18}$$

where

$$L(x) = 1 + i\vec{\theta}(x).\vec{\tau} \quad \text{and}$$

$$G = 1 + i\vec{\psi}.\vec{\tau}$$

Let us define

$$\rho_\mu = \vec{\rho}_\mu.\vec{\tau} \tag{2.19}$$

and

$$\pi = \vec{\pi}.\vec{\tau} \tag{2.20}$$

The transformation of ρ_μ and π is

$$\rho_\mu \to L(x)\ \rho_\mu\ L(x)^{-1} + \frac{i}{g} L(x)\ \partial_\mu(L(x)^{-1}) \tag{2.21}$$

$$\pi \to L(x)\ \pi\ L(x)^{-1} \tag{2.22}$$

The transformation properties (2.14), (2.21) and (2.22) require that under $SU(2)^L \times SU(2)^G$,

$$(\partial_\mu \rho_\nu - \partial_\nu \rho_\mu - ig\,[\rho_\mu, \rho_\nu]) \to L(x)(\partial_\mu \rho_\nu - \partial_\nu \rho_\mu - ig\,[\rho_\mu, \rho_\nu]) \times L(x)^{-1} \times L(x)^{-1} \tag{2.23},$$

$$(\partial_\mu \pi - ig\,[\rho_\mu, \pi]) \to L(x)\,(\partial_\mu \pi - ig\,[\rho_\mu, \pi])\,L(x)^{-1} \tag{2.24},$$

$$(\partial_\mu \phi - ig\rho_\mu \phi) \to L(x)(\partial_\mu \phi - ig\,\rho_\mu \phi)\,G^{-1} \tag{2.25}.$$

Therefore we can write the Lagrangian invariant under $SU(2)^L \times SU(2)^G$ as,

$$\begin{aligned}\mathcal{L} = &-\frac{1}{8}\,\mathrm{tr}\,[(\partial_\mu \rho_\nu - \partial_\nu \rho_\mu - ig\,[\rho_\mu, \rho_\nu])^2] \\ &+ \frac{1}{4}\,\mathrm{tr}\,[(\partial_\mu \pi - ig\,[\rho_\mu, \pi])^2] \\ &+ \frac{1}{4}\,\mathrm{tr}\,[(\partial_\mu \phi - ig\,\rho_\mu \phi)(\partial^\mu \phi^\dagger + ig\,\phi^\dagger \rho^\mu)] \\ &+ \frac{\alpha^2}{4}\,\mathrm{tr}\,[\phi^\dagger \phi] - \frac{\beta}{4}\,(\mathrm{tr}\,[\phi^\dagger \phi])^2 - \frac{\gamma}{2}\,[(\phi^\dagger \phi)^2] \\ &- \frac{\delta}{4}\,\mathrm{tr}\,[\pi^2 \phi^\dagger \phi] - \frac{\lambda}{4}\,(\mathrm{tr}\,[\pi^2])^2 \end{aligned} \tag{2.26}.$$

Simplified, and expressed in terms of M_o, $\vec{M}$ etc. (see (2.13)), it becomes,

$$\begin{aligned} = &-\frac{1}{4}\,(\partial_\mu \vec{\rho}_\nu - \partial_\nu \vec{\rho}_\mu + 2g\,\vec{\rho}_\mu \times \vec{\rho}_\nu)^2 \\ &+ \frac{1}{2}\,(\partial_\mu \vec{\pi} + 2g\,\vec{\rho}_\mu \times \vec{\pi})^2 \\ &+ \frac{1}{2}\,(\partial_\mu M_o)^2 + \frac{1}{2}\,(\partial_\mu N_o)^2 + \frac{1}{2}\,(\partial_\mu \vec{M})^2 + \frac{1}{2}\,(\partial_\mu \vec{N})^2 \end{aligned}$$

$$
\begin{aligned}
&- g\vec{\rho}_\mu \cdot (M_o \partial^\mu \vec{N} - \partial^\mu \pi_o \vec{N}) \\
&+ g\vec{\rho}_\mu \cdot (N_o \partial^\mu \vec{M} - \partial^\mu N_o \vec{M}) \\
&- g\vec{\rho}_\mu \cdot (\vec{M} \times \partial^\mu \vec{M}) \\
&- g\vec{\rho}_\mu \cdot (\vec{N} \times \partial^\mu \vec{N}) \\
&+ \frac{1}{2} g^2 \vec{\rho}_\mu^{\,2} (M_o^2 + N_o^2 + \vec{M}^2 + \vec{N}^2) \\
&+ \frac{\alpha^2}{2} (M_o^2 + N_o^2 + \vec{M}^2 + \vec{N}^2) \\
&- (\beta + \gamma) (M_o^2 + N_o^2 + \vec{M}^2 + \vec{N}^2)^2 \\
&- 2\gamma (M_o \vec{M} + N_o \vec{N})^2 - 4\gamma ((\vec{M}.\vec{N})^2 - \vec{M}^2 \vec{N}^2) \\
&- \frac{\delta}{2} \vec{\pi}^2 (M_o^2 + N_o^2 + \vec{M}^2 + \vec{N}^2) - \lambda \vec{\pi}^4 \qquad (2.27).
\end{aligned}
$$

2.3 SPONTANEOUS SYMMETRY BREAKING

Let us choose the vacuum expectation values of ϕ as

$$\langle \phi \rangle_o = \eta \qquad (2.28).$$

Then we can rewrite the fields ϕ in terms of fields ϕ' with zero vacuum expectation value simply by 'shifting' ϕ as

$$\phi = \phi' + \eta \qquad (2.29)$$

For convenience we shall use the same symbols M_o, $\vec{M}$, N_o, $\vec{N}$ for the decomposition of the type (2.17) for ϕ'. Substituting (2.29) in (2.27), and equating the coefficient

$$\alpha^2 - 4\eta^2 (\beta + \gamma) \qquad (2.30)$$

of the linear terms in the Lagrangian equal to zero, we obtain for $\mathcal{L}$,

$$\begin{aligned}
\mathcal{L} = & -\frac{1}{4} (\partial_\mu \vec{\rho}_\nu - \partial_\nu \vec{\rho}_\mu + 2g\vec{\rho}_\mu \times \vec{\rho}_\nu)^2 \\
& + \frac{1}{2} (\partial_\mu \vec{\pi} + 2g\vec{\rho}_\mu \times \vec{\pi})^2 + \frac{1}{2} g^2\eta^2 \vec{\rho}_\mu^{\,2} - \frac{1}{2} \delta\eta^2 \vec{\pi}^2 \\
& + \frac{1}{2} (\partial_\mu M_o)^2 + \frac{1}{2} (\partial_\mu N_o)^2 + \frac{1}{2} (\partial_\mu \vec{M})^2 \\
& + \frac{1}{2} (\partial_\mu \vec{N})^2 - \alpha^2 M_o^{\,2} - 4\gamma\eta^2 \vec{M}^2 \\
& - g\vec{\rho}_\mu \cdot (M_o \partial^\mu \vec{N} - \partial^\mu N_o \vec{N}) \\
& - g\eta\vec{\rho}_\mu \cdot \partial^\mu \vec{N} + g\vec{\rho}_\mu \cdot (N_o \partial^\mu \vec{M} - \partial^\mu N_o \vec{M}) \\
& - g\vec{\rho}_\mu \cdot (\vec{M} \times \partial^\mu \vec{M}) - g\vec{\rho}_\mu \cdot (\vec{N} \times \partial^\mu \vec{N}) \\
& + \frac{g^2}{2} \vec{\rho}_\mu^{\,2} [M_o^{\,2} + N_o^{\,2} + \vec{M}^2 + \vec{N}^2 + 2\eta M_o] \\
& - (\beta + \gamma) [M_o^{\,4} + 4M_o^{\,3}\eta + 2(M_o^{\,2} + 2M_o\eta) \times \\
& \times (N_o^{\,2} + \vec{M}^2 + \vec{N}^2) + 2N_o^{\,2}\vec{M}^2 + 2N_o^{\,2}\vec{N}^2 + 2\vec{M}^2\vec{N}^2] \\
& - 2\gamma [M_o^{\,2}\vec{M}^2 + N_o^{\,2}\vec{N}^2 + 2\eta M_o \vec{M}^2 + 2\eta M_o \vec{M}\cdot\vec{N} + 2M_o N_o \vec{M}\cdot\vec{N} \\
& + 2(\vec{M}\cdot\vec{N})^2 - 2\vec{M}^2\vec{N}^2] \\
& - \frac{\delta}{2} \vec{\pi}^2 (M_o^{\,2} + N_o^{\,2} + \vec{M}^2 + \vec{N}^2 + 2\eta M_o) - \lambda\vec{\pi}^4 \qquad (2.31).
\end{aligned}$$

We notice that vector meson, pion, M_o and M all get masses. N_o and $\vec{N}$ remain massless. We also notice that under transformations characterized by $\theta(x)$ independent of x and equal to $\vec{\psi}$, the Lagrangian (2.31) is still invariant. This is immediately clear from (2.17).

2.4 CHOICE OF GAUGE

As we have three gauge particles we can choose three conditions to fix the gauge. We could for example choose a gauge such that

$$\vec{N} = 0 \tag{2.32}$$

This corresponds to the unitary gauge. This has the effect of removing three massless particles in the theory, as well as the term,

$$-g\eta\vec{\rho}_\mu \cdot \partial^\mu\vec{N} \tag{2.33}$$

from the Lagrangian.

Another choice to fix the gauge is to add an explicitly gauge non-invariant term to the Lagrangian. For example we can add,

$$\mathcal{L}_1 = -\frac{1}{2}(\partial_\mu\vec{\rho}^\mu + g\eta\vec{N})^2 \tag{2.34}.$$

Such a choice corresponds to working in the so-called t'Hooft-Feynman gauge. It has the advantage that three

things are achieved simultaneously. Firstly, (2.33) combines with the cross-term of (2.34) to form a total divergence and so does not contribute. Secondly, $\vec{N}$ gets a mass whose square is $g^2\eta^2$. Thirdly, the vector meson propagator becomes the simple Feynman propagator

$$-ig_{\mu\nu}/(k^2-M^2).$$

However, we know that in deriving the Feynman rules by functional integration method, we have to take into account the explicit change in $\mathcal{L}_1$ under gauge transformation. In other words, we have to introduce fictitious particles - the so-called Faddeev-Popov ghosts. That is taken into account if we add to the Lagrangian yet another term,

$$\begin{aligned}\mathcal{L}_2 = {} & \partial^\mu \omega^{i\dagger} (\partial_\mu \delta_{ij} - 2g\varepsilon_{ijk}\rho_\mu{}^k)\, \omega^j \\ & - g^2\eta^2 \omega^{i\dagger}\omega^i - g^2\eta [M_o \omega^{i\dagger}\omega^i \\ & - \varepsilon_{ijk}\omega^{i\dagger}\omega^j N^k]\end{aligned} \tag{2.35}$$

with the specific requirement that a factor -1 should be inserted for each closed loop of the ghosts.

In the following we shall work in the t'Hooft-Feynman gauge only.

A remark must be made concerning the presence of N_o in our Lagrangian. It is still massless.

We could have avoided N_o by either choosing small number of Higgs scalars, for example breaking symmetry by giving non-zero vacuum expectation value to some component of just one complex doublet instead of two. Or, we could have retained the similarity with the Bardacki-Halpern model, and extended the group to U(2). In the latter case, one has to introduce another vector meson corresponding to U(1) part of $U(2) = U(1) \times SU(2)$. Then we can choose another gauge condition and eliminate N_o. However, as in our work that follows, we don't require these couplings, we have not explicitly written them down.

2.5 ORDER OF MAGNITUDE OF COUPLING CONSTANT AND SYMMETRY-BREAKING PARAMETER

To lowest order the $\rho \to \pi\pi$ width Γ is easily found to be,

$$\Gamma/M = \frac{g^2}{12\pi}\left(1 - \left(\frac{2m}{M}\right)^2\right)^{3/2} \tag{2.36}$$

with m the mass of pion and M that of rho meson. (We shall use this convention for mass of π and ρ throughout). Using $M = 765$ MeV, $\Gamma = 135$ MeV, $m = 140$ MeV, we find

$$g^2/4\pi = .43 \tag{2.37}$$

On the other hand, as

$$M^2 = g^2\eta^2$$

and

$$m^2 = \delta\eta^2$$

we find

$$\eta = 330 \text{ MeV}$$

$$\delta = .18 \qquad (2.38)$$

This fixes the parameters g, η and δ.

CHAPTER THREE

In this chapter we shall very briefly review the experimental and theoretical studies of A_1 and its status as a $\rho\pi$ resonant system.

3.1 OBSERVATION OF MASS ENHANCEMENT IN DIFFRACTIVE PRODUCTION

In a diffractive production process like $\pi N \to (\rho\pi)N \to (\pi\pi\pi)N$ with no quantum numbers exchanged and small momentum transfer one observes a broad bump in the s-wave of the $\rho\pi$ system with $\rho\pi$ invariant mass about 1.1 GeV. On first observations[14-16] the interpretation was, of course, to regard it as a resonant state A which decays into ρ and π

$$\pi p \to Ap \to (\rho\pi)p \to (\pi\pi\pi)p \qquad (3.1)$$

Later, the original peak resolved into two peaks[17,18], called A_1 (around 1.1 GeV) and A_2 (around 1.4 GeV). The spin-parity assignment of A_1 has been established to be 1^+.[19] Thus there is an unmistakable enhancement in diffractive processes in 1^+ channel and at 1.1 GeV.[20-27]

However, the mere presence of a bump in the cross-section is not enough to justify a resonance. There should also be the phase-shift behaviour characteristic of a resonance. With the phase shift analyses[28] made of the

$A_1\rho\pi$ system, the conclusion seems to be that A_1 does not exhibit any phase shift variation characteristic of a resonance. This, coupled with the possibility of explaining the A_1 enhancement by Deck effect or similar mechanisms (to be discussed later in this chapter), has cast a strong doubt on the very existence of A_1 as a particle.[29]

3.2 A_1 IN NONDIFFRACTIVE PROCESSES

As the diffractive production of A_1 is open to doubt whether it is a true resonance or a kinematic enhancement peculiar to the diffraction process, it has been of considerable interest to observe it in some process which is free of such kinematic complications so that the resonant or non-resonant character of A_1 can be established.

Contrary to the situation in diffractive processes, the evidence for A_1 peak in non-diffractive processes like charge-exchange, backward scattering and in inelastic processes like $\pi^+p \to \pi^+\pi^-\pi^0\ \Delta^{++}$ and $p\bar{p}$ annihilation is very small.

In backward π^-p scattering there is an indication of A_1 but the data is of limited statistical significance.[30] Recent analyses of $(3\pi)^0$ system produced by charge exchange donot find any evidence for A_1 production.[30] Analysing $\pi^+n \to \pi^+\pi^-\pi^0p$ at 4 GeV/c, Emms et al[31] observe no A_1 about 1.1 GeV.

In $p\bar{p}$ annihilation experiment there is an indication of A_1[33,34], but the peak is not very significant above the background.

In K^+p processes,[35-37] there is some evidence for A_1 but as Berlinghieri points[38] out that a purely kinematic enhancement is not ruled out.

Recently Wagner et al[39] have studied the reaction $\pi^+p \rightarrow \pi^+\pi^-\pi^0 \Delta^{++}$ at 7 GeV/c, and have set an upper limit of 2μb on the A_1 production cross section. If A_1 exists then, as pointed out by Kane[29], the expected cross section should be of the order of 30 μb.

Thus we see that the evidence of A_1 in non-diffractive processes is slender and insufficient.

3.3 THEORETICAL MODELS TO UNDERSTAND A_1 PEAK AS A KINEMATIC ENHANCEMENT

Even before the discovery of the A_1 peak, it was suggested by Nauemberg and Pais[40] in 1962 that purely kinematic peaks may occur in 2π and 3π systems. This suggestion is based on the Pierls Mechanism[41], originally conceived to understand the second pion-nucleon resonance. The basic idea is the following. Consider the scattering of X and Y with the exchange of Z as shown in Fig. 1a. If the mass of X, m_X is greater than $m_Y + m_Z$ then the two vertices are decay vertices

and the scattering amplitude has a pole at $p_Z^2 = m_Z^2$. However, for physical values of s (the centre of mass energy squared) it is possible for p_Z to be on mass-shell, and thus contribute a pole to the scattering amplitude. This pole will of course depend on the scattering angle, and as the scattering angle θ runs over the entire range, the pole will trace a segment in the s plane above the threshold. The scattering amplitude shows an enhancement over this region. Analysing the (X, Y, Z) = (ρ, π, π) system they predicted an enhancement at 1090 MeV, just where A_1 peak is seen. However this analysis presumes the dominance of the exchange diagram of Fig. 1a over any other process and does not take into account the unitarity of the amplitude over the physical region.

Immediately after the observation of the A_1 bump, Deck pointed out[42] that the effect could be due to the particular mechanism of production. Analysing the process $\pi p \to 3\pi p$ he assumed the dominance of the pion exchange diagram shown in Fig. 1b. The differential cross section for such a process will be of the form (with the notation of Fig. 1b).

$$d\sigma = (\text{kinematical factors}) \times \frac{F(\Delta^2)}{(\Delta^2 - m^2)^2} |M'_{\pi N}|^2 \, dq_1 \, dq_2 \, dq,$$

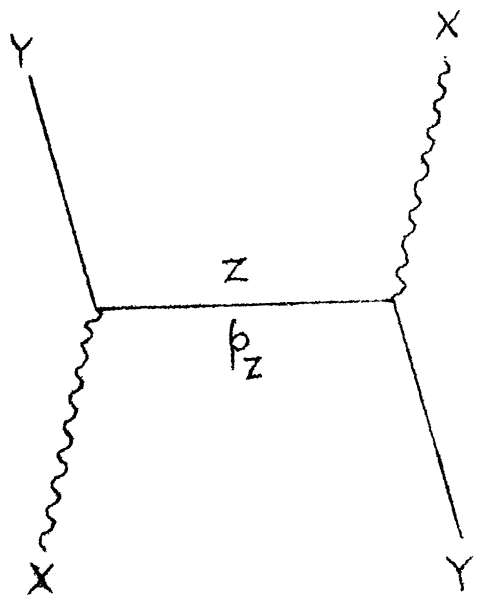

Fig. 1a: Diagram responsible for Pierls Mechanism

$m_X > m_Y + m_Z$

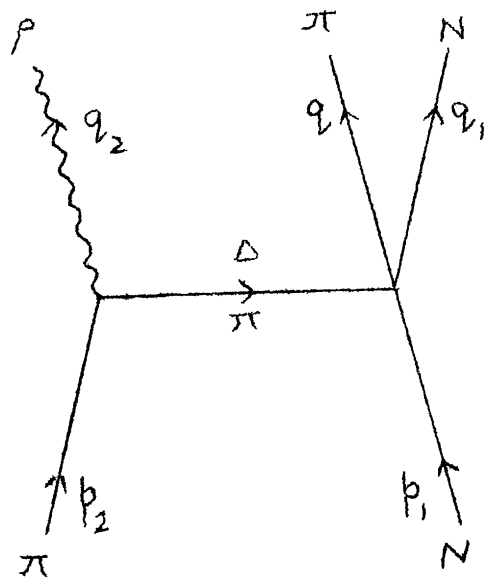

Fig. 1b: Dominant diagram in Deck Effect.

where $F(\Delta^2)$ is the form-factor associated with the pion propagator, and $M'_{\pi N}$ is the off-shell scattering amplitude for $\pi N \to \pi N$, which is approximated by the on-shell matrix element. Now the $\pi N \to \pi N$ cross section (proportional to $|M'_{\pi N}|^2$) shows a peak in the forward direction for diffractive reaction, i.e. for small momentum transfer to the nucleon. Approximating the peak in $d\sigma_{\pi N}/d\Omega$ by a functional form $e^{\lambda t^2}$ where $t^2 = (p_1 - q_1)^2$ is the momentum transfer, and making some simplifying assumptions about $F(\Delta^2)$ one finds, after integrating in the neighbourhood of $t^2 = 0$, that the differential cross-section with respect to $\rho\pi$ invariant mass shows a peak about 1100 MeV.

Later, the idea of Deck model has been extended and generalized to include exchange of Regge pole and trajectories[43-4] However, as pointed out by Chew and Pignotti[50], the concept of duality implies that when periferal models of the Deck type predict large cross section at low subenergies, there probably are resonances present even though there is no explicit insertion of a resonance in the amplitude. So the Deck model, rather than explaining away the resonance, in fact predicts a resonance. This startling conclusion has somewhat confused the situation. We shall not go into the details of these arguments. Suffice is to say that Reggerized Deck model has been able to explain the data of A_1 production without explicitly requiring a resonance.

Recently Brayshaw[51] has constructed a model in which the lack of variation of the phase shift is compatible with an A_1 resonance pole. The model is based on the boundary-condition formalism developed earlier by him for relativistic three particle systems.[52] The amplitude for $N\pi \to N(3\pi)$ is written as,

$$T = T_p \cdot T_3$$

where T_p is the production amplitude and T_3 the 3-pion amplitude. If A_1 is indeed a dynamical effect then T_3 should contain the resonance pole. After properly unitarizing the amplitude one obtains an A_1 state of approximately the right mass and width and with negligible phase variation.

3.4 REMARKS

We shall not discuss the many calculations involving A_1 which explicitly assume the existence of A_1 and then explore its consequence. These include hard-pion calculations, quark model calculations, current-algebra and superconvergence calculations, and Veneziano model calculations.

Recently Bowler et al[53] have constructed a model amplitude for diffractive production of resonant states in the presence of Deck amplitudes. It is found that the resonance may get grossly distorted and may show very slow phase variation. The model successfully explains the detailed features of A_1 production, if only the mass of A_1 be about 1.3 GeV and width about 240 MeV.

CHAPTER FOUR

As reviewed in the previous chapter, the present status of A_1 as a particle is very unclear. A number of analyses of the experimental data have been made, and all agree on the absence of a resonant A_1 state. A_1 phase variation is quite flat. On the other hand quark model and chiral symmetry require the existence of A_1. Weinberg's sum rules[3], if vector and axial vector spectral functions are saturated with ρ and A_1, require $m_{A_1} = \sqrt{2}\, m_\rho$, just about the place where $\pi\rho$ mass enhancement in $\pi N \to (3\pi) N$ is seen. Similarly in the meson spectrum generated by the quark model it is natural to expect A_1.

In this chapter we shall investigate the presence of A_1 by solving the N/D equations for $J^P(I) = 1^+(1)$ partial wave amplitudes of $\rho\pi$ scattering. Generally in using the N/D equations ... one either treats the discontinuity across the left hand cuts as a parameter to be fitted or supplies this information from some source. We have obtained the discontinuities from lowest order diagrams of a gauge model, in which global isospin is preserved and vector mesons are given masses by breaking the symmetry spontaneously.

In fact we can do two things. First to consider only the isospin group and consider the scattering of ρ and π as in the model of Chapter Two and see if in N/D solutions any A_1 resonance appears. Secondly, one can consider the broken chiral SU(2) X SU(2) Bardakci model (described in Appendix Two) and consider whether the assumption of A_1 as a particle which couples to ρ and π in u-channel implies an A_1 resonance in the $\rho\pi$ s-channel.

We have carried out both the calculations, and the result is, for both the cases, there is definite absence of a peak in the cross-section near A_1 mass region.

In sections 4.1 and 4.2 we study the helicity amplitudes for $\rho\pi$ scattering and in 4.3 the N/D equations for them. In section 4.4 we find the expressions for discontinuity on the left hand cut of these equations and using these as input, solve the equations numerically. The results obtained are discussed in section 4.5. Details of kinematics, and the discontinuities of partial wave amplitudes obtained from the Bardakci Model are given in Appendix One and Two respectively.

4.1 HELICITY AMPLITUDES FOR $\rho\pi$ SCATTERING:

Let us define the scattering amplitude for $\rho\pi$ scattering with the indices 1,2,3,4 referring to ingoing ρ and π and outgoing ρ and π respectively, as,

$$S^{i_3 i_4, i_1 i_2}_{\lambda_3 \lambda_1}(p_3 p_4, p_1 p_2) = 2p_1{}^{o}\ 2p_2{}^{o}\ \delta^3(\vec{p}_1-\vec{p}_3)\ \delta^3(\vec{p}_2-\vec{p}_4)$$

$$\times\ \delta_{\lambda_3\lambda_1}\ \delta_{i_3 i_1}\ \delta_{i_4 i_2}$$

$$+\ i(2\pi)^4\ T^{i_3 i_4, i_1 i_2}_{\lambda_3 \lambda_1}(s,t) \quad (4.1).$$

The invariant amplitude $T^{i_3 i_4, i_1 i_2}_{\lambda_3 \lambda_1}(s,t)$ can in general be decomposed as,

$$T^{i_3 i_4, i_1 i_2}_{\lambda_3 \lambda_1}(s,t) = \frac{1}{(2\pi)^6}\ \varepsilon^{\nu *}_{\lambda_3}(p_3)\ \varepsilon^{\mu}_{\lambda_1}(p_1)$$

$$\times\ [A g_{\nu\mu} + B p_{2\nu} p_{2\mu} + C\ p_{1\nu} p_{2\mu} + D\ p_{2\nu}\ p_{3\mu}$$

$$+ E\ p_{1\nu} p_{3\mu}] \qquad (4.2)$$

where we have omitted the superscript $i_3 i_4, i_1 i_2$ in A to E.

We note that actually there are only four independent invariant amplitudes, because time reversal invariance requires that,

$$C = B + D \qquad (4.3)$$

As shown in detail in Appendix One, in the center of mass system the parity conserving amplitudes, i.e. amplitudes with definite total angular momentum and parity, can be written, for the case of $J^P = 1^+$, in terms of the above invariant amplitudes as follows

$$T^{1^+}_{(11)} = \frac{\pi p}{2\sqrt{s}} \frac{1}{(2\pi)^6} \int_{-1}^{1} dx \left[-\frac{A}{2}(1+x^2) + \frac{D-E}{2} p^2 x (1-x^2) \right] \quad (4.4)$$

$$T^{1^+}_{(10)} = \frac{\pi p \Omega}{\sqrt{2s}\, M} \frac{1}{(2\pi)^6} \int_{-1}^{1} dx \frac{1-x^2}{2} \left[-A + (B-C) \frac{p^2\sqrt{s}}{\Omega} + (D-E)\, p^2 (1-x) \right] \quad (4.5)$$

$$T^{1^+}_{(01)} = T^{1^+}_{(10)} \quad (4.6)$$

$$T^{1^+}_{(00)} = \frac{\pi p \Omega^2}{2\sqrt{s}\, M^2} \cdot \frac{1}{(2\pi)^6} \int_{-1}^{1} dx \left[A\left(\frac{p^2}{\Omega^2} - x\right) + \frac{p^2\sqrt{s}}{\Omega} \left(\frac{B\omega + C\Omega}{\Omega} + x(B-C) \right) + p^2(1-x) \left(\frac{D\omega + E\Omega}{\Omega} + x\,(D-E) \right) \right] \quad (4.7),$$

where the definition of center of mass variables is given in (A1.32) and it is understood that the amplitudes A, B etc. have been projected to the isospin 1 with the help of (A1.41). We note that for $J^P = 1^+$ we have four amplitudes $T^{1^+}_{(\alpha\beta)}$ because out of $\rho\pi$ helicity states one can construct two independent positive parity states with angular momentum 1, namely the one corresponding to ρ-helicity zero and the other corresponding to a linear combination of helicity +1 and -1. In $T^{1^+}_{(\alpha\beta)}$, α or $\beta = 1$ corresponds to helicity $\pm$ 1 combination. Note also that $T^{1^+}_{(\alpha\beta)}$ is symmetric as required by time reversal

invariance (cf. eqn. (A1.21)). Alternately, we can look at it in this way. $J^P = 1^+$ amplitudes mix the centre-of-mass orbital angular momentum s- and d- waves. In the basis of orbital angular momentum $\ell = 0, 2$ the amplitudes are given by,

$$t_{00} = \frac{1}{3}\left(2T^{1^+}_{(11)} + 2\sqrt{2}\, T^{1^+}_{(10)} + T^{1^+}_{(00)}\right) \tag{4.8}$$

$$t_{22} = \frac{1}{3}\left(2T^{1^+}_{(00)} - 2\sqrt{2}\, T^{1^+}_{(10)} + T^{1^+}_{(11)}\right) \tag{4.9}$$

$$t_{02} = \frac{\sqrt{2}}{3}\left(T^{1^+}_{(11)} - \frac{1}{\sqrt{2}}\, T^{1^+}_{(10)} - T^{1^+}_{(00)}\right) \tag{4.10}$$

$$t_{20} = t_{02} \tag{4.11}$$

4.2 SINGULARITIES OF THE HELICITY AMPLITUDES:

The amplitude matrix $T^{1^+}_{(\alpha\beta)}$ introduced in the previous section satisfies the unitarity condition,

$$i\left(T^{1^+\dagger} - T^{1^+}\right) = (2\pi)^4\, T^{1^+}\, T^{1^+\dagger} \tag{4.12}.$$

This condition requires that $T^{1^+}_{(\alpha\beta)}$ have a cut in the s-plane from $(M+m)^2$ to ∞. This is the 'physical' or unitarity cut. Apart from it these amplitudes will have the so called 'unphysical cuts' or 'left-hand cuts' arising from dynamical singularities of invariant amplitude A(s, t), B(s, t) etc. corresponding to exchange of particles in other channels. Apart from the physical and unphysical cuts these amplitudes also have kinematical singularities coming from factors like

$p = ((s - (M+m)^2)(s-(M-m)^2)/4s)^{\frac{1}{2}}$ which has branch points at threshold $(M+m)^2$ and 'pseudo-threshold' $(M-m)^2$, and occurence of $\sqrt{s}$ at various places.

The reason we have constructed parity conserving amplitudes is that the kinematical singularities can be removed very easily from these amplitudes[54]. We define the following amplitudes,

$$\tilde{T}_{00} = \pi(2\pi)^4 \frac{m^2}{p\sqrt{s}} T^{1^+}_{(00)} \tag{4.13}$$

$$\tilde{T}_{10} = \pi(2\pi)^4 \frac{m}{p} T^{1^+}_{(10)} \tag{4.14}$$

$$\tilde{T}_{11} = \pi(2\pi)^4 \frac{\sqrt{s}}{p} T^{1^+}_{(11)} \tag{4.15}$$

$$\tilde{T}_{01} = \tilde{T}_{10} \tag{4.16}$$

Except for pole at $s = 0$ these are free of kinematical singularities in the physical region and satisfy the following unitarity condition,

$$i(\tilde{T} - \tilde{T}^\dagger) = -\tilde{T}\,\rho\,\tilde{T}^\dagger \tag{4.17}$$

where ρ is the diagonal matrix,

$$\rho_{00} = \frac{p\sqrt{s}}{\pi m^2} \tag{4.18a}$$

$$\rho_{11} = \frac{p}{\pi\sqrt{s}} \tag{4.18b}$$

$$\rho_{10} = \rho_{01} = 0 \tag{4.18c}$$

It should be emphasized that our approach is not intended to be a purely dispersion theoretic approach. For us the problem of kinematic singularities is, in a sense, academic. The singularity structure of the amplitudes is given to us by the perturbation theory, and we impose on it only the physical cut. We need not have cared at all about the kinematical singularities, and still would have written N/D equations. The only reason why we have defined $\tilde{T}_{\alpha\beta}$ in (4.13-16) by factoring out p, $\sqrt{s}$ etc. is that we are able to get equations for N and D which are relatively much simpler to work with. Similarly, we notice that in the partial wave amplitudes (e.g. in T_{00}^{1+}) terms like $\omega^2/\sqrt{s}$ occur. By multiplying them by $1/\sqrt{s}$ (as in 4.13) we are apparently introducing a $1/s^2$ singularity at $s = 0$. We could have multiplied $T_{(00)}^{1+}$, $T_{(10)}^{1+}$, $T_{(11)}^{p+}$ respectively by $s\sqrt{s}/p$, s/p and $\sqrt{s}/p$ apart from other trivial factors. In that case we would have obtained,

$$\rho_{00} = p/s\sqrt{s}\,\pi \quad , \quad \rho_{11} = p/\sqrt{s}\,\pi \quad ,$$

$$\rho_{10} = \rho_{01} = 0 \qquad (4.19).$$

If we do this, we can avoid the factor $1/s^2$ in $\tilde{T}_{\alpha\beta}$ at the cost of making its asymptotic behaviour worse - the equation for N (See (4.23) in Section 4.3) becomes singular. We are at liberty to choose from the following alternatives: 'subtract' N at an arbitrary point with undetermined residue

or cut off the integral in (4.23) and treat the cut off point as a parameter. We resort to neither of these and instead shift the pole at $s = 0$ by multiplying T^{1+}_{00} by $(\frac{s}{s-a})^2$ and $T^{1+}_{(10)}$ by $(\frac{s}{s-a})$. Accordingly,

$$\rho_{00} \to (\frac{s-a}{s})^2 \qquad \rho_{11} \to \rho_{11} \tag{4.20}$$

This does not change the asymptotic behaviour of ρ. We have verified that the choice of a in the neighbourhood of o does not change the results compared to results without using this device. In the following we have written formulas with $a = 0$, i.e. without shifting the pole, for simplicity.

An amplitude, apart from satisfying unitarity condition should also satisfy the correct threshold behaviour and kinematic constraints.

The correct threshold behaviour for $T^{1}_{(\alpha\beta)}$ is that it should behave like $(p)^{2\ell_{min}+1}$ near the threshold.[55] In our case $\ell_{min} = 0$, therefore $T^{1+}_{(\alpha\beta)}$ should go as p near $s = (M+m)^2$. This means that amplitudes $\tilde{T}_{\alpha\beta}$ should behave like constants near thresholds. However, our numerical calculation, with points in the s-plane at interval of 2 pion mass-squared, is too rough to say anything on this point. Similarly, an amplitude calculated at a finite number of points on the left and right-hand singularities cannot be expected to satisfy the kinematical constraints[56] at points like $s = 0$ which a true amplitude should satisfy.

We have given most importance to unitarity and symmetry of the S-matrix and not discussed above questions in any detail.

4.3 N/D FORMALISM:

Let us write the matrix $\tilde{T}$ in the form

$$\tilde{T} = N D^{-1} \qquad (4.21),$$

where N and D are 2 x 2 matrices.

We assume that D is analytic in the s-plane except for the physical cut whereas N is analytic except for the unphysical cuts.

The equations for N and D, taking account of their analytic properties and the unitarity condition (4.17) are,

$$D(s) = 1 - \frac{s-s_0}{2\pi} \int_P ds' \frac{\rho(s')\, N(s')}{(s'-s_0)(s'-s)} \qquad (4.22)$$

$$N(s) = \int_U ds'' \frac{\Delta(s'')D(s'')}{(s''-s)} \qquad (4.23)$$

The integrals in (4.22) and (4.23) go over the physical (P) and unphysical (U) cuts respectively, and $\Delta(s'')$ is the discontinuity in $\tilde{T}(s'')$ across the unphysical cut divided by $2\pi i$. Note that we have normalized D at s_0.

By substituting the second of these equations in the first we get the following integral equation for D,

$$D(s) = 1 - \frac{s-s_o}{2\pi} \int_U ds'' \; R(s,s'') \, \Delta(s'') \, D(s'') \qquad (4.24)$$

where,

$$R(s,s'') = \int_P ds' \; \frac{\rho(s')}{(s'-s_o)(s'-s)(s''-s')} \qquad (4.25).$$

It is obvious that the above equation cannot be inverted to solve for D if the kernel is badly behaved. In particular R(s, s") should exist. Our choice (4.18,20) for ρ makes this possible.

Once the discontinuity Δ across the unphysical cut is obtained, we can solve the integral equation (4.24) for values of D on the unphysical cut. These values can then be used to obtain N on the physical cut by (4.23). This, in turn, determines D on the physical cut as,

$$\text{Re } D(s) = 1 - \frac{s-s_o}{2\pi} P \int_P ds' \; \frac{\rho(s') \, N(s')}{(s'-s_o)(s'-s)} \qquad (4.26)$$

$$\text{Im } D(s) = -\frac{1}{2} \rho(s) \, N(s) \qquad (4.27)$$

where the letter P before the integral in (4.26) means that Cauchy principal value is to be taken. We shall use this procedure for solving N/D equations in the following section.

An important remark due to Bjorken and Nauemberg[57] about these equations for N and D is that it is essential that the matrix $\tilde{T}$ be symmetric in order that it satisfies

the unitarity condition. If ρ and Δ are given to be symmetric then the analytic properties of N and D imply that $\tilde{T}$ will be symmetric. We have verified that even in a relatively simple numerical calculation the symmetry and unitarity of $\tilde{T}$ are very well obtained.

Finally, we should mention that poles and zeros of N and D are not uniquely fixed. In particular there is the ambiguity due to CDD poles[58]. However, as we are neglecting the inelastic processes, an argument due to Mandelstam[59] can be advanced that physically relevant solutions of N/D equations are free of CDD ambiguity. We shall assume that there are no CDD poles.

4.4 CALCULATION OF Δ FROM PERTURBATION THEORY:

In N/D equations the discontinuities across the unphysical cuts are supposed to be given. With these as input one calculates N and D, satisfying the unitarity condition.

For the input of this physical information, we use the simple model of ρ and π given in Chapter Two. We consider the lowest order diagrams to $\rho\pi$ scattering and calculate the amplitudes A, B, etc. of eqn. (4.2). The diagrams which contribute to the 1^+ channel are shown in Fig. 2. The discontinuities Δ for these diagrams are easily evaluated from

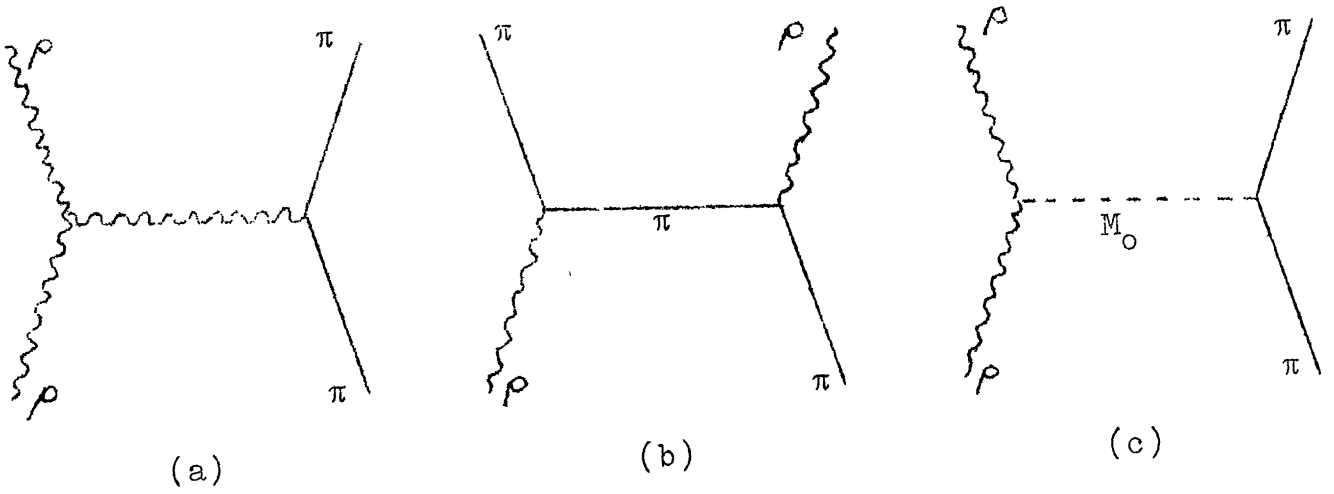

Fig. 2: Born diagrams contributing to left-hand cut in 1^+ channel. Wavy line denotes ρ, straight line π and broken line M_o.

equations (4.4-7). The unphysical cuts of l^+ partial wave amplitudes corresponding to Born diagrams of Fig. 2. are shown in Figs. 3 to 5. The signs + and - in the figure mean the following: $\tilde{T}_{(\alpha\beta)}$ on the + side of the cut minus $\tilde{T}_{(\alpha\beta)}$ on the - side is equal to $2\pi i \ \Delta_{\alpha\beta}$. We give below the $\Delta_{\alpha\beta}$ corresponding to different diagrams.

4.4.1 ρ-EXCHANGE IN THE t-CHANNEL:

$$\Delta^{\rho}_{00}(s) = \frac{g^2}{4}\left(\frac{m^2\Omega^2}{M^2 s}\right) y_\rho \left[-\frac{s-u'}{p^2}\left(\frac{p^2}{\Omega^2} - y_\rho\right) + \left(y + \frac{2\omega}{\Omega} + 1\right)(1-y_\rho)\right] \tag{4.28}$$

$$\Delta^{\rho}_{10}(s) = \frac{g^2}{4\sqrt{2}}\left(\frac{m\Omega}{M\sqrt{s}}\right)\left[\frac{s-u'}{p^2} - \frac{4\omega}{\Omega} - 4y_\rho\right]$$

$$x\,(1-y_\rho{}^2) = \Delta^{\rho}_{01}(s) \tag{4.29}$$

$$\Delta^{\rho}_{11}(s) = \frac{g^2}{8}\left[\frac{s-u'}{p^2}(1+y_\rho{}^2) + 4y_\rho\,(1-y_\rho{}^2)\right] \tag{4.30}$$

where,

$$y_\rho = 1 + \frac{M^2}{2p^2} \tag{4.31}$$

and

$$u' = 2M^2 + 2m^2 - s + 2p^2\,(1-y_\rho) \tag{4.32}$$

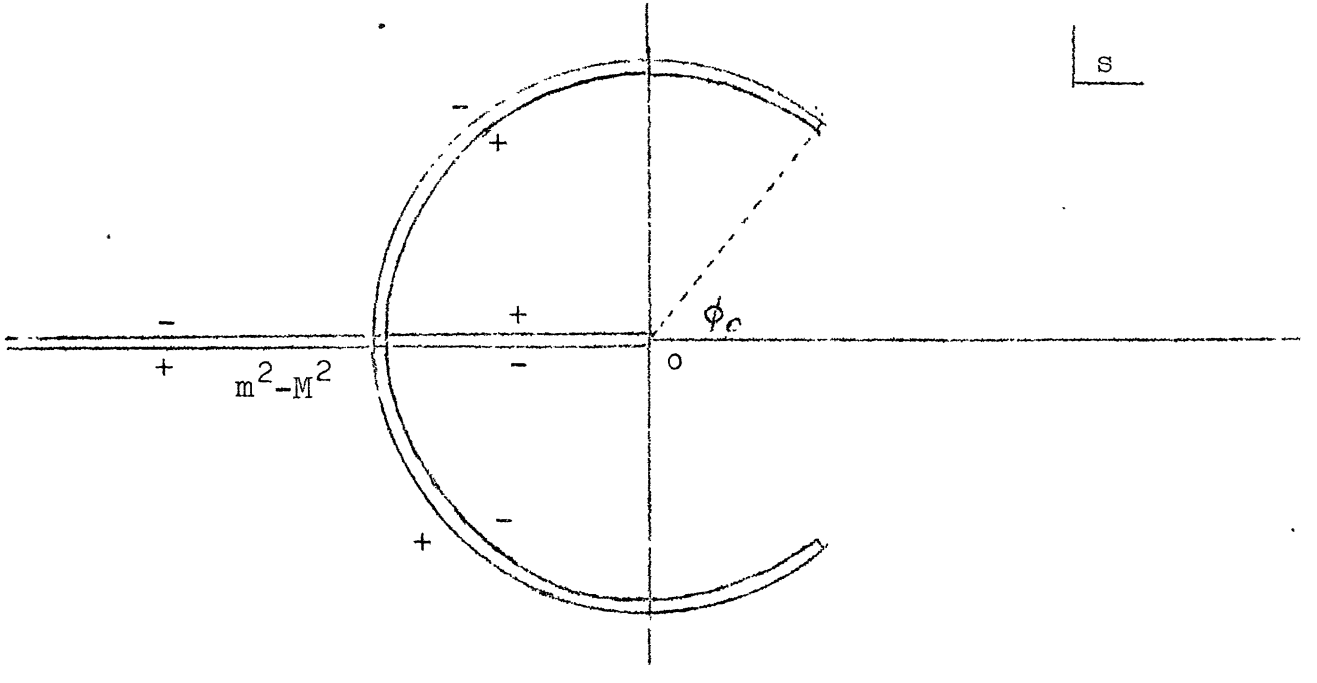

lig. 3: Left-hand discontinuities for diagram (a) in Fig. 2.
$\phi_o = \cos^{-1}((m^2+M^2/2)/(M^2-m^2))$.

4.4.2 π-EXCHANGE IN THE u-CHANNEL:

$$\Delta^{\pi}_{00}(s) = g^2 \left(\frac{m^2\Omega^2}{M^2 s}\right) y_\pi \left(y_\pi + \frac{\omega}{\Omega}\right)^2 \tag{4.33}$$

$$\Delta^{\pi}_{10}(s) = \frac{g^2}{\sqrt{2}} \left(\frac{m\Omega}{M\sqrt{s}}\right) (1-y_\pi^2) \left(y_\pi + \frac{\omega}{\Omega}\right) = \Delta^{\pi}_{01} \tag{4.34}$$

$$\Delta^{\pi}_{11}(s) = -g^2 y_\pi (1-y_\pi^2) \tag{4.35}$$

where,

$$y_\pi = 1 + \frac{2M^2 + m^2 - s}{2p^2} \tag{4.36}$$

It is interesting to note that because of the light mass of the pion, a part of the unphysical cut lies entirely within the physical cut. This happens because $\rho\pi \to 3\pi$ is kinematically possible. Such a situation can occur if we have unstable particles. Such cases need special attention in a purely dispersion theoretic approach. Work in this direction has been done by Ball, Frazer Nauemberg[60] and others[61]. A detailed treatment of such a case is not within the scope of the present thesis. In solving the N/D equations we shall therefore include only the cut from $-\infty$ to 0 as belonging to the unphysical cut, the amplitude all over the physical cut being determined by the N/D equations.

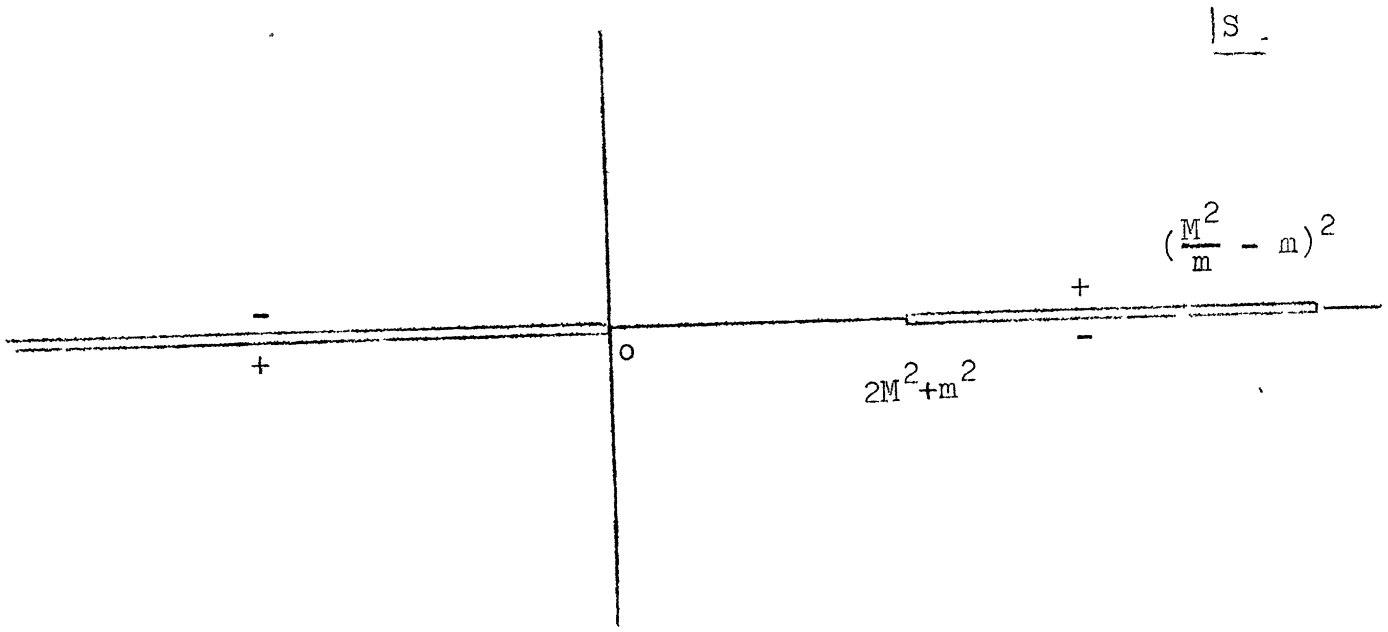

Fig. 4: Left-hand discontinuities for diagram (b) in Fig. 2.

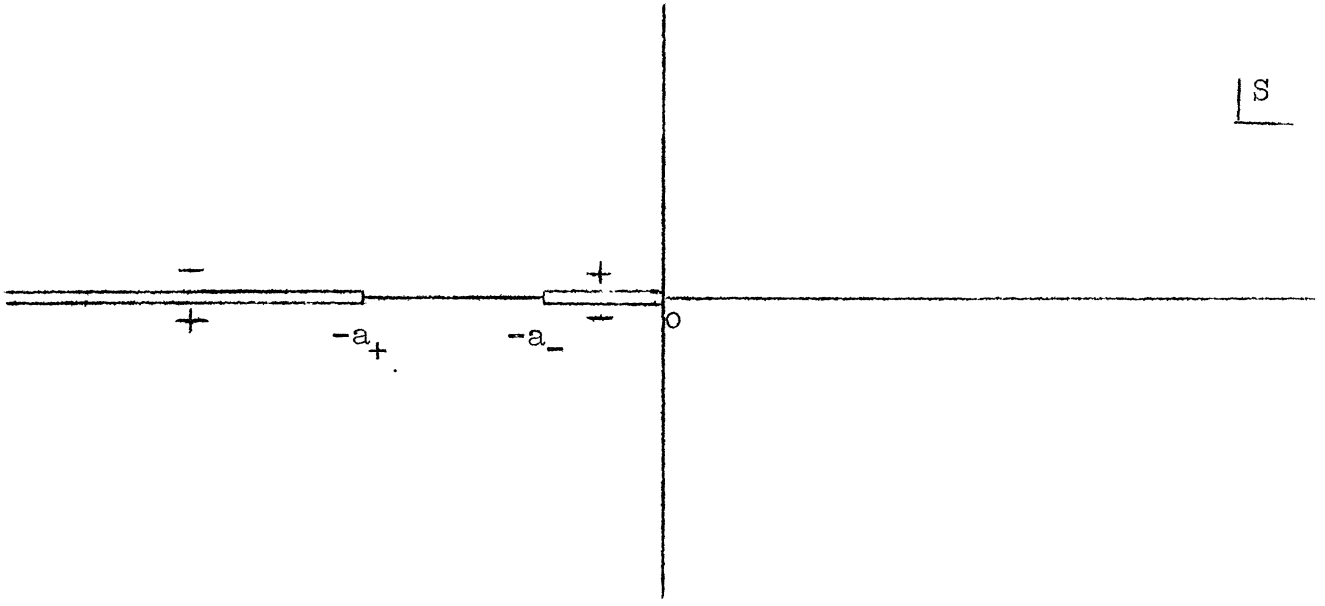

Fig. 5: Left-hand discontinuities for diagram (c) in Fig. 2.

$a_\pm = \frac{\mu^2}{2} - M^2-m^2 \pm [(\frac{\mu^2}{2} - M^2-m^2)^2 - (M^2-m^2)^2]^{\frac{1}{2}}$.

μ is the M_o-mass and assumed to be $\geqslant 2M$.

4.4.3 SCALAR-EXCHANGE IN THE t-CHANNEL:

Corresponding to diagram (c) in Fig. 2, we have,

$$\Delta^{M}_{00}(s) = -\frac{g^2}{4}\,\frac{\eta^2\delta}{p^2}\left(\frac{m^2\Omega^2}{M^2 s}\right)\left(\frac{p^2}{\Omega^2} - y_M\right) y_M \tag{4.37}$$

$$\Delta^{M}_{10}(s) = \frac{g^2}{4\sqrt{2}}\,\frac{\eta^2\delta}{p^2}\,\frac{m\Omega}{M\sqrt{s}}\left(1 - y_M{}^2\right) = \Delta^{M}_{01} \tag{4.38}$$

$$\Delta^{M}_{11}(s) = \frac{g^2}{8}\,\frac{\eta^2\delta}{p^2}\left(1 + y_M{}^2\right) \tag{4.39}$$

$$y_M = 1 + \frac{\mu^2}{2p^2} \tag{4.40}$$

where μ is the mass of the scalar particle.

4.5 SOLUTION OF N/D EQUATIONS AND DISCUSSION OF RESULTS:

In order to solve (4.24) numerically we first convert it into a matrix equation and then solve for D on the left hand cut by inverting the matrix. N on the right-hand cut is then evaluated from (4.23). From the knowledge of N on the right-hand cut, D is evaluated on the right-hand cut using (4.26) and (4.27). An outline of this procedure is given in Appendix Three.

We calculate in units of the pion mass. We choose s_o as well as a to be equal to one (cf. (4.20) and (4.22)). The amplitudes obtained are shown in Figs. 6,7 and 8 for discontinuities due to diagrams shown in Fig. 2 calculated in the model

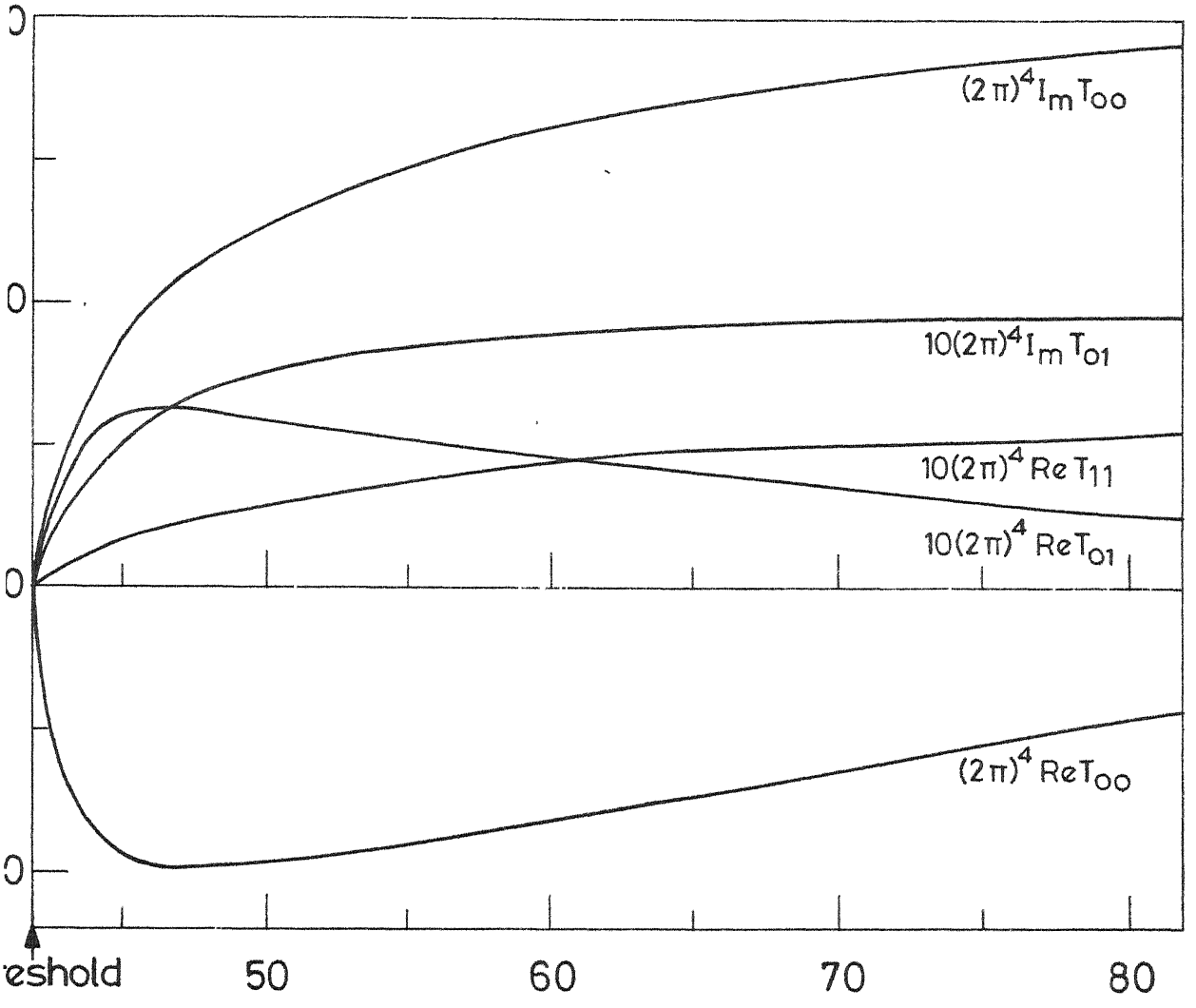

Fig. 6 $(2\pi)^4 T_{\alpha\beta}$ obtained by solving N/D equations. M_0 mass is taken to be infinity. s is in units of pion mass. $I_m T_{11}$ is too small to be shown.

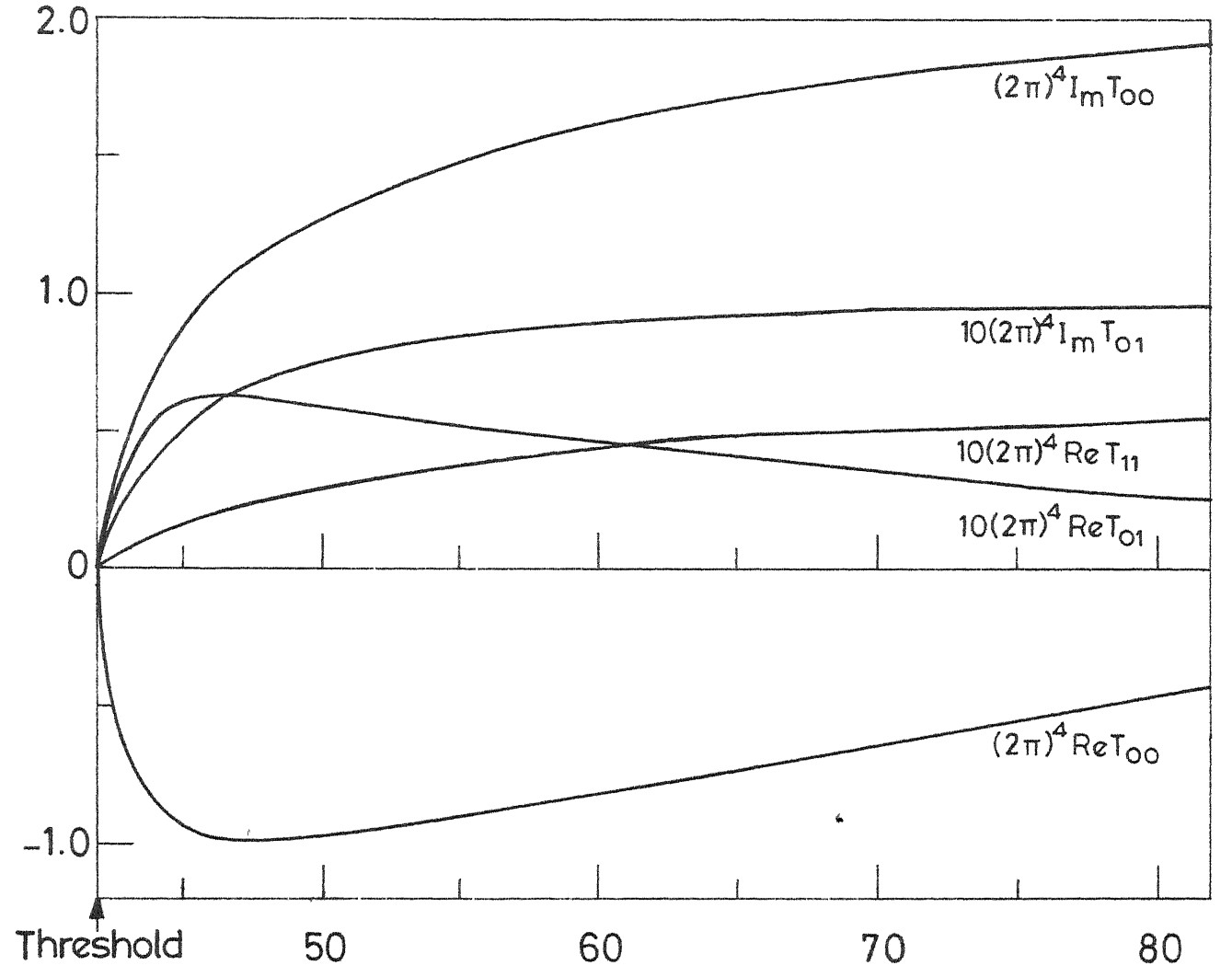

Fig. 7 $(2\pi)^4 T_{\alpha\beta}$ with M_o mass six times the rho mass. $I_m T_{11}$ too small to be shown.

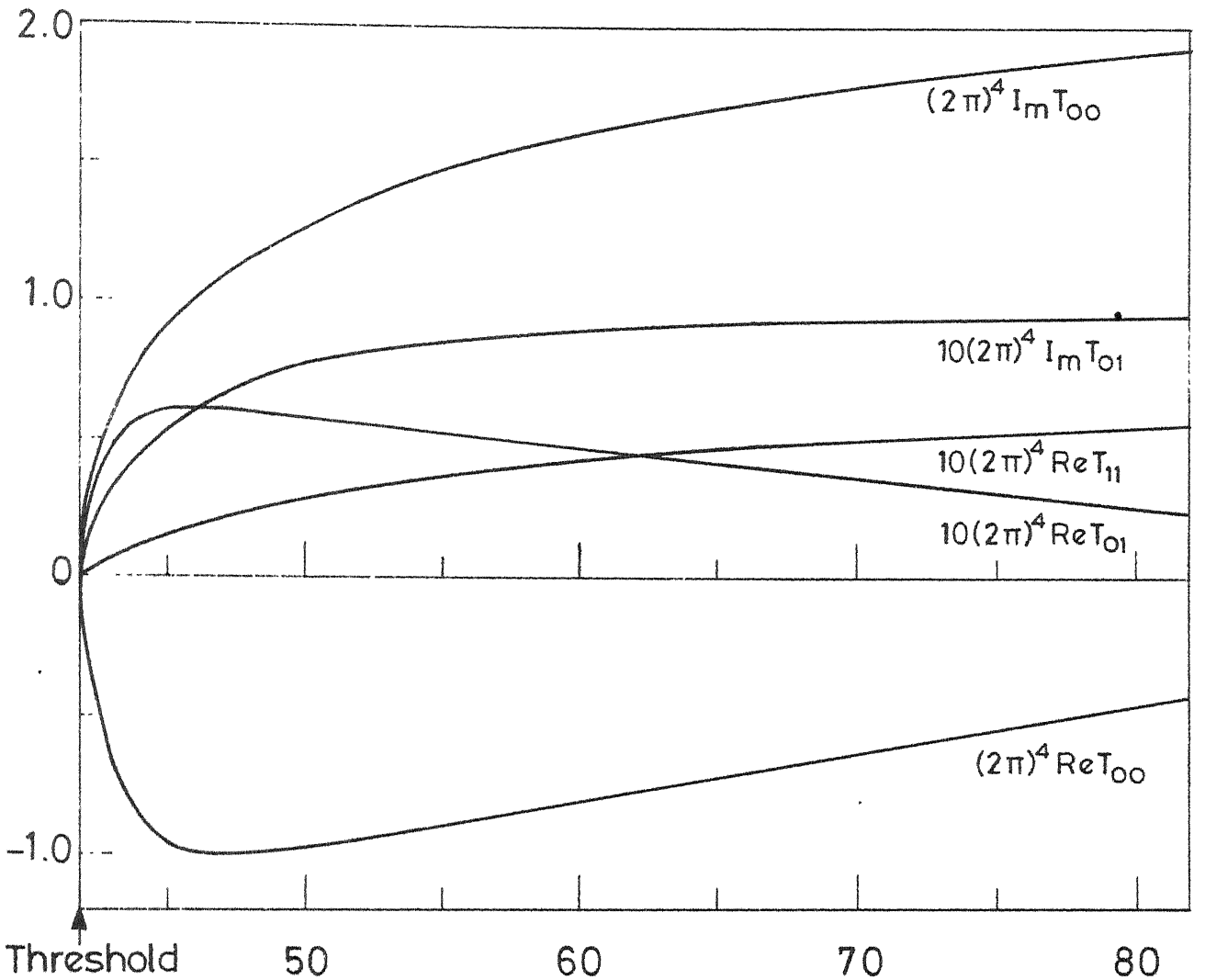

Fig. 8 $(2\pi)^4$ $T_{\alpha\beta}$ with M_0 mass twice the rho mass. $I_m T_{11}$ is too small to be shown.

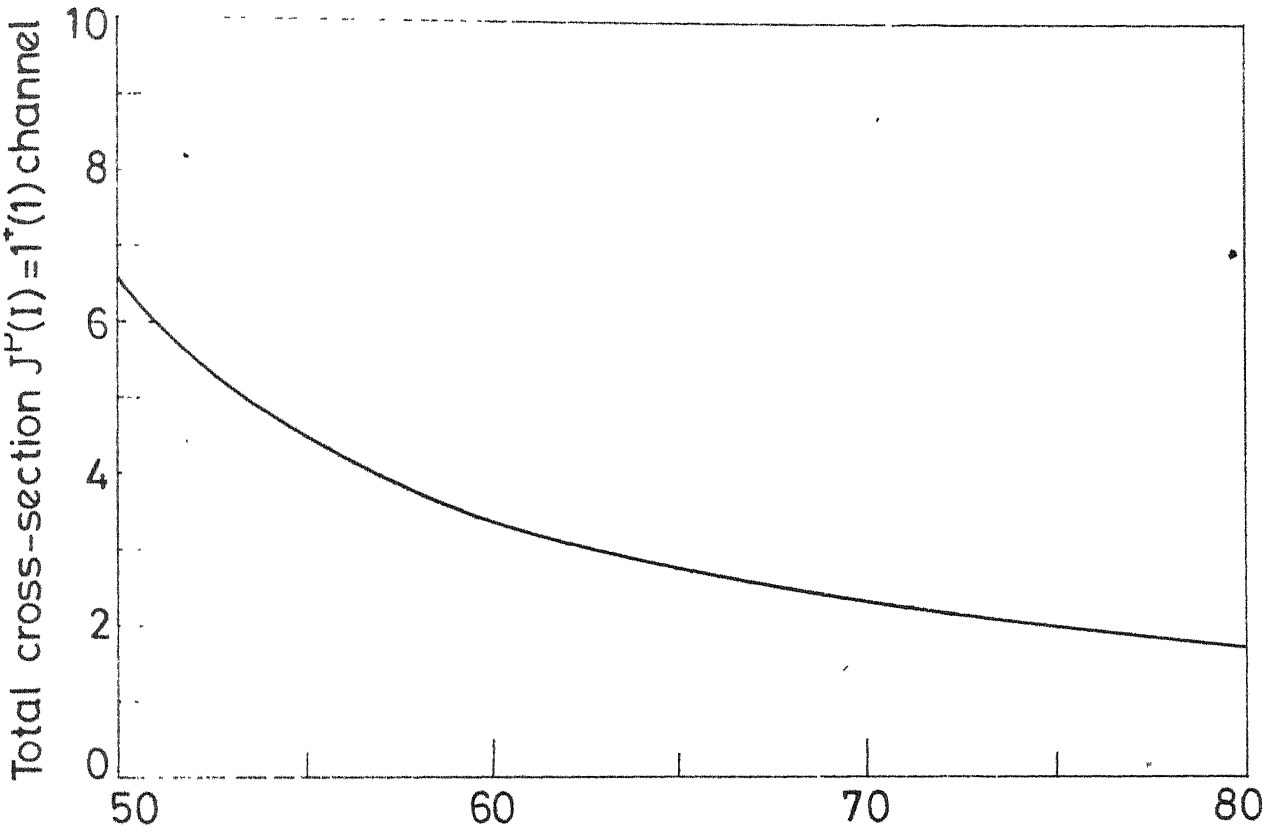

Fig. 9 Cross-section (in poin mass units) as a function of s obtained from amplitudes of fig. 8. A_1 mass region is about s = 62.

discussed in Chapter Two. They correspond respectively, to cases in which the mass of M_o is taken to be infinity (so that the cuts shown in Fig. 5 are entirely omitted), six times the rho mass and twice the rho mass. There is very little variation of amplitudes with the M_o mass.

In Fig. 9 we plot the partial cross-section in 1^+ channel near 1.1 GeV. Evidently there is no peak.

To confirm that there is no characteristic resonant variation of amplitudes, it is sufficient to observe that

$$g_{\alpha\beta}(s) = (s - M_A + iM_A\,r)\,T_{\alpha\beta}(s) \qquad (4.41)$$

which would vary slowly near $s = M_A$ if there were a pole in the second sheet at $M_A - iM_A r$, do not vary slowly. We do not find $g_{\alpha\beta}(s)$ varying slowly for a typical value like 1.1 GeV for M_A and 200 MeV for r.

The same calculation can be done with Bardakci model couplings. Apart from ρ and π exchanges, we can have A_1 itself in the u-channel. A_1 exchange gives left hand cuts as shown in Fig. 10. Omitting the contribution of scalar exchange, which we know from previous calculation causes little change, we get amplitudes shown in Fig. 11, and cross-section in Fig. 12. The results are qualitatively the same as for previous calculation. There is no bump in cross-section and $g_{\alpha\beta}(s)$ vary appreciably in the region under study.

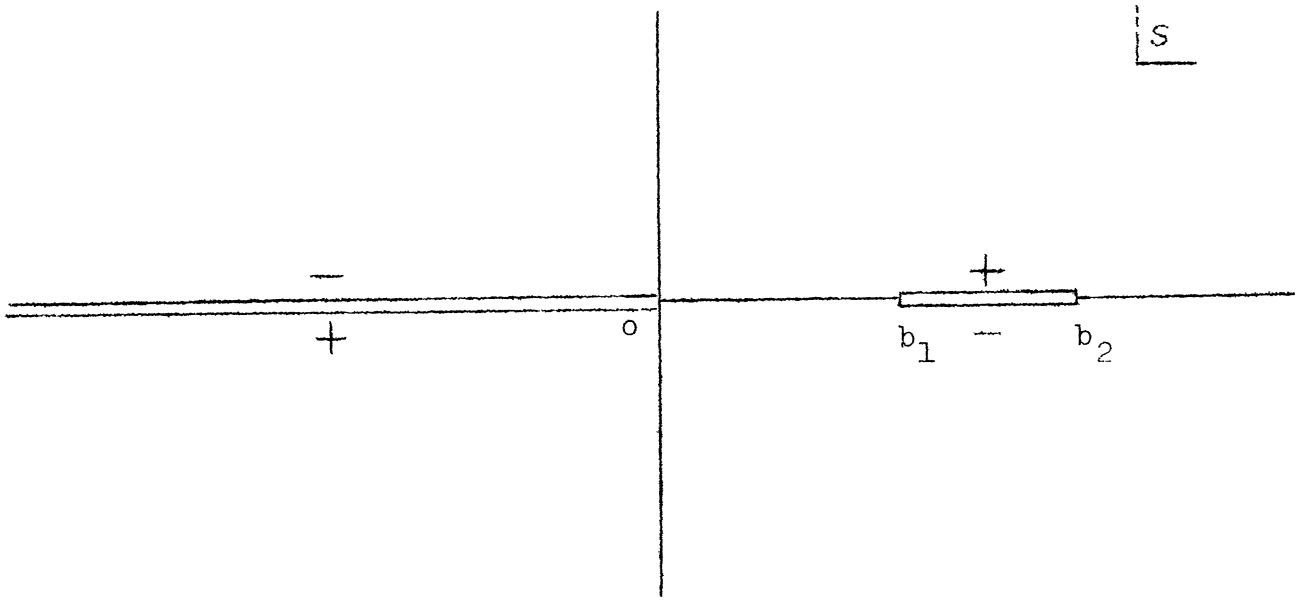

Fig. 10: Left-hand discontinuities due to ρ_1 exchange.

$$b_1 = 2M^2 + 2m^2 - m_A^2 , \quad b_2 = (M^2-m^2)^2/m_A^2 .$$

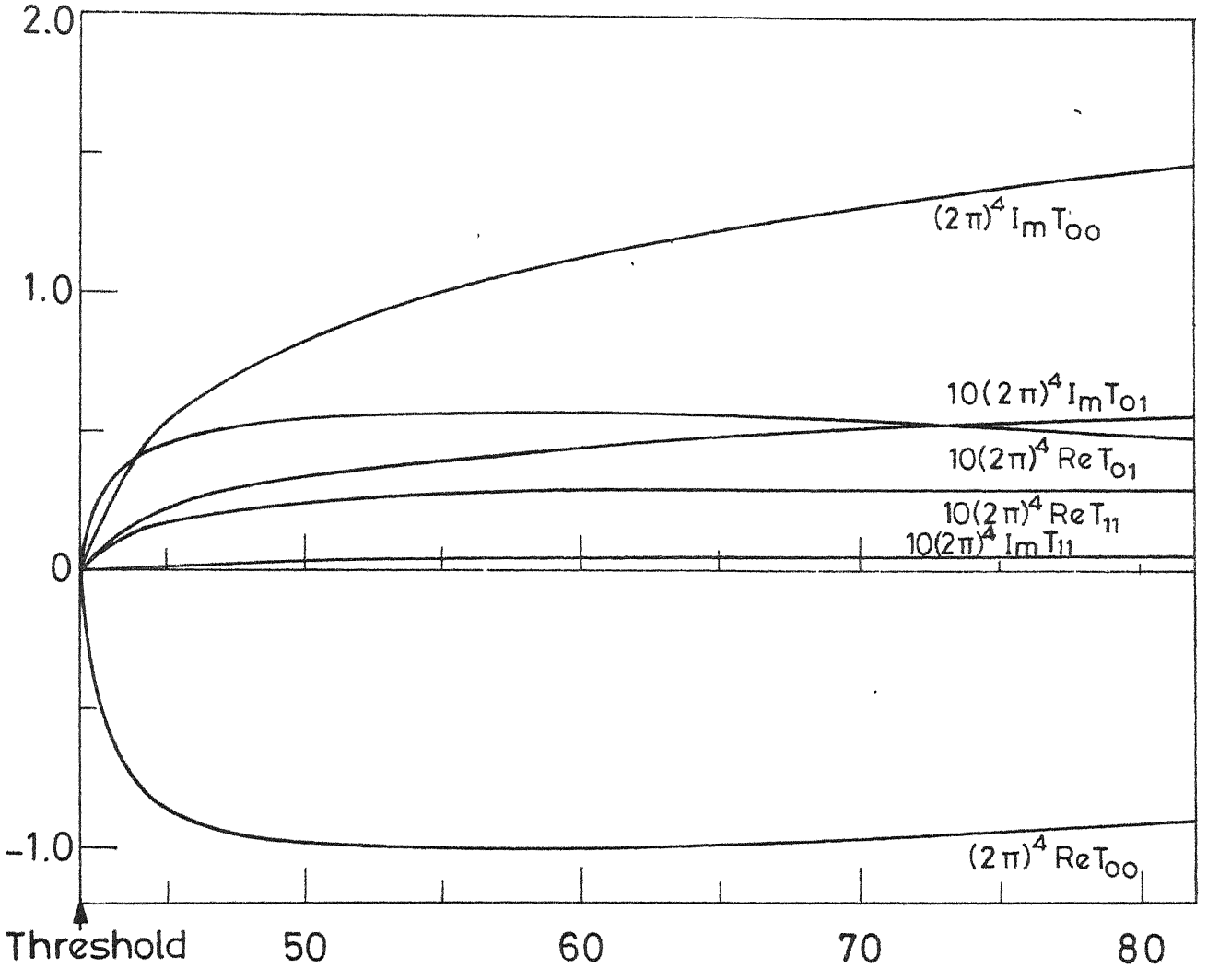

Fig. 11 $(2\pi)^4 T_{\alpha\beta}$ obtained by solving N/D equations in Bardakci model.

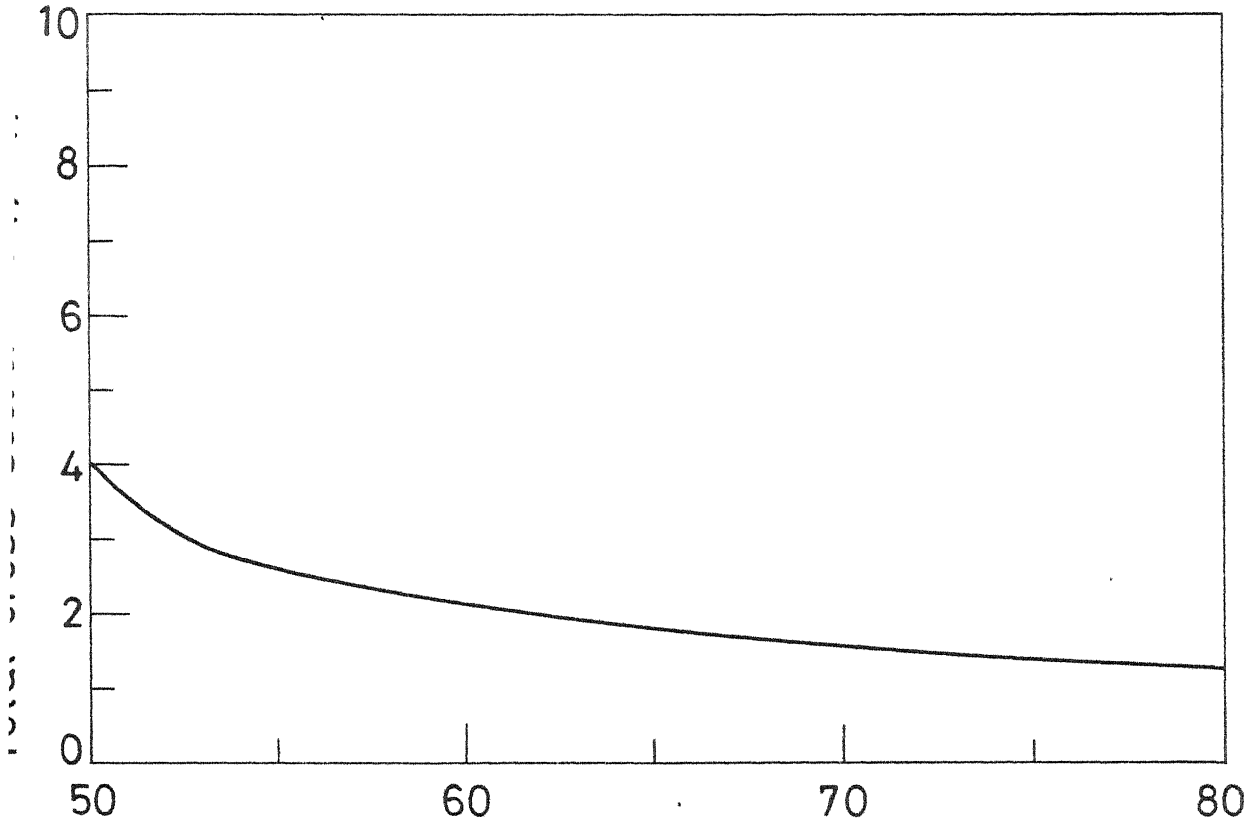

Fig. 12 Cross-section (in pion mass units) as a function of s obtained from amplitudes of fig. 11. A_1 mass region is about s = 62.

In the above calculation we have checked the following points carefully:

(i) $D_{\alpha\beta}(s)$ is a conjugate symmetric function in its domain of analyticity, in particular, real on the negative real axis. We find that in a typical calculation the ratio of imaginary part to the real part of $D_{\alpha\beta}(s)$ on negative real axis is of the order of 10^{-10}.

(ii) $N_{\alpha\beta}(s)$ is real on the right hand cut. The ratio of imaginary part to real part is less than 10^{-7} in a typical case.

(iii) $T_{\alpha\beta}(s)$ is symmetric to a great extent. In the calculations done with the model of Chapter Two, the maximum value of $|T_{10} - T_{01}| \; / \; |T_{10} + T_{01}|$ is less than .05. This is indeed quite good when we realise that our calculation is quite coarse, with only six points on the left hand cut for gaussian quadrature. For calculation with the Bardakci model, however, the symmetry is not so good. The corresponding ratio is of the order of .15. We realise that the symmetry of $T_{\alpha\beta}$ depends on the exact analytic properties[57] of D and N. With additional cuts due to A_1 exchange, and their approximation numerically, it is understandable that symmetry is not so good. We could have improved it by making the computation finer; but we have not done so.

(iv) Unitarity condition for the amplitudes is very well satisfied. We have calculated the two eigenvalues x_1 and x_2 of $S_{\alpha\beta} = 1 + i\,(2\pi)^4\, T_{\alpha\beta}$ as a function of s, and found that their modulus is very near 1. For example, for amplitudes shown in Fig. 8 the maximum difference of $|x_1|$ or $|x_2|$ from 1 is less than .06, for amplitudes shown in Fig. 11, it is less than .02.

In the end, we would like to emphasize that our aim in the above calculation has been to see whether the lowest order $\rho\pi$ amplitudes in gauge theories when unitarized by N/D formalism produce a resonant behaviour for A_1. We find that they do not. It is possible to do this calculation at much more sophisticated level, for example, by continuing in the mass-variable of ρ to take account of its being unstable. We have not done that. Another shortcoming of the present calculation related to the previous one is that we have assumed elastic unitarity for $\rho\pi$ scattering. Over and above all these, there is of course the question whether the lowest order amplitudes in perturbation theory with strong coupling are any good as input, that is, any approximation at all to the real amplitudes. Our hope is that at least qualitative features of strong interactions are not lost in perturbation theory.

CHAPTER FIVE

In this chapter we shall briefly review the various attempts to study the high energy behaviour of Feynman diagrams in field theory. To a limited extent we shall also discuss the calculational methods used to determine the asymptotic behaviour.

5.1 HIGH ENERGY BEHAVIOUR OF FEYNMAN DIAGRAMS IN PERTURBATION THEORY: MOTIVATION

In any theory it is of interest to find the behaviour of physical quantities of interest as some variables, on which it depends, take on limiting values. It is all the more so in perturbation theory because there is a possibility that, order by order, some regularity may be found, which can be generalized to all orders and some meaningful statement may be made about the total amplitude.

A considerable impulse to study the high-energy behaviour of amplitudes in quantum field theory came from the generalization[62-65] of Regge's fundamental work[66,67] in non-relativistic potential scattering. Regge's result, generalized to relativistic case, avoids the usual difficulty of bad high energy behaviour in field theory when higher

spin particles are exchanged, by providing a high energy behaviour of the type $c(t)s^{\alpha(t)}$. If for physical values of the momentum transfer $\alpha(t)$ can decrease to a value ≤ 1, the high energy behaviour is good. One can conjecture that all bound and resonant states are Regge poles. Experimentally, such a hypothesis has fared very well. Theoretically, one may try to see whether high energy behaviour of the Regge type is obtained in the amplitudes in field theory. When a given elementary particle - by which we simply mean a particle described by a field in the theory -- does exhibit such a behaviour we can generally say that it 'Reggeizes'.

It was shown by Gell-Mann and Goldberger[68] that the nucleon cannot be treated as a Regge pole if we consider nucleon-pion interaction of the ps-ps type. However, if we replace the pion by a neutral vector meson, then the nucleon, upto second order considered by them, Reggeizes. Apart from the characteristic high energy behaviour, there are other conditions to be satisfied for a particle to be a Regge pole. The conditions have been widely discussed[69-77] but we shall not go into the details.

Because of its simplicity, a considerable attention has been paid to the $\lambda\phi^3$ theory to study its high energy behaviour. It was found that in a three boson field theory, the Bethe-Salpeter amplitudes in the ladder approximation give

Regge-behaviour.[78] The same is the case with scattering amplitudes[79,80] for some special classes of diagrams. Later, Regge behaviour was obtained for even wider class of diagrams[81-84]. It was pointed out by Trueman and Yao[85] that merely summing the series of leading terms of each order is not sufficient, as was done by previous authors. Sometimes the next to leading order amplitude, when summed to all orders in the coupling constant, destroys the Regge behaviour. However, when all graphs of a well defined class are added, the Regge behaviour is restored.[86]

It must be emphasized that Regge behaviour obtained by summing ladders or other suitably chosen subclass of diagrams was only a partial success. Regge pole model is, after all, based on an intuitive generalization of non-relativistic potential scattering. There are other models which also have their roots in potential theory. For example the so-called 'droplet' model[87-89] or eikonal model.[90] These models predict high energy behaviour different from Regge behaviour. To test whether these generalizations from non-relativistic domain are justified, one can study the field theory and see what it predicts. The most well established theory both theoretically and experimentally, is, of course, quantum electrodynamics. In a series of papers[91-95] Cheng and Wu thoroughly examined the high energy behaviour of

various processes in quantum electrodynamics. They found that the forward elastic electron-electron, electron-positron, electron-photon and photon-photon scattering amplitudes with two photon exchange at large s go like sf(t) at fixed t. This result was generalized to include multiphoton exchange processes[96-98]. It was found that it is neither the Regge-type behaviour, nor the droplet model form that emerges[99-105]. The asymptotic amplitude cannot be reconciled with Regge-form without introducing complications, in particular, the Pomeranchuk trajectory cannot be a pole with factorizable residues. The result can rather be described in terms of the 'impact diagrams' which represent the high energy process.[106]

Recently there has been a revival of interest in the study of high energy behaviour of field theories. To a large extent it is due to the realization that spontaneously broken gauge theories are renormalizable, and therefore one expects a good high energy behaviour in them. In 1974, Nieh and Yao[107] pointed out some miraculous cancellations that take place in higher order diagrams of a Yang-Mills theory, as a result of which the high energy behaviour is like $s\ln^3 s$ and $s\ln^5 s$ to sixth and eighth order respectively. This result seems to be in error, as was pointed out by McCoy and Wu[108,109] the behaviour is even better than that! The leading part to

sixth order goes not as $s\ln^3 s$ but as $s\ln^2 s$. A number of calculations[110-112] have since been done and verified the latter result. Tyberski[110] has found that in fermion-fermion scattering, the amplitude upto sixth order can be written as the first three terms of

$$T = T_{Born} \left(\frac{s}{m^2}\right)^{-F(t)} \tag{5.1}$$

where,

$$T_{Born} = \frac{g^2}{8} \frac{1}{\mu^2-t} \cdot \frac{s}{m^2} (\lambda_a)_{i_1,i_3} (\lambda_a)_{i_2,i_4}$$

$$F(t) = \frac{g^2}{8\pi^2} (\mu^2-t) \int_0^1 d\alpha_1 \int_0^1 d\alpha_2 \frac{\delta(\alpha_1+\alpha_2-1)}{(-t)\,\alpha_1\alpha_2 + \mu^2 - i\varepsilon}$$

and λ_a's are isospin matrices.

This is typical Regge behaviour. Thus the result suggests that the vector boson in renormalizable non-Abelian gauge theory lies on a Regge trajectory with $\alpha(t) = 1-F(t)$ which becomes 1 at $t = \mu^2$, the vector boson mass. There is further support obtained from the study of factorization properties of amplitudes.[113]

A similar result is found by Lo and Cheng[111] upto eighth order in fermion-fermion scattering and by Yeung[112] upto eigth order in both fermion-fermion and boson-boson scattering. In particular the existence of Regge trajectory is seen to be insensitive to the details of spontaneous

symmetry breaking as Yeung has verified by calculating in several models. But that does not mean that spontaneous symmetry breaking is irrelevant. On the contrary, in all these calculations the entire machinery of spontaneous symmetry breaking is required to produce the subtle cancellations necessary for Reggeization to occur in non-Abelian gauge theory.

In conclusion, it seems that non-Abelian gauge theories have very interesting high energy behaviour and open up a place to study qualitative phenomena at high energy which may be of value for providing some insight into the hadron interactions.

5.2 HIGH ENERGY BEHAVIOUR OF FEYNMAN DIAGRAMS: METHOD

In this section we shall discuss briefly the calculational methods used for obtaining the high energy behaviour of Feynman diagrams.

First, for simplicity consider the $\lambda\phi^3$ theory. The amplitude corresponding to a Feynman diagram can generally be written down[114,115] in terms of Feynman parameters α after the loop integrals have been performed as

$$F(s,t) = \int_0^1 \int_0^1 d\alpha_1 .. d\alpha_I \cdot \frac{[c(\alpha)]^{L-1}}{[D(s,t,\alpha)]^{I+1}} \delta(\sum \alpha - 1) \tag{5.2}$$

where, $D(s, t, \alpha)$ is of the form

$$D(s, t, \alpha) = f(\alpha)\, s + g(\alpha)t + h(\alpha) \qquad (5.3),$$

L is the number of loops and I the number of internal lines.

In (5.3), f, g and h are polynomials in $\alpha_1, \ldots, \alpha_I$. Evidently, for any $\varepsilon > 0$, the region of integration in α space defined by $|f(\alpha)| > \varepsilon$ gives an asymptotic contribution of the form s^{-L-1}. Thus the strongest asymptotic contribution for $s \to \infty$ comes from an arbitrarily small neighbourhood of the surface defined by $f(\alpha) = 0$. Tiktopoulos[80] has used this fact to evaluate the asymptotic behaviour of $\lambda\phi^3$ theory. By his method the asymptotic behaviour can be directly obtained from the topological properties of the diagram, because $f(\alpha)$ will depend on parameters α accordingly.

One can apply the technique of Mellin transforms with great advantage to determine the asymptotic behaviour. This was done by Bjorken and Wu[84], Trueman and Yao[85] and Polkinghorne[8(

The situation becomes a little complex when one considers spin. The straightforward application of the methods used for spinless case lead to quite involved formulas[116,117]. New techniques have to be used and here the network analogy and graph theory have been found to be very useful.[118-120]

Intimately connected with the problem of finding the asymptotic behaviour of a particular diagram is the problem of classifying the diagrams according to their asymptotic behaviour. With increasing order in perturbation theory, the number of diagrams increases. We shall not discuss the details of beautiful topological methods devised by Tiktopoulos[80] and Lam and Lebrun[118].

In gauge theories we have a three fold increase in the complexity of the problem compared to spinless case: (i) there is complication due to spin (ii) due to derivative couplings and (iii) there are enormous number of diagrams because of a large number of couplings.

It is here that the 'infinite momentum technique' or the 'momentum space technique', first used by Chang and Ma[97] and later amply used by McCoy and Wu[109], comes very handy. As we shall use a variant of this method in the next chapter, it may not be out of place to illustrate this method by a simple example.

Suppose the amplitude is written,

$$\int \frac{F(p,k)}{\prod_i [(p_i + k)^2 - m_i^2 + i\varepsilon]} d^4k \qquad (5.4)$$

where p's are external momenta and k is internal momentum. For fixed momentum transfer and large s, the external

momenta will have high momentum in, say, +z or -z direction. If p has high momentum in +z direction then $p^+ = p^0 + p^3 = O(\sqrt{s})$ and $p^- = p^0 - p^3 = O(1/\sqrt{s})$. Similarly for other momenta (See Appendix Four).

Write,

$$(p_i+k)^2-m_i^2 + i\varepsilon = (p_i^+ + k^+)(p_i^- + k^-) - (\vec{p}_{i_\perp} + \vec{k}_\perp)^2 - m_i^2 + i\varepsilon \qquad (5.5).$$

One now puts a cut-off on $\vec{k}_\perp$ and integrates over k^+ keeping k^- fixed, closing on the poles of the integrand of (5.4) at

$$k_{(i)}^+ = ((\vec{p}_{i_\perp} + \vec{k}_\perp)^2 + m_i^2 - i\varepsilon)/(p_i^- + k^-) \qquad (5.6)$$

The main point is that p_i^- are all either of $O(\sqrt{s})$ or $O(1/\sqrt{s})$. Therefore for k^- greater than the greatest of p_i^- all poles (5.6) lie below the real line in k^+ plane, and, for all k^- less than the smallest of p_i^-, above. Thus only for k^- in a finite region, when some poles lie above and some below the real axis, that the contribution of k^+ integral is non-zero. The k^+ integration performed - it is just a matter of collecting residues - the k^- integration ranges over a finite segment. One now expresses the asymptotic expansion of the integral, which is obtained easily as we have a single integral over a finite range, $\vec{k}_\perp$ still having the cut-off. (In the general

case we have a finite L-tuple integral if there are L integration momenta. Compare this with Feynman parameter method where there is one parameter for each internal line). After the limit $s \to \infty$ is taken and asymptotic formula obtained, one lets $\vec{k}_\perp$ go to ∞. Usually, even if $\int d\vec{k}_\perp$ are divergent for individual diagrams, divergences cancel on adding all diagrams of a given order.

This method has obvious lack of rigour. In particular, $s \to \infty$ being taken before $\vec{k}_\perp$ integration cannot be justified mathematically. However, so far the calculations based on it have given consistent results[121]. Because of its enormous simplicity it has recently been applied with great success in formion exchange process in massive electrodynamics to calculate asymptotic behaviour of amplitude upto 12th order.[122]

5.3 REMARKS:

We shall make a few remarks before concluding this chapter.

In the above brief review of an extensive literature, we have omitted works on high energy behaviour where the limit $s \to \infty$ is taken without keeping t constant. These omissions include the very important work of Weinberg[123] and its elaboration[124-126]. They consider the limit when all the four components of the four momentum become high. Similarly,

we have omitted the works on fixed angle high energy behaviour.[127]

In sections 5.1 and 5.2 we have described the high energy behaviour of two particle elastic scattering. We have not been able to find much discussion of high energy behaviour of production amplitudes. Halliday and Polkinghorne[128] considered bosons interacting via Yukawa interaction. By summing ladders they find Regge pole behaviour of production amplitudes. The asymptotic amplitude depends on the way kinematic variables are taken to infinity. Cheng and Wu[129] have studied the high energy pair production and bremsstrahlung in quantum electrodynamics. Their results confirm the 'impact picture' they found by studying the high energy scattering process in quantum electrodynamics.

In the next chapter we shall use a variant of the momentum-space technique to study in detail the high energy behaviour of scattering as well as one particle production amplitude at the one-loop level.

CHAPTER SIX

In this chapter we shall discuss a general formalism for the asymptotic behaviour of one-loop scattering and one particle production Feynman diagrams. In section 6.1 we express the scattering amplitude in terms of asymptotic parameters keeping the transverse part of integration momentum fixed. In 6.2 topological properties of one-loop scattering diagrams are discussed, and one-loop diagrams are divided into five classes A, B, C, D, E. A theorem is proved in this section for diagrams of class (A), which greatly facilitates the determination of their asymptotic behaviour, discussed in section 6.3. We discuss the asymptotic behaviour of diagrams of other classes in section 6.4.

In section 6.5 we consider one-loop production graphs. As in the case of scattering graphs, they are classified, and for graphs of class analogous to the class (A) of scattering graphs, an analogous result is proved. The asymptotic behaviour is obtained for production graphs in section 6.6.

The results obtained in this rather long chapter are summarised in section 6.7.

6.1 GENERAL EXPRESSION FOR THE AMPLITUDE OF ONE LOOP DIAGRAMS:

In general the amplitude M for a given one-loop Feynman diagram can be written in the form

$$M = \int d^4k \; n d^{-1} \tag{6.1}$$

where n is a polynomial in the external momenta and the internal momentum k, and d is of the form,

$$d = \prod_{i=1}^{N} [(p_i + k_i)^2 - m_i^2 + i\varepsilon].$$

Here N is the number of internal lines, p_i is the flow of external momentum in the i-th line, and k_i is the flow of internal (or loop) momentum through the i-th line. As there is only one loop, k_i is of the form,

$$k_i = \sigma_i k$$

where $\sigma_i = 0$ or ± 1.

It is important to emphasize here that the line for which $\sigma_i = 0$ gives an explicit dependence on external momenta, and therefore the factor $(p_i^2 - m_i^2)^{-1}$ can be conveniently included in the numerator as far as our analysis is concerned. It has the advantage that $(p_i^2 - m_i^2)$ gives us the complete dependence on s, and not an approximation which it might in the general analysis. However, in the following analysis we donot make this assumption, though for calculation we shall always factor out such explicit dependence.

As shown in Appendix Four, the longitudinal parts $p^{\pm}$ of external momenta can be written as,

$$p_i^{\pm} = \sqrt{s}\ \lambda_i^{\pm} + \frac{1}{\sqrt{s}}\ \mu_i^{\pm}$$

where $\lambda_i^{\pm}$ are real constants and $\mu_i^{\pm}$ are functions of p_i which tend to a constant as $s \to \infty$.

Introducing parameters α_i for the internal lines, we can write d^{-1} in the usual manner as,

$$d^{-1} = (-i)^N \left(\prod_{i=1}^{N} \int_0^{\infty} d\alpha_i\right) \exp\left[i \sum_{i=1}^{N} \alpha_i \left((p_i + k_i)^2 - m_i^2 + i\varepsilon\right)\right] \qquad (6.2)$$

Writing,

$$\sum_{i=1}^{N} \alpha_i \left[(p_i + k_i)^2 - m_i^2 + i\varepsilon\right]$$

as

$$\sum_i \alpha_i\, p_i^{+}\, k_i^{-} + \alpha k^{+}k^{-} + k^{+}\beta^{-} + k^{-}\beta^{+} - \sum_i \alpha_i \left(\Delta_i^2 - i\varepsilon\right) \qquad (6.3)$$

where

$$\beta^{\pm} \equiv \sum_i \alpha_i\, \sigma_i\, p_i^{\pm},$$

$$\alpha \equiv \sum_i (\sigma_i)^2\, \alpha_i,$$

and

$$\Delta_i^2 = (\vec{p}_{i\perp} + \sigma_i \vec{k}_\perp)^2 + m_i^2 .$$

Let the numerator n in (6.1) be written as,

$$n = \sum_{mm_+m_-} a_{mm_+m_-} (\sqrt{s})^m (k^+)^{m_+} (k^-)^{m_-} \qquad (6.4),$$

where m, m_+, m_- are integers and $a_{mm_+m_-}$ are functions of external momenta and $\vec{k}_\perp$ which are of $O(1)$ as $s \to \infty$ with t remaining constant.

With these expressions for n and d^{-1}, (6.1) becomes,

$$M = \frac{1}{2} \sum_{mm_+m_-} \int d^2\vec{k}_\perp \int dk^+ \int dk^- \left(\prod_i d\alpha_i \right)$$

$$\cdot a_{mm_+m_-} (\sqrt{s})^m (k^+)^{m_+} (k^-)^{m_-} \exp\left[i \sum_i \alpha_i p_i^+ p_i^- \right.$$

$$\left. + i\alpha k^+ k^- + ik^+\beta^- + ik^-\beta^+ - i \sum_i \alpha_i (\Delta_i^2 - i\varepsilon) \right] \qquad (6.5)$$

We put a cut-off on the transverse part $\vec{k}_\perp$ of loop momentum and integrate over k^+ and k^-, using,

$$\int dk^+ (k^+)^{m_+} \exp\left[ik^+(\alpha k^- + \beta^-) \right] = 2\pi(-i)^{m_+} \delta^{(m_+)}(\alpha k^- + \beta^-)$$

and

$$\int dk^- F(k^-) \delta^{(m_+)}(\alpha k^- + \beta^-) = (-1)^{m_+} \alpha^{-1} \left(\frac{\partial}{\partial \tilde{k}}\right)^{m_+} \tilde{F}(\tilde{k}) \Big|_{\tilde{k}=\beta^-}$$

where

$$\tilde{k} = \alpha k^- + \beta^-$$

and

$$\tilde{F}(\tilde{k}) = F\left(\frac{\tilde{k} - \beta^-}{\alpha} \right) .$$

The result is

$$M = \sum_{mm_+m_-} \sum_{r=0}^{\min(m_+,m_-)} \int d^{2\vec{k}} \left(\prod_i d\alpha_i \right) x$$

$$x\, C_{mm_+m_-r} (\alpha)^{r-m_+-m_-1} (\beta^-)^{m_--r} (\beta^+)^{m_+-r}$$

$$x\, (\sqrt{s})^m \exp i\Big[\sum_i \alpha_i p_i^+ p_i^- - \alpha^{-1} \beta^+ \beta^-$$

$$- \sum_i \alpha_i (\Delta_i^2 - i\varepsilon)\Big] \qquad (6.6),$$

where

$$C_{mm_+m_-r} \equiv \pi(-i)^N (-1)^{m_++m_-} (i)^r \frac{m_+!\ m_-!}{r!\ (m_+-r)!\ (m_--r)!}$$

$$x\ a_{mm_+m_-} \qquad (6.7)$$

6.2 CLASSIFICATION OF ONE-LOOP SCATTERING DIAGRAMS:

When we consider the high energy behaviour of a scattering graph for a process $\underline{1} + \underline{2} \to \underline{3} + \underline{4}$, we find that it depends crucially on the way in which the external momentum can be distributed in the graph. As shown in Appendix Four, when $s \to \infty$ and t remains fixed, the $p^+ = p^0 + p^3$ component of external momenta corresponding to particles $\underline{1}$ and $\underline{3}$, is very large (of the order $\sqrt{s}$). Similarly, the p^- component of $\underline{2}$ and $\underline{4}$ is of order $\sqrt{s}$. The conservation of external momentum at each vertex demands that there should be a continuous path from the external line corresponding to particle $\underline{1}$ to that

corresponding to $\underline{3}$ such that only on lines i of this path p_i^+ is of order $\sqrt{s}$. Similarly, there exists a path from external line $\underline{2}$ to $\underline{4}$ such that only on lines of this path p_i^- is of order $\sqrt{s}$. We shall call these paths as $\underline{1}$-$\underline{3}$ - path and $\underline{2}$-$\underline{4}$-path.

For a particular graph the way its amplitude behaves as $s \to \infty$ depends, among other things, on how the $\underline{1}$ - $\underline{3}$ - path and $\underline{2}$ - $\underline{4}$ - path can be chosen. The topological properties of these paths are characterized by numbers $\lambda_i^{\pm}$ and σ_i.

For our purpose we can classify the one loop scattering graphs as graphs for which it is possible to choose the flow of external momenta in such a way that,

(A) $\lambda_i^+ \lambda_i^- = 0$ for all i, and there exists k and j such that $\sigma_k \lambda_k^+ \neq 0$ and $\sigma_j \lambda_j^- \neq 0$,

(B) $\lambda_i^+ \lambda_i^- = 0$ for all i, but either $\sigma_k \lambda_k^+ = 0$ for all k or $\sigma_j \lambda_j^- = 0$ for all j or both,

(C) there exists an i with $\lambda_i^+ \lambda_i^- \neq 0$, and either $\sigma_k \lambda_k^+ = 0$ for all k or $\sigma_j \lambda_j^- = 0$ for all j.

(D) there is an i such that $\lambda_i^+ \lambda_i^- \neq 0$, $\sigma_i \lambda_i^+ \lambda_i^- = 0$ for all i, and there exist k and j with $\sigma_k \lambda_k^+ \neq 0$ and $\sigma_j \lambda_j^- \neq 0$.

(E) there exist lines i, k, j such that, $\sigma_i \lambda_i^+ \lambda_i^- \neq 0$, $\sigma_k \lambda_k^+ \neq 0$, $\sigma_j \lambda_j^- \neq 0$.

As the source and sink of high (i.e. of order $\sqrt{s}$) p^+ or p^- momentum is fixed, the arbitrariness in the choice of distribution of external momenta comes only from choosing the internal momentum in different ways, which can be removed by a translation of the integration variable k. Thus the above classification is in fact independent of the actual distribution of momenta in the internal lines. Put differently, and, perhaps, in a less clumsy manner, the diagrams of class (A) to (D) correspond to those in which

(A) paths $\underline{1} - \underline{3}$ and $\underline{2} - \underline{4}$ can be chosen to have no line common to them (we call the paths $\underline{1} - \underline{3}$ and $\underline{2} - \underline{4}$ to be 'disjoint' in such a case, though they may have vertices common to them), and both the paths have at least one line of the loop.

(B) Paths $\underline{1} - \underline{3}$ and $\underline{2} - \underline{4}$ can be chosen to be disjoint and at least one of them does not pass through the loop, i.e. does not have a line belonging to the loop.

(C) $\underline{1} - \underline{3}$ and $\underline{2} - \underline{4}$ cannot be chosen to be disjoint, but the line they have common can be chosen to not to belong to the loop. Also, at least one of the two paths does not pass through the loop.

(D) $\underline{1} - \underline{3}$ and $\underline{2} - \underline{4}$ both pass through the loop and have necessarily a common line, though the common line does not belong to the loop.

(B) In whatever way the paths $\underline{1}$ - $\underline{3}$ and $\underline{2}$ - $\underline{4}$ are chosen, they pass through the loop and have a line common which belongs to the loop.

Typical diagrams of class (A) to (B) are shown in Figs. 13-16.

We shall see that the most important class, as for as leading high energy behaviour is concerned, is the class (A). For one-loop graphs of this class we have the following theorem.

Theorem: For graphs of class (A) there is exactly one k and one j with $\sigma_k \lambda_k^+ \neq 0$ and $\sigma_j \lambda_j^- \neq 0$.

Proof: Let us suppose that there are k and k' for which $\sigma_k \lambda_k^+ \neq 0$ and $\sigma_{k'} \lambda_{k'}^+ \neq 0$. Then lines k and k' both lie on the $\underline{1}$ - $\underline{3}$ path. As σ_k and $\sigma_{k'}$ are non -zero k, k' also belong to the loop. Similarly, line j belongs to the $\underline{2}$ - $\underline{4}$ path as well as the loop. Since a path is always linearly ordered, the lines in the path $\underline{1}$ .. $\underline{3}$ get divided into three sets, those that lie between line $\underline{1}$ and, say, k; those between k and k', and those between k' and $\underline{3}$. If there is no line between k and k', then k and k' have a common vertex v. Lines $\underline{1}$ and $\underline{3}$ cannot be incident on v. Nor can any other loop line do the same, as there are two and only two loop lines at any vertex in a loop and k and k' are already incident on v. Thus j, being a loop line, does not join v. Since k, k' and j

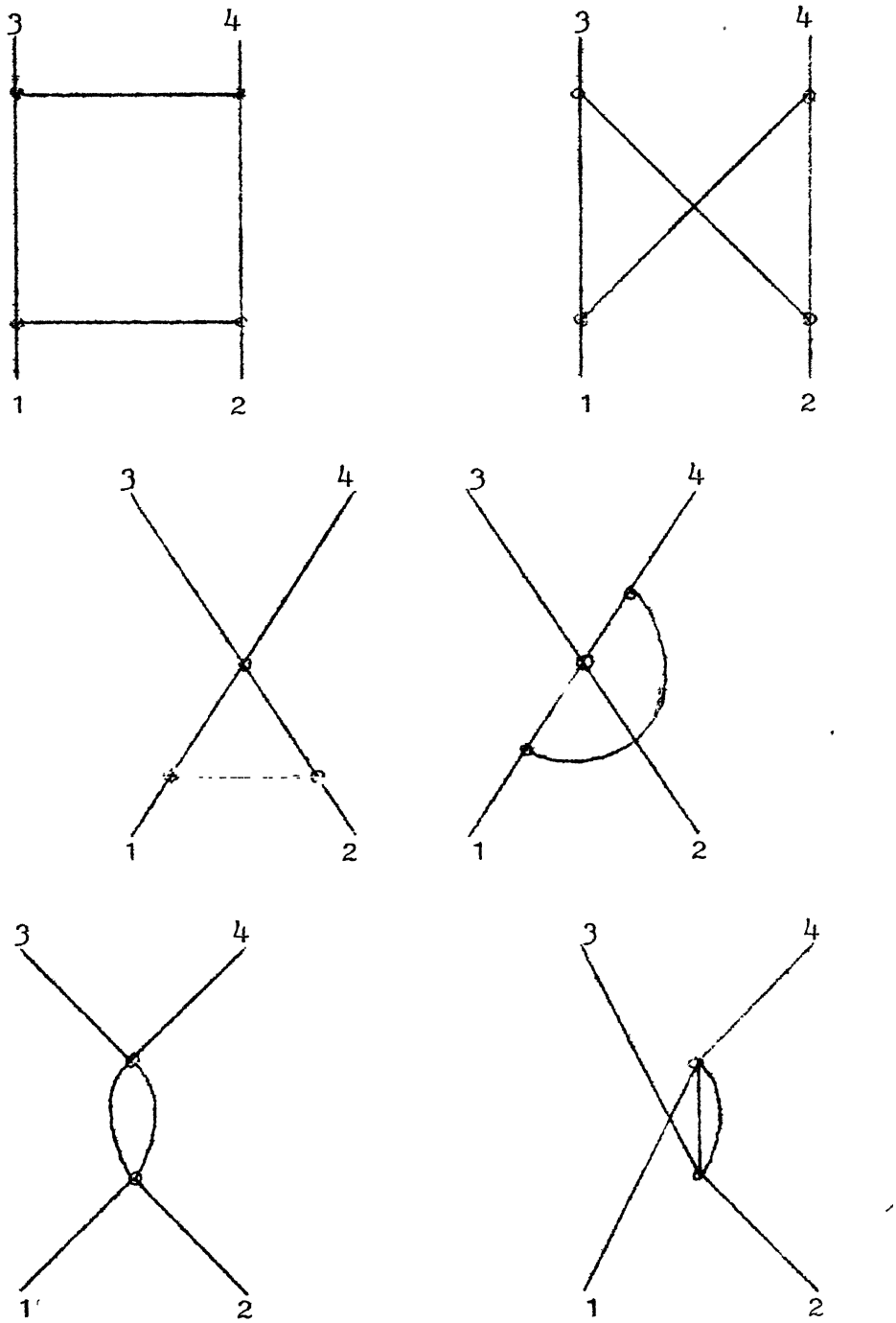

Fig. 13: Typical diagrams of class (A).

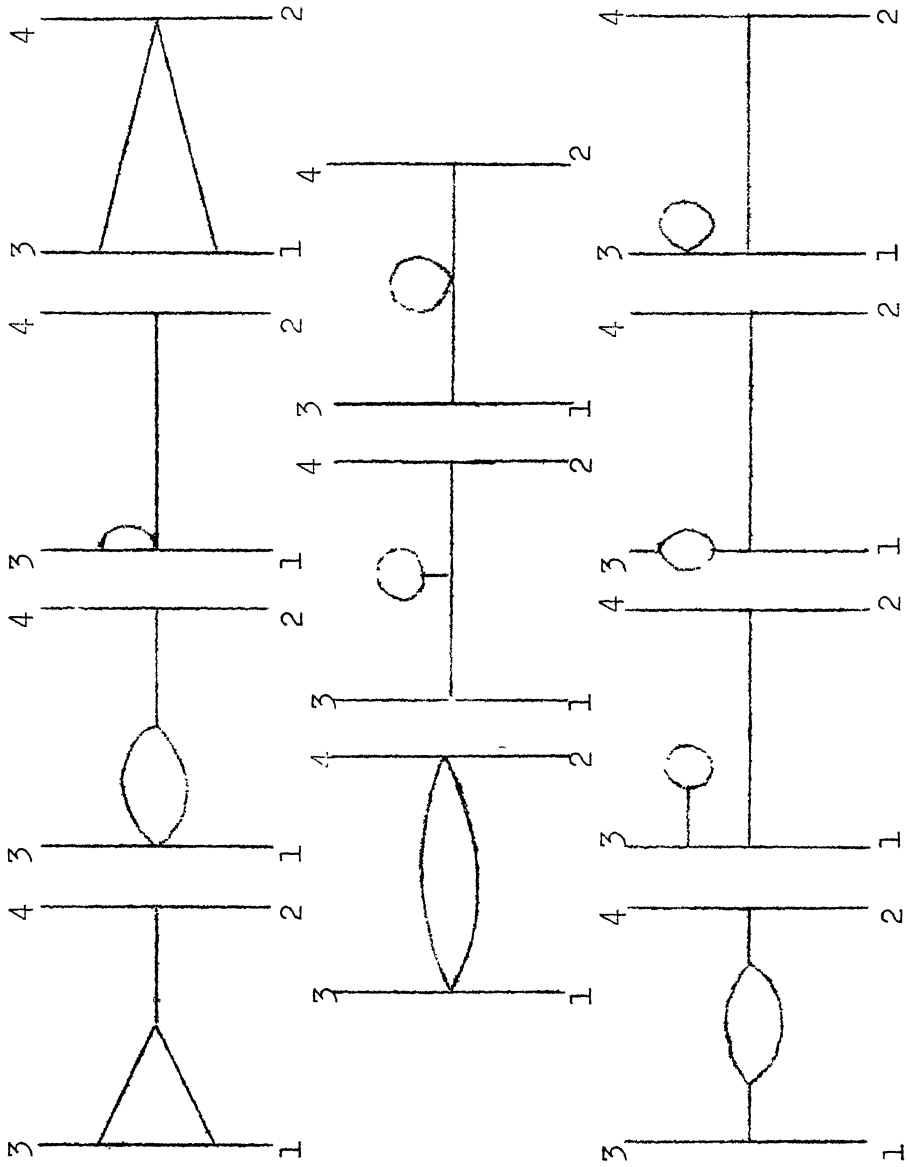

Fig. 14: Typical diagrams of Class (B).

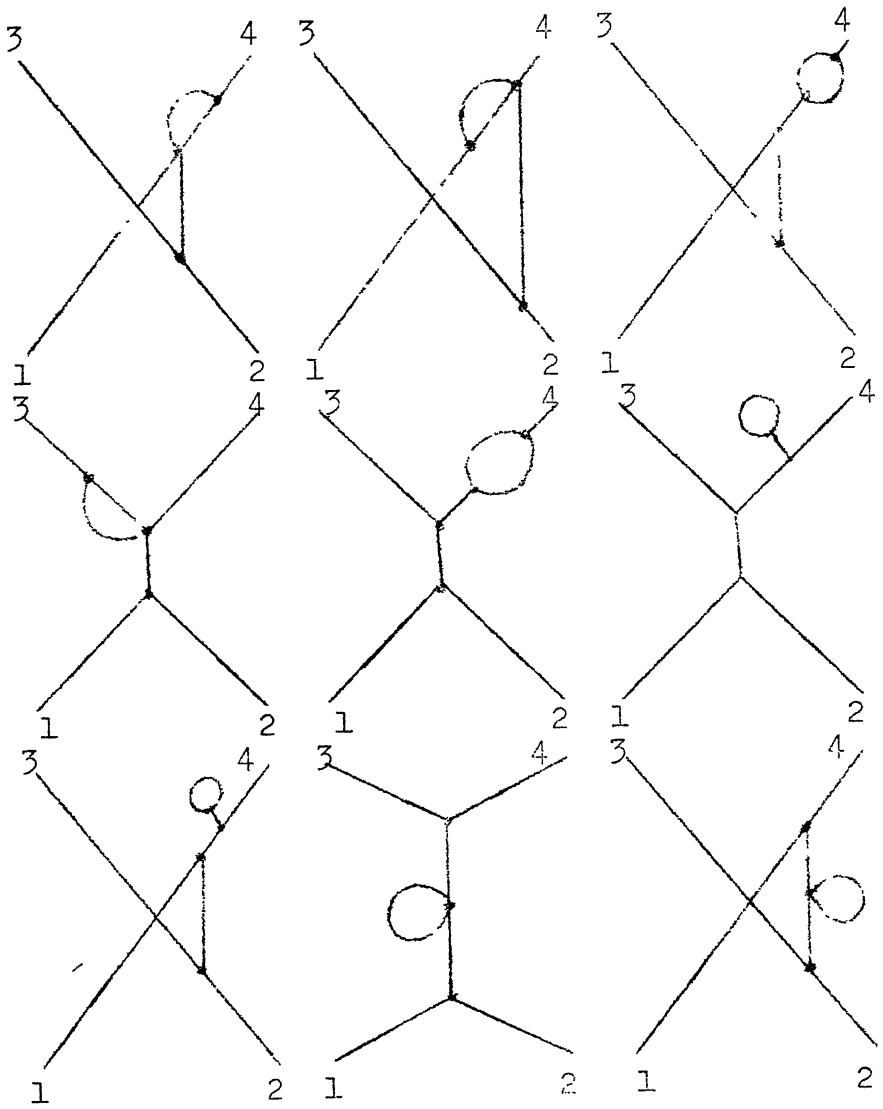

Fig. 15: Typical diagrams of Class (C).

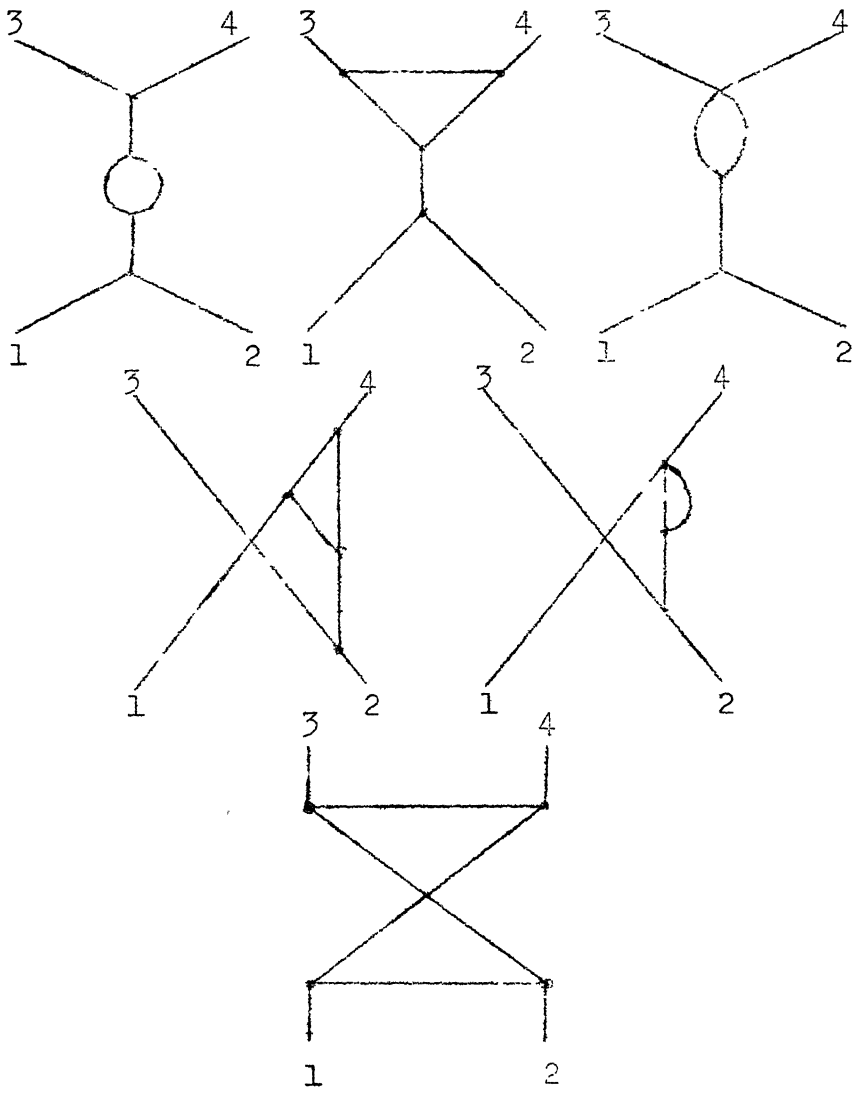

Fig. 16: Typical diagrams of Class (D) (first five) and the only diagram of Class (E).

all belong to the loop, all paths (and there are exactly two of them) joining v to either end point of j have to include either k or k'. As $\lambda_i^+ \lambda_i^- = 0$ for each i, $\underline{2}$ and $\underline{4}$ cannot be incident on v. Thus v cannot be joined to any external line by a path other than passing through k or k'. As none of the external line and none of the loop lines other than k and k' is incident on v, there is (for there have to be at least three lines incident on a vertex) a line ℓ without loop momentum incident on v. As both the ends of any internal line of a connected graph are joined to some external line by a path, the other end of ℓ can be joined to a vertex on which one of the external lines is also incident. Thus a path can be found from v to one of the external lines. If this path does not contain k or k', then we have shown the existence of an independent loop, namely joining v to say $\underline{1}$ through two paths; one including ℓ the other including k. If this path does contain k or k', then again, an independent loop exist, because v will fall again on the path, forming an independent loop. As there is only one loop in the diagram, the result follows (for this case).

When there exist lines between k and k' on the $\underline{1}$ - $\underline{3}$ path, there exist vertices v_k and $v_{k'}$ which are one of the end points of k and k' respectively, and on which $\underline{1}$ and $\underline{3}$ are not incident. v_k and $v_{k'}$ are connected by lines of $\underline{1}$-$\underline{3}$ pa

v_k and $v_{k'}$ are also connected by a path containing loop momentum as both of them belong to the loop. For a graph containing only one loop there can be just two independent paths containing two vertices of a loop, and both these paths carry loop momentum. Thus there exists a line k" distinct from k, carrying the loop momentum, belonging to $\underline{1} - \underline{3}$ path and incident on v_k. The argument of the previous paragraph applies here with vertex v_k as the vertex v of that paragraph. The result follows for this case too.

An exactly similar argument holds for there being just one j with $\sigma_j \lambda_j^- \neq 0$. The theorem is thus proved.

In the next section we shall find the asymptotic behaviour at high energy of the amplitude of a graph of class (A).

6.3 ASYMPTOTIC BEHAVIOUR OF ONE LOOP SCATTERING GRAPHS OF CLASS (A):

By the theorem proved in the previous section the amplitude (6.6) for a graph of class (A) takes the form,

$$M = \sum_{mm_+m_-r} \int d^2\vec{k}_\perp \left(\prod_i \int d\alpha_i \right) C_{mm_+m_-r}(\alpha)^{r-m_+-m_--1} (\nu_{kj})^{m_+-r} (\sigma_j \lambda_j^-)^{m_--m_+} (\alpha_k)^{m_+-r} (\alpha_j)^{m_--r} \times s^{M-r} \exp\left[-i\alpha^{-1} \nu_{kj} \sigma_k \alpha_j s - i \sum_i \alpha_i (\Delta_i^2 - i\varepsilon)\right] \tag{6.8}$$

where,

$$\nu_{kj} \equiv \sigma_k \lambda_k^+ \sigma_j \lambda_j^- \tag{6.8a}$$

is either +1 or -1, and

$$M \equiv \frac{1}{2}(m_+ + m_- + m) \tag{6.8b}$$

is an integer by Lorentz invariance of n. We have also neglected terms of order $1/\sqrt{s}$ in comparison to $\sqrt{s}$.

As $s \to \infty$, the contribution in (6.8) comes mainly from the neighbourhood of $\alpha_k = 0$, $\alpha_j = 0$. The asymptotic behaviour of (6.8) can be found out by using the Mellin transforms. (See Appendix Five for some useful formulas).

We note that the Mellin transform of a function like exp (-as) is .

$$\int_0^\infty \exp(-as)\, s^{z-1}\, ds = a^{-z}\, r(z) \tag{6.9}$$

where

$a > o.$

In (6.9) we can let a take complex values with Re $a > o$. However, the continuation of values for Re $a \leq o$ is not unambiguous because of the logarithmic branch cut, which, as is the common practice, we take along the negative real axis. In finding the asymptotic behaviour of the amplitude we encounter an expression like exp (ias) occuring inside an integral

over real values of a. Looking closely one finds that using the analytic property of the integrand one can shift the contours in such a way that exp (iαs) is brought to the form exp (-bs). One can then take the Mellin transform without ambiguity.

Coming back to (6.8) we realize that in the α-planes one can deform the contour $\alpha_i = (0, \infty)$ to any other between these points as long as Re $\alpha_i \geq 0$ and $I_m\ \alpha_i \leq 0$, for any i.

As the contribution at large s comes mainly from $\alpha_k \sim 0$ and $\alpha_j \sim 0$, we first neglect α_k and α_j in α. Next we discuss the cases when ν_{kj} > or < 0 separately.

6.3.1 $\nu_{kj} = -1$ OR THE CASE OF PLANAR GRAPHS:

In this case we rotate the contours ($0 \leq \alpha_i \leq \infty$; $i \neq k, j$) to run along the negative imaginary axis. Writing

$$\alpha_i = -iy_i,$$

we find that

$$M = \sum_{mm_+m_-r} \int d^{2\vec{k}_1} C^1_{mm_+m_-r} \left(\prod_i{}' \int_0^\infty dy_i \right)$$
$$\times (y')^{r-m_+-m_--1} \exp\left[-\sum_i{}' y_i \left(\Delta_i{}^2 - i\varepsilon \right) \right] \int_0^\infty d\alpha_k$$
$$\times \int_0^\infty d\alpha_j \, (\alpha_k)^{m_+-r} \, (\alpha_j)^{m_--r} \, s^{M-r} \exp\left[-(y')^{-1} \alpha_k \alpha_j s \right.$$
$$\left. -i\alpha_k \Delta_k{}^2 - i\alpha_j \Delta_j{}^2 \right] \qquad (6.10)$$

where,

$$C^{1}_{mm_+m_-r} \equiv C_{mm_+m_-r}\,(-1)^{m_+-r}\,(-i)^{N-2+r-m_+-m_--1}\,(\sigma_j\lambda_j^{-})^{m_--m_+}$$

$$= -i\pi\,(-1)^{N}\,(-i)^{m_++m_-}\,\frac{m_+!\;m_-!}{r!\,(m_+-r)!\,(m_--r)!}\,a_{mm_+m_-}$$

$$\times\,(\sigma_j\,\lambda_j^{-})^{m_--m_+}\;\;(-1)^{m_+-r} \qquad (6.10a),$$

$$y' \equiv \sum_i{}' \; y_i(\sigma_i)^2 \qquad (6.10b),$$

and a prime on $\prod_i$ or $\sum_i$ denotes that $i \neq k, j$.

The Mellin transform of (6.10) is

$$M(z) \equiv \int_0^\infty M\,s^{z-1}\,ds = \sum_{mm_+m_-r}\int d^2\vec{k}_\perp\; C^{1}_{mm_+m_-r}\left(\prod_i{}'\;\int_0^\infty dy_i\right)$$

$$= \exp\left[-\sum_i y_i\,(\Delta_i^{\,2}-i\varepsilon)\right]\,(y')^{z+M-m_+-m_--1}$$

$$\times\,(\Delta_k^{\,2})^{z+M-m_+-1}\,(\Delta_j^{\,2})^{z+M-m_--1}\;\;\Gamma(z+M-r)$$

$$\times\,\Gamma(-z-M+m_++1)\;\Gamma(-z-M+m_-+1)\;\exp\left[i\pi\left(z+M-\frac{m_++m_-}{2}-1\right)\right]$$

(6.11),

where in the above we have also carried out the α_k, α_j integrations.

6.3.2 $\nu_{kj} = 1$ OR THE CASE OF NON-PLANAR GRAPHS:

In this case we rotate all the contours $0 \leq \alpha_i \leq \infty$ to run along the negative imaginary axis, to get,

$$M = \sum_{mm_+m_-r} \int d^2\vec{k}_i \; C^2_{mm_+m_-r} \left(\prod_i{}' \int_0^\infty dy_i \right)$$
$$x \; (y')^{r-m_+-m_--1} \exp\left[- \sum_i{}' y_i \left(\Delta_i{}^2 - i\varepsilon \right) \right] \int_0^\infty dy_k$$
$$\int_0^\infty dy_j \; (y_k)^{m_+-r} \; (y_j)^{m_--r} \; s^{M-r} \exp\left[-(y')^{-1} \, y_k y_j s \right.$$
$$\left. - y_k \, \Delta_k{}^2 - y_j \, \Delta_j{}^2 \right] \qquad (6.12)$$

where

$$C^2_{mm_+m_-r} = i\pi \, (-1)^{m_++m_-} \, (-1)^r \, \frac{m_+! \; m_-!}{r!(m_+-r)!(m_--r)!} \, a_{mm_+m_-}$$
$$x \; (\sigma_j \lambda_j^-)^{m_- - m_+} (-1)^M \qquad (6.13).$$

The Mellin transform of (6.12) is

$$M(z) = \sum_{mm_+m_-r} \int d^2\vec{k}_i \; C^2_{mm_+m_-r} \left(\prod_i{}' \int_0^\infty dy_i \right)$$
$$x \exp\left[- \sum_i{}' y_i \left(\Delta_i{}^2 - i\varepsilon \right) \right] (y')^{z+M-m_+-m_--1}$$
$$x \; (\Delta_k{}^2)^{z+M-m_+-1} \; (\Delta_j{}^2)^{z+M-m_--1} \; \Gamma(z+M-r)$$
$$x \; \Gamma(-z-M+m_++1) \; \Gamma(-z-M+m_-+1) \qquad (6.14).$$

We are now in a position to discuss the asymptotic behaviour of expressions (6.11) and (6.14) which are, respectively the Mellin transforms of the amplitudes of planar and non-planar graphs of class (A). The asymptotic behaviour of M as $s \to \infty$, depends on the poles of (6.11) and (6.14) in the z plane.

According to the theorem quoted in Appendix Five, the leading asymptotic behaviour is determined by poles lying in the region

$$\mathrm{Re}(z+m-r) > 0 \qquad (6.15)$$

and having their real parts as small as possible.

The poles of $\Gamma(-z+M+m_{\pm}+1)$ lie at

$$z = n_{\pm} + 1 - M + m_{\pm} \qquad (6.16),$$

where $n_{\pm} = 0, 1, 2, \ldots$.

The poles (6.16) automatically satisfy (6.15) as $r - m_{\pm} \leq 0$. Of these poles, those which are left most will be called the 'contributing poles'. We have the following cases.

6.3.3 $m_+ < m_-$: THE CONTRIBUTING POLE IS AT $z = 1-M+m_+$:

The asymptotic expression for M, using the theorem given in Appendix Five, is

$$M \simeq \sum_{mm_+m_-r} (\sqrt{s})^{m+\Delta m-2} \int \ldots \int_{+} C^{3}_{mm_+m_-r} \times (\Delta_j^{\,2})^{-\Delta m} \left(\prod_i' \int_0^{\infty} dy_i \right) (y')^{-\max(m_+,m_-)} \exp\left[-\sum_i' y_i(\Delta_i^{\,2} - i\varepsilon) \right] \qquad (\nu_{kj} = -1) \qquad (6.17),$$

where,

$$\Delta m = |m_+ - m_-|,$$

$$C^{3}_{mm_+m_-r} \equiv -i\pi(-1)^{N}(-1)^{m_+ + m_- - r} (\sigma_j \lambda_j^{-})^{\Delta m} \times \frac{m_+!\, m_-!\, (\Delta m-1)!}{r!(\max(m_+,m_-)-r)!} a_{mm_+m_-} \qquad (6.18),$$

for $\nu_{kj} = -1$, and

$$M \simeq \sum_{mm_+m_-r} (\sqrt{s})^{m+\Delta m-2} \int d^2\vec{q}_\perp \; C^4_{mm_+m_-r}$$

$$\times (\Delta_j^2)^{-\Delta m} \left(\prod_i' \int_0^\infty dy_i \right) (y')^{\max(m_+,m_-)}$$

$$\times \exp\left[-\sum' y_i (\Delta_i^2 - i\varepsilon)\right] \qquad (\nu_{kj} = 1) \qquad (6.19)$$

where,

$$C^4_{mm_+m_-r} \equiv i\pi(-1)^N(-1)^{m_++m_-}(-1)^r (\sigma_j \lambda_j^-)^{\Delta m}$$

$$\times \frac{m_+!\, m_-!\, (\Delta m-1)!}{r!(\max(m_+,m_-)-r)!} \cdot a_{mm_+m_-} \qquad (6.20)$$

for the other case.

6.3.4 $m_- < m_+$: THE CONTRIBUTING POLE IS $z = 1-M+m_-$:

The asymptotic expression for this case is given by expressions similar to (6.17) and (6.19) for the cases $\nu_{kj} = -1$ and $+1$ respectively with these changes: Δ_j^2 to be replaced by Δ_k^2, $\sigma_j \lambda_j^-$ by $\sigma_k \lambda_k^+$.

6.3.5 $m_+ = m_- = m_0$: THE CONTRIBUTING DOUBLE POLE IS $z = 1-M+m_0$:

In this case,

$$M \simeq \sum_{mm_+m_-r} (\sqrt{s})^{m-2} (\ln s - i\pi) \int d^2\vec{k}_\perp \; C^5_{mm_+m_-r} \left(\prod_i' \int_0^\infty dy_i\right)$$

$$x\,(y')^{-m_0} \exp\left[-\sum_i' y_i(\Delta_i^2 - i\varepsilon)\right] \quad (\nu_{kj} = -1) \qquad (6.21)$$

with $$C^5_{mm_+m_-r} \equiv -i\pi(-1)^N(-1)^r \frac{(m_0!)^2}{r!(m_0-r)!}\, a_{mm_+m_-} \qquad (6.22),$$

and $$M \simeq \sum_{mm_+m_-r} (\sqrt{s})^{m-2} \ln s \int d^2\vec{k}_\perp \; C^6_{mm_+m_-r} \left(\prod_i' \int_0^\infty dy_i\right)$$

$$x\,(y')^{-m_0} \exp\left[-\sum_i' y_i(\Delta_i^2 - i\varepsilon)\right] \quad (\nu_{kj} = 1) \qquad (6.23)$$

where,

$$C^6_{mm_+m_-r} = -C^5_{mm_+m_-r} \qquad (6.24)$$

Expressions (6.17), (6.19), (6.21) and (6.23) give us the required asymptotic expressions for high energy behaviour of diagrams of class (A).

6.4 ASYMPTOTIC BEHAVIOUR OF SCATTERING DIAGRAMS OF OTHER CLASSES:

In the previous section we considered the diagrams of class (A) and found their asymptotic behaviour. We shall consider the asymptotic behaviour of diagrams of other classes in this section.

6.4.1 CLASS (B):

According to the definition given in section 6.2, for diagrams of class (B), we have $\lambda_i^+ \lambda_i^- = 0$ for all i, and either $\sigma_i\lambda_i^+ = 0$ for all i, or $\sigma_j \lambda_j^- = 0$ for all j. For the sake of definiteness, let us assume that it is $\lambda_i^-\sigma_i$ which is zero for all i, the same is not true of $\lambda_i^+ \sigma_i$, then,

$$\sum_i \alpha_i p_i^+ p_i^- \simeq \sum_i \alpha_i \left(\lambda_i^+ \mu_i^- + \lambda_i^- \mu_i^+ \right) \tag{6.25}$$

and defining,

$$L^{\pm} = \sum_i \alpha_i \sigma_i \lambda_i^{\pm} \tag{6.26}$$

and $$M^{\pm} = \sum_i \alpha_i \sigma_i \mu_i^{\pm} \tag{6.27}$$

we get, $$\beta^+ = \sqrt{s}\, L^+ \tag{6.28}$$

$$\beta^- = 1/\sqrt{s}.\ M^- \tag{6.29},$$

where we have neglected terms of one order down in s.

Thus the asymptotic behaviour of amplitude is obtained from (6.6) trivially in this case as,

$$M = \sum_{m m_+ m_- r} (\sqrt{s})^{m+m_+-m_-} \left(\prod_i d\alpha_i \right) (\alpha)^{r-m_+-m_--1} (L^+)^{m_+-r} \times \int d^2\vec{k}_\perp\, C_{m m_+ m_- r} (M^-)^{m_--r} \exp i\left[\sum_i \alpha_i \left(\lambda_i^+ \mu_i^- + \lambda_i^- \mu_i^+ \right) - \alpha^{-1} L^+ (l^2 - \sum_i \alpha_i (\Delta_i^2 - i\varepsilon)) \right] \tag{6.30}.$$

The other case when $\lambda_i^+ \sigma_i = 0$ for all i, but $\lambda_i^- \sigma_i$ are not all zero, is completely symmetric to the one above, we only have to interchange + and -.

When both $\lambda_i^+ \sigma_i$ and $\lambda_i^- \sigma_i$ are zero for all i, then

$$M = \sum_{mm_+m_-r} (\sqrt{s})^{m-m_+-m_-+2r} \left(\prod_i \int d\alpha_i\right) \times (\alpha)^{r-m_+-m_--1} \int d^{2}\vec{k}_{\perp} C_{mm_+m_-r} (\mu^+)^{m_+-r} \times (\mu^-)^{m_--r} \exp i\Big[\sum_i \alpha_i (\lambda_i^+ \mu_i^- + \lambda_i^- \mu_i^+) - \sum_i \alpha_i (\Delta_i^2 - i\varepsilon)\Big] \tag{6.31}$$

6.4.2 CLASS (C):

Let $\sigma_i \lambda_i^- = 0$ for all i.

Then,

$$M = \sum_{mm_+m_-r} (\sqrt{s})^{m+m_+-m_-} \int d^{2}\vec{k}_{\perp} \left(\prod_i \int d\alpha_i\right) \times C_{mm_+m_-r} (\alpha)^{r-m_+-m_--1} (\mu^+)^{m_+-r} \times (\mu^-)^{m_--r} \exp i\Big[s \sum_i \lambda_i^+ \lambda_i^- \alpha_i - \sum_i \alpha_i \times (\Delta_i^2 - i\varepsilon)\Big] \tag{6.32}$$

It is easily seen that one can choose the 1-3 and 2-4 paths kin such a manner that if only one line is common to both the paths, then,

$$\sum_i \lambda_i^+ \lambda_i^- \alpha_i = \lambda_{i_1}^+ \lambda_{i_1}^- \alpha_{i_1}$$

where i_1 is the common line. Then, as $\lambda_{i_1}^- \neq 0$, $\sigma_{i_1} = 0$. Thus in the expression for $\alpha = \sum \alpha_i (\sigma_i)^2 \alpha_{i_1}$ does not occur, and one can perform the integration over α_{i_1}. The result is a factor 1/s. This could have been seen directly, because the typical graphs of class (C) are one loop corrections to external lines of tree graphs having an s. or u-channel pole. Thus, as t is constant, their asymptotic behaviour is down by a factor of s. Two common lines give s^{-2}.

6.4.3 CLASS (D):

Let i_1, i_2 be the lines (there are at most two) for which $\lambda_{i_1}^+ \lambda_{i_1}^- \neq 0$ and $\lambda_{i_2}^+ \lambda_{i_2}^- \neq 0$. Then surely, σ_{i_1}, $\sigma_{i_2} = 0$. Therefore as in Class (C) α_{i_1} (and α_{i_2})'decouples' entirely, i.e. can be integrated over to get a factor 1/s. The rest of the integral is of the same form as (6.8) of class (A) and can be treated in exactly the same manner. We avoid repeating the details. Suffice is to say that generally the asymptotic behaviour of diagrams of this class can be obtained in the same way as for class (A), only, it is down by a factor

s or s^2 depending on whether there is one line with $\lambda_i^+\lambda_i^- \neq 0$ or two.

6.4.4 CLASS (E):

Essentially there is only one diagram of this kind. It is shown in Fig. 16 . We shall not discuss it in detail as, in company with other diagrams which have a line lying on both $\underline{1}$-$\underline{3}$ and $\underline{2}$-$\underline{4}$ paths, it is down by a factor s with respect to similar graphs of class (A).

6.5 ONE-LOOP ONE-PARTICLE PRODUCTION DIAGRAMS:

We now come to discuss the high energy behaviour of one-particle production diagrams at one loop level. With a final state of three particles we see immediately that high energy can be distributed in various possible ways. Let the reaction described be,

$$\underline{1} + \underline{2} \rightarrow \underline{3} + \underline{4} + \underline{5} \qquad (6.37)$$

This reaction can be described by five invariant variables three 'sub-energies' s_{34}, s_{35}, s_{45}, and two momentum transfer variables t_{13} and t_{24}. These variables are defined in Appendix Four. If we let the centre of mass energy squared $s = s_{34} + s_{35} + s_{45} - m_3^2 - m_4^2 - m_5^2$ go to infinity, and keep t_{13} and t_{24} constant, we find that there are five kinematic regions corresponding to whether only one out of the three sub-energies s_{34}, s_{35}, s_{45} go to infinity as fast as s,

or two. Note that s_{35} and s_{45} cannot both grow as fast as s because t_{13} and t_{24} being fixed, particles $\underline{3}$ and $\underline{4}$ move in opposite directions in the center of mass system. If the particle $\underline{5}$ stays put (i.e. has momentum of O(1)) then s_{35} and s_{45} go as $\sqrt{s}$. If it moves alongwith either $\underline{3}$ or $\underline{4}$, the corresponding subenergy is small.

Out of the five kinematical regions we shall work in the regions where all the final state particles have high energies. Explicitly, the region with s_{34}, $s_{35} \sim s$, and the one with s_{34}, $s_{45} \sim s$. As we are concerned with the process where particles $\underline{3}$ and $\underline{4}$ are the same, for reasons of symmetry, it suffices to actually work with only one of these two.

So, let us consider the case where,

$$p_1^+ = \sqrt{s} + O(1/\sqrt{s}), \quad p_1^- = O(1/\sqrt{s}), \quad \vec{p}_{1_\perp} = 0 \qquad (6.38a)$$

$$p_2^+ = O(1/\sqrt{s}), \quad p_2^- = \sqrt{s}+O(1/\sqrt{s}), \vec{p}_{2_\perp} = 0 \qquad (6.38b)$$

$$p_3^+ = \lambda\sqrt{s}+O(1/\sqrt{s}), \quad p_3^- = O(1/\sqrt{s}), \quad \vec{p}_{3_\perp} = O(1) \qquad (6.38c)$$

$$p_4^+ = O(1/\sqrt{s}), \quad p_4^- = \sqrt{s}+O(1/\sqrt{s}), \vec{p}_{4_\perp} = O(1) \qquad (6.38d)$$

$$p_5^+ = (1-\lambda)\sqrt{s}+O(1/\sqrt{s}), p_5^- = O(1/\sqrt{s}), \quad \vec{p}_{5_\perp} = O(1) \qquad (6.38e)$$

$$\vec{p}_{3_\perp} + \vec{p}_{4_\perp} + \vec{p}_{5_\perp} = 0 \qquad (6.38f)$$

Just as discussed in the case of scattering diagrams, so here for production graphs, one can choose the flow of external momenta in the internal lines in such a way that lines for which $\lambda_i^+ \neq 0$ form a connected tree (with two branches), which, in analogy to the case of scattering discussed previously, and with some abus de langage, we call the $\underline{1} - \underline{3}\ \underline{5}$ path. The other path, i.e. the one of lines for which $\lambda_i^- \neq 0$ is called, as before, $\underline{2} - \underline{4}$ path.

Classification of one-loop diagrams for production of one particle can be done along the same lines as for the scattering case. Indeed, we can use the same classification defined by (A) to (E) in section 6.2, but with the understanding that path $\underline{1} - \underline{3}$ is now to be read as $\underline{1} - \underline{3}\ \underline{5}$.

Once again we have, for diagrams of class (A), a result corresponding to the theorem of section 6.2.

Theorem: For one-loop, one particle diagrams of class (A), there is exactly one line j for which $\sigma_j \lambda_j^- \neq 0$ and there are at most two lines k and k' such that $\sigma_k \lambda_k^+ \neq 0$ and $\sigma_{k'} \lambda_{k'}^+ \neq 0$.

The proof is similar to that of the theorem in section 6.2. In fact, for the existence of exactly one j with $\sigma_j \lambda_j^- \neq 0$ it is identical.

Let us suppose that it is possible that there are three lines k, k' and k'' with $\sigma_k \lambda_k^+ \neq 0$, $\sigma_{k'} \lambda_{k'}^+ \neq 0$ and $\sigma_{k''} \lambda_{k''}^+ \neq 0$. All these lines belong to the $\underline{1}$-$\underline{2}$ $\underline{5}$ path, as well as to the loop. These three lines will have at least four distinct vertices as their end points. (For, if they had three or less, they will form a closed loop by themselves. The line j, also belonging to the loop will lie on an independent loop, but there is only one loop in all, and $\lambda_i^+ \lambda_i^- = 0$ for all i). Now as there are only three external lines with $p^+ = O(\sqrt{s})$, namely $\underline{1}$, $\underline{2}$ and $\underline{5}$, there is at least one vertex, out of these four, on which none of the external lines join. The rest of the argument is the same as in the proof of the theorem in section (6.2).

6.6 ASYMPTOTIC BEHAVIOUR OF ONE-LOOP ONE-PARTICLE PRODUCTION DIAGRAMS:

We shall consider only the most important class of diagrams as far as asymptotic behaviour is concerned, namely, the class (A).

From the theorem in the previous section it follows that we have two different cases, namely those for which there is only one line k with $\lambda_k^+ \sigma_k \neq 0$, and the case where there are two such lines.

6.6.1 DIAGRAMS WITH ONE LINE k WITH $\sigma_k \lambda_k^+ \neq 0$:

This is identical to the scattering case, except that $\nu_k \equiv \sigma_k \lambda_k^+ \sigma_j \lambda_j^-$ need not be of modulus unity. The sign of ν_k of course determines the planarity of the graph as before,

$\nu_k < 0$ for planar graph

> 0 for nonplanar graph.

Accordingly, the expression for asymptotic behaviour is again given by the formulas (6.17), (6.19), (6.21), (6.23), except that the factor $|\nu_k|^{-1}$ is to be inserted in $C^3{}_{mm_+m_-r}$, $C^4{}_{mm_+m_-r}$, $C^5{}_{mm_+m_-r}$, $C^6{}_{mm_+m_-r}$ in (6.18), (6.20), (6.22) and (6.24) respectively.

6.6.2 DIAGRAMS WITH TWO LINES k AND k' WITH $\sigma_k \lambda_k^+ \neq 0 \neq \sigma_{k'} \lambda_{k'}^+$:

The general expression for the amplitude (6.6) becomes, in this case,

$$M = \sum_{mm_+m_-r} \int d^{2}\vec{k}_1 \left(\prod_i \int d\alpha_i\right) C_{mm_+m_-r}$$

$$\times (\alpha)^{r-m_+-m_--1} (\sigma_j \lambda_j^-)^{m_--m_+} (\nu_k \alpha_k + \nu_{k'} \alpha_{k'})^{m_+-r}$$

$$\times (\alpha_j)^{m_--r} s^{M-r} \exp\left[-i \frac{\alpha_j s}{\alpha} (\nu_k \alpha_k + \nu_{k'} \alpha_{k'})\right.$$

$$\left. - \sum_i \alpha_i (\Delta_i^2 - i\varepsilon)\right] \qquad (6.39)$$

where

$$\nu_k = \sigma_k \lambda_k^+ \sigma_j \lambda_j^-$$

$$\nu_{k'} = \sigma_{k'} \lambda_{k'}^+ \sigma_j \lambda_j^- \qquad (6.40)$$

Two distinct cases arise.

6.6.2.1 ν_k AND $\nu_{k'}$ HAVE THE SAME SIGN:

In this case we can neglect α_k and $\alpha_{k'}$ and α_j in α. As before we rotate all the α-contours except α_k, $\alpha_{k'}$, α_j, to run along negative imaginary axis, then,

$$M = \sum_{mm_+m_-r} \int d^2\vec{k}_\perp \left(\prod_i \int dy_i \right) C^7_{mm_+m_-r} (y'')^{r-m_+-m_--1}$$
$$\times \exp\left[- \sum_i'' y_i (\Delta_i^2 - i\varepsilon) \right] P(s) \qquad (6.41)$$

with

$$C^7_{mm_+m_-r} = \pi(-1)^N(-i)^{m_++m_-} \frac{m_+!\, m_-!}{r!(m_+-r)!(m_--r)!} a_{mm_+m_-} \qquad (6.42)$$

$$y'' = \sum_i'' (\sigma_i)^2 y_i$$

$$P(s) = \int_0^\infty d\alpha_k \int_0^\infty d\alpha_{k'} \int_0^\infty d\alpha_j \; (\sigma_j \lambda_j^-)^{m_- - m_+}$$
$$\times (\nu_k \alpha_k + \nu_{k'} \alpha_{k'})^{m_+ - r} (\alpha_j)^{m_+ - r} s^{M-r}$$
$$\times \exp\left[(y'')^{-1} (\nu_k \alpha_k + \nu_{k'} \alpha_{k'}) \alpha_j s \cdot \right.$$
$$\left. - i\alpha_k \Delta_k^2 - i\alpha_{k'} \Delta_{k'}^2 \cdot\cdot i\alpha_j \Delta_j^2 \right] \qquad (6.43)$$

and a double prime on Π, $\sum$ indicates omission of k, k' and j.

If ν_k and $\nu_{k'}$ are both < 0, we can take the Mellin transform of P as it stands and get

$$P(z) \equiv \int_0^\infty s^{z-1} P(s)\, ds$$

$$= \Gamma(z+M-r)(y'')^{z+M-r} (\sigma_j \lambda_j^-)^{m_- - m_+} (-1)^{m_+ - r} \int d\alpha_k \int d\alpha_{k'}$$

$$\int d\alpha_j \left(|\nu_k|\, \alpha_k + |\nu_{k'}|\, \alpha_{k'}\right)^{-z-M+m_+} (\alpha_j)^{-z-M+m_-}$$

$$\exp\left[-i\alpha_k\, \Delta_k^2 - i\alpha_{k'}\, \Delta_{k'}^2 - i\alpha_j\, \Delta_j^2\right]$$

$$= i(y'')^{z+M-r} (\sigma_j \lambda_j^-)^{m_- - m_+} (-1)^{m_+ - r}$$

$$\times \left(|\nu_{k'}|\, \Delta_k^2 - |\nu_k| \Delta_{k'}^2\right)^{-1} \left[\left(\frac{\Delta_k^2}{|\nu_k|}\right)^{z+M-m_+-1}\right.$$

$$\left. - \left(\frac{\Delta_{k'}^2}{|\nu_{k'}|}\right)^{z+M-m_+-1}\right] (\Delta_j^2)^{z+M-m_--1}$$

$$\times \Gamma(-z-M+m_++1)\, \Gamma(-z-M+m_-+1)\, \Gamma(z+M-r)$$

$$\times \exp\left[i\pi\left(z+M-1-\frac{m_+ + m_-}{2}\right)\right] \qquad (\nu_k, \nu_{k'} < 0) \quad (6.44).$$

If ν_k and $\nu_{k'}$ are both positive, then we rotate the contours α_k, $\alpha_{k'}$ and α_j too, and obtain

$$P(s) = (-i)^{3+m_++m_--2r} \int_0^\infty dy_k \int_0^\infty dy_{k'} \int_0^\infty dy_j\, (\sigma_j \lambda_j^-)^{m_- - m_+}$$

$$\times (\nu_k y_k + \nu_{k'} y_{k'})^{m_+ - r} y_j^{m_- - r} \exp\left[-(y'')^{-1}\right.$$

$$\left. \times (\nu_k y_k + \nu_{k'} y_{k'})\, y_j s - y_k \Delta_k^2 - y_{k'} \Delta_{k'}^2 - y_j \Delta_j^2\right]$$

(6.45)

Its Mellin transform is

$$P(z) = (-i)^{-2r+3+m_+ +m_-} (\quad)^{z+M-r} (\sigma_j \lambda_j^{-})^{m_- - m_+} \cdot$$

$$\text{x } \Gamma(z+M-r) \int dy_k \int dy_{k'} \int dy_j \; (\nu_k y_k + \nu_{k'} y_{k'})^{-z-M+m_+}$$

$$\text{x } y_j^{-z-M+m_-} \exp\left[-y_k \Delta_k^2 - y_{k'} \Delta_{k'}^2 - y_j \Delta_j^2\right]$$

$$= (-i)^{-2r+3+m_+ +m_-} (\quad)^{z+M-r} (\sigma_j \lambda_j^{-})^{m_- - m_+} (-1)$$

$$\text{x } (\nu_{k'} \Delta_k^2 - \nu_k \Delta_{k'}^2)^{-1} \left[\left(\frac{\Delta_k^2}{\nu_k}\right)^{z+M-m_+-1}\right.$$

$$\left. - \left(\frac{\Delta_{k'}^2}{\nu_{k'}}\right)^{z+M-m_+-1}\right] (\Delta_j^2)^{z+M-m_--1}$$

$$\text{x } \Gamma(-z-M+m_++1)\, \Gamma(-z-M+m_-+1)\, \Gamma(z+M-r)$$

$$(\nu_k, \nu_{k'} > 0) \qquad (6.46)$$

6.6.2.2 ν_k AND $\nu_{k'}$ HAVE OPPOSITE SIGN:

We shall assume specifically that $\nu_k > 0$ and $\nu_{k'} < 0$; the opposite case can be obtained simply by the interchange of k and k' in the formulas.

In this case we notice that as the contribution to the integral as $s \to \infty$ comes from the neighbourhood of $\nu_k \alpha_k - |\nu_{k'}|\, \alpha_{k'} = 0$ and $\alpha_j = 0$, we can no longer neglect α_k and $\alpha_{k'}$ in α.

Let us define

$$\gamma = \nu_k \alpha_k - |\nu_{k'}|\, \alpha_{k'} \qquad (6.47)$$

Then,

$$\int_0^\infty d\alpha_k \int_0^\infty dk_{k'} = \frac{1}{|\nu_{k'}|} \int_{-\infty}^{0} d\gamma \int_0^\infty d\alpha_k + \frac{1}{\nu_k} \int_0^\infty d\gamma \int_0^\infty d\alpha_{k'} \tag{6.48}$$

Correspondingly, the amplitude M can be written as a sum of two integrals:

$$M = M_1 + M_2$$

$$M_1 = \sum_{mm_+m_-r} \int d^{2\vec{k}}_{\perp} \left(\prod_i'' \int d\alpha_i \right) C_{mm_+m_-r} \int_0^\infty d\gamma \int_0^\infty d\alpha_k$$

$$\int_0^\infty d\alpha_j \frac{1}{|\nu_{k'}|} \left(\sigma_j \lambda_j^{-}\right)^{m_- - m_+} \left(\tilde{\alpha}_1\right)^{r-m_+-m_--1}$$

$$x \left(-\gamma\right)^{m_+-r} \left(\alpha_j\right)^{m_--r} s^{M-r} \exp\left[-i\,\tilde{\alpha}_1^{-1}\,\alpha_j \gamma s\right.$$

$$- i \sum_i'' \alpha_i \left(\Delta_i^2 - i\varepsilon\right) - i\alpha_j \left(\Delta_j^2 - i\varepsilon\right)$$

$$\left. - i\,\alpha_k \left(\Delta_k^2 - i\varepsilon\right) - i \left(\frac{\nu_k\,\alpha_k + \gamma}{|\nu_{k'}|}\right) \left(\Delta_{k'}^2 - i\varepsilon\right)\right] \tag{6.50}$$

$$M_2 = \sum_{mm_+m_-r} \int d^{2\vec{k}}_{\perp} \left(\prod_i'' \int d\alpha_i \right) C_{mm_+m_-r} \int_0^\infty d\gamma \int_0^\infty d\alpha_{k'}$$

$$x \int_0^\infty d\alpha_j \frac{1}{\nu_k} \left(\sigma_j\, \lambda_j^{-}\right)^{m_- - m_+} \left(\tilde{\alpha}_2\right)^{r-m_+-m_--1} \left(\gamma\right)^{m_+-r}$$

$$x \left(\alpha_j\right)^{m_--r} s^{M-r} \exp\left[i\,\tilde{\alpha}_2^{-1}\,\alpha_j\,\gamma s - i \sum_i'' \alpha_i \left(\Delta_i^2 - i\right.\right.$$

$$- i\alpha_j \left(\Delta_j^2 - i\varepsilon\right) - i\nu_k^{-1} \left(\gamma + |\nu_{k'}|\,\alpha_{k'}\right)$$

$$\left. x \left(\Delta_k^2 - i\varepsilon\right) - i\alpha_{k'} \left(\Delta_{k'}^2 - i\varepsilon\right)\right] \tag{6.51}$$

where neglecting γ and α_j, as the main contribution comes from the region where they are small;

$$\tilde{\alpha}_1 = \sum_i'' \alpha_i(\sigma_i)^2 + \alpha_k \left(1 + \frac{\nu_k}{|\nu_{k'}|}\right) \qquad (6.52),$$

$$\tilde{\alpha}_2 = \sum_i'' \alpha_i(\sigma_i)^2 + \alpha_{k'}\left(1 + \frac{|\nu_{k'}|}{\nu_k}\right) \qquad (6.53).$$

We shall discuss the asymptotic behaviour of M_1 and M_2 separately.

We notice that in M_1 and M_2, we have the freedom of rotating the contour in γ to $-i\eta$. In M_1 we rotate all the contours to get,

$$M_1 = \sum_{mm_+m_-r} \int d^2\vec{k}_\perp \; C^8 \left(\prod_i'' \int dy_i\right) \int_0^\infty d\eta \int_0^\infty dy_k \int_0^\infty dy_j$$
$$\times (\tilde{y})^{r-m_+-m_--1} (\eta)^{m_+-r} (y_j)^{m_--r} s^{M-r} \times$$
$$\times \exp\left[-s\tilde{y}^{-1} y_j\eta - \sum_I'' y_i \Delta_i^2 - y_j \Delta_j^2\right.$$
$$\left. - y_k \left(\Delta_k^2 + \frac{\nu_k}{|\nu_{k'}|} \Delta_{k'}^2\right) - \eta \Delta_{k'}^2\right] \qquad (6.54),$$

$$C^8 = C_{mm_+m_-r} (-i)^{N-r-1} (-1)^{m_+-r} (\sigma_j \lambda_j^-)^{m_--m_+} \frac{1}{|\nu_{k'}|} \qquad (6.55)$$

The Mellin transform of M_1 is

$$M_l(z) = \sum_{m m_+ m_- r} \int d^2\vec{k}_\perp \; C^8 \left(\prod_i'' \int dy_i\right) \int_0^\infty d\eta \int_0^\infty dy_k \int_0^\infty dy_j$$

$$\times (\tilde{y}_l)^{z+M-m_+-m_--1} (\eta)^{-z-M+m_+} (y_j)^{-z-M+m_-}$$

$$\times \exp\left[-\sum_i'' y_i \Delta_i^2 - y_j \Delta_j^2 - y_k \left(\Delta_k^2 + \frac{\nu_k}{|\nu_{k'}|} \Delta_{k'}^2\right)\right.$$

$$\left. - \eta \Delta_k^2\right] \times \Gamma(z+M-r) \qquad (6.56),$$

with $\tilde{y}_l = \sum_i'' y_i (\sigma_l)^2 + y_k \left(1 + \frac{\nu_k}{|\nu_{k'}|}\right)$.

The integration over y_j and η can be immediately performed. For integration over y_k we use,

$$\int_0^\infty e^{-ty} (t + x)^{\alpha-1} dt = y^{-\alpha} e^{xy} \Gamma(\alpha, xy)$$

where $\mathrm{Re}\, y > 0$, $x > 0$, $\mathrm{Re}\, \alpha > 1$, and $\Gamma(\alpha, xy)$ is the incomplete gamma function[130].

This gives,

$$M_l(z) = \sum_{m m_+ m_- r} \int d^2\vec{k}_\perp \; C^8 \left(\prod'' \int dy_i\right) \exp\left[-\sum'' y_i \Delta_i^2\right.$$

$$+ \left(|\nu_{k'}| + \nu_k\right)^{-1} \left(|\nu_{k'}| \Delta_k^2 + \nu_k \Delta_{k'}^2\right)$$

$$\left. \times \left(\sum'' y_i \sigma_i^2\right)\right] \Gamma\left(z+M-m_+-m_-, \left(|\nu_{k'}| + \nu_k\right)^{-1}\right.$$

$$\times \left.\left(|\nu_{k'}| \Delta_k^2 + \nu_k \Delta_{k'}^2\right)\left(\sum'' y_i \sigma_i^2\right)\right)$$

$$\times |\nu_{k'}| \left(|\nu_{k'}| + \nu_k\right)^{-1}$$

$$\times \left[\frac{|\nu_{k'}| \Delta_k^2 + \nu_k \Delta_{k'}^2}{|\nu_{k'}| + \nu_k}\right]^{-z-M+m_++m_-}$$

$$\times \left(\frac{\Delta_{k'}^2}{|\nu_{k'}|}\right)^{z+M-m_+-1} \left(\Delta_j^2\right)^{z+M-m_--1} \Gamma\left(-z-M+m_++1\right)$$

$$\times \Gamma\left(-z-M+m_-+1\right) \Gamma(z+M-r) \qquad (6.57).$$

Similarly, in M_2 we rotate all the contours except γ and α_j, and take the Mellin transform. We obtain,

$$M_2(z) = \sum_{mm_+m_-r} \int d^2\vec{k}_\perp \, C^9 \left(\prod_i{}'' \int dy_i\right) \int_0^\infty d\gamma \int_0^\infty dy_{k'} \int_0^\infty d\alpha_j \, (\tilde{y}_2)^{z+m-m_+-m_--1} (\alpha_j)^{-z-M+m_-} \Gamma(z+M-r) \exp\left[-\sum_i{}'' y_i \Delta_i^2 - i\alpha_j (\Delta_j^2 - i\varepsilon) - i\frac{\gamma \Delta_k^2}{\nu_k} - y_{k'} \left(\Delta_{k'}^2 + \frac{|\nu_{k'}|}{\nu_k} \Delta_k^2\right)\right] \qquad (6.58)$$

where,

$$C^9 = C_{mm_+m_-r} (-i)^{N-3+r-m_+-m_-} (\sigma_j \lambda_j^-)^{m_--m_+} \frac{1}{\nu_k}$$

and $$\tilde{y}_2 = \sum_i{}'' y_i (\sigma_i)^2 + y_{k'} \left(1 + \frac{|\nu_{k'}|}{\nu_k}\right).$$

Carrying out the integrations over α_j, y_k, and γ, we obtain,

$$M_2(z) = \sum_{mm_+m_-r} \int d^2\vec{k}_\perp \, C^9 \left(\prod_i{}'' \int dy_i\right) \exp\left[-\sum_i{}'' y_i \Delta_i^2 + (|\nu_{k'}| + \nu_k)^{-1} (|\nu_{k'}| \Delta_k^2 + \nu_k \Delta_{k'}^2) \times \left(\sum_i{}'' y_i \sigma_i^2\right)\right] \Gamma(z+M-m_+-m_-) (|\nu_{k'}| + \nu_k)^{-1} \times \left(|\nu_{k'}| \Delta_k^2 + \nu_k \Delta_{k'}^2\right) \left(\sum_i{}'' y_i \sigma_i^2\right)) \times \nu_k (|\nu_{k'}| + \nu_k)^{-1}$$

$$x \left(\frac{|\nu_{k'}| \Delta_k^2 + \nu_k \Delta_{k'}^2}{|\nu_{k'}| + \nu_k} \right)^{-z-M+m_+ +m_-} \left(\frac{\Delta_k^2}{\nu_k} \right)^{z+M-m_+ -1}$$

$$x \left(\Delta_j^2 \right)^{z+M-m_- -1} \Gamma(-z-M+m_+ +1) \Gamma(-z-M+m_- +1) \; x$$

$$x \Gamma(z+M-r) \exp \left[i\pi \left(z+M+1 - \frac{1_+ +m_-}{2} \right) \right] \qquad (6.59)$$

Therefore, adding $M_1(z)$, we obtain, finally,

$$M(z) = \sum_{mm_+m_-r} \int d^2\vec{k}_i \; C^{10} \left(\prod_i'' \int dy_i \right) \exp \left[-\sum_i'' y_i \Delta_i^2 \right.$$

$$+ \left(|\nu_{k'}| + \nu_k \right)^{-1} \left(|\nu_{k'}| \Delta_k^2 + \nu_k \Delta_{k'}^2 \right)$$

$$\left. x \left(\sum_i'' y_i \sigma_i^2 \right) \right] \Gamma(z+M-m_+ -m_-, \left(|\nu_{k'}| + \nu_k \right)^{-1}$$

$$x \left(|\nu_{k'}| \Delta_k^2 + \nu_k \Delta_{k'}^2 \right) \left(\sum_i'' y_i \sigma_i^2 \right))$$

$$x \left(\Delta_j^2 \right)^{z+M-m_- -1} \left(\frac{|\nu_{k'}| \Delta_k^2 + \nu_k \Delta_{k'}^2}{|\nu_{k'}| + \nu_k} \right)^{-z-M+m_+ +m_-}$$

$$x \Gamma(-z-M+m_+ +1) \Gamma(-z-M+m_- +1) \Gamma(z+M-r)$$

$$x \left[\left(\frac{\Delta_{k'}^2}{|\nu_{k'}|} \right)^{z+M-m_+ -1} \cdot \exp \left[i\pi(z+M-m_+ -1) \right] \right.$$

$$\left. x \left(\frac{\Delta_k^2}{\nu_k} \right)^{z+M-m_+ -1} \right] \left(|\nu_{k'}| + \nu_k \right)^{-1} \qquad (6.60),$$

where C^{10} is a constant.

6.6.2.3 ASYMPTOTIC BEHAVIOUR OF DIAGRAMS WITH TWO LINES k, k' SUCH THAT $\sigma_k \lambda_k^+ \neq 0$ $\sigma_{k'} \lambda_{k'}^+ \neq 0$.

The asymptotic behaviour of diagrams with two lines k and k' with $\sigma_k \lambda_k^+ \neq 0$ and $\sigma_{k'} \lambda_{k'}^+ \neq 0$ can be easily seen from

their Mellin transforms given by (6.44), (6.46) and (6.60) for different cases.

We notice immediately that these expressions contain an explicit factor,

$$\left(\frac{\Delta_k^2}{|\nu_k|}\right)^{z+M-m_+-1} - \left(\frac{\Delta_{k'}^2}{|\nu_{k'}|}\right)^{z+M-m_+-1} \qquad (6.61),$$

for (6.44) and (6.46) and

$$\left(\frac{\Delta_{k'}^2}{|\nu_{k'}|}\right)^{z+M-m_+-1} - \exp\left[i\pi\,(z+M-m_+-1)\right]\left(\frac{\Delta_k^2}{|\nu_k|}\right)^{z+M-m_+-1} \qquad (6.62),$$

in (6.60).

As we discussed in section 6.3, the left most pole of the Mellin transform of the amplitude in the region $\mathrm{Re}(z+M-r) > 0$ gives the leading asymptotic behaviour. However, we see that the above factors give a zero at $z = -M+m_+ +1$. Therefore the pole at $z = -M+m_+ +1$ is always killed. We saw in section 6.3 that the double pole at $m_+ = m_-$ gives the ln s behaviour. This behaviour would be absent because of the cancellation of one of the poles.

Thus we have shown that production diagrams of class (A) with two lines k, k' with $\lambda_k^+ \sigma_k \neq 0$ and $\lambda_{k'}^+ \sigma_{k'} \neq 0$ are not the leading ones compared to diagrams with only one such line because of the occurrance of factors like (6.61) and (6.62) in

them. So, effectively the study of asymptotic behaviour of production diagrams of class (A) reduces to those with only one line j and k with $\lambda_j^- \sigma_j \neq 0$ and $\lambda_k^+ \sigma_k \neq 0$.

6.6.3 OTHER PRODUCTION DIAGRAMS:

We can study the asymptotic behaviour of other classes (B), (C), (D) and (E) along the same lines as for scattering diagrams (see section 6.4). The details need not be repeated here. It is enough to bear in mind that generally diagrams of these other classes do not contribute to leading asymptotic behaviour.

6.7 SUMMARY:

We have found in this chapter that leading asymptotic behaviour at high energy and fixed momentum transfer of Feynman diagrams at one-loop level comes mainly from a class of diagrams in which the high forward and backward momenta can be directed along lines which donot intersect and both of which have a line each carrying the loop momentum. The asymptotic behaviour for such diagrams is given by (6.17), (6.19), (6.21) and (6.23) for scattering diagrams, and for production diagrams, by these same formulas, but with modification mentioned in section 6.6.1. We have also found that in general in production graphs of class (A) if there are two loop lines which carry high energy momentum then they are dominated by graphs in which

there is only one such line.

We shall use the formalism of this section in the next chapter to evaluate the asymptotic behaviour of the processes $\pi\rho \to \pi\rho$ and $\pi\pi \to \pi\pi\rho$.

CHAPTER SEVEN

In this chapter we shall consider the high energy behaviour of the processes $\rho\pi \to \rho\pi$ and $\pi\pi \to \rho\pi\pi$ using the method of Chapter Six.

7.1 HIGH ENERGY BEHAVIOUR OF $\rho\pi$ SCATTERING TO ORDER g^4:

In the notation of Chapter Six, we take ρ to be the particle $\underline{1}$ and $\underline{3}$ and π to be $\underline{2}$ and $\underline{4}$. The second order leading amplitude is given by the diagram in Fig. 2.a.

$$M^{\rho\pi\to\rho\pi}_{Born} = -\frac{(2g)^2}{(2\pi)^6}\,\varepsilon^{i_3 i_1 k}\,\varepsilon^{i_4 i_2 k}\,\varepsilon^{*}_{\lambda_3}(p_3).\varepsilon_{\lambda_1}(p_1)\,\frac{2s}{t-M^2} \qquad (7.1)$$

Coming to the fourth order, consider first the box diagrams of class (A). They are shown in Fig. 17. All of them have the same structure of the denominator d (cf. equation (6.1)). The numerator n, however, differs from diagram to diagram. Because of the derivative couplings, the numerator is a polynomial in external and loop momenta. In order to contribute to the leading order, it is evident from the asymptotic formulas (6.17-23), that a diagram of Class (A) should have in its numerator as high a power of $\sqrt{s}$ as possible. There are four vertices in all these diagrams, and a derivative coupling on all the four vertices can produce $(\sqrt{s})^4$. However, it does not

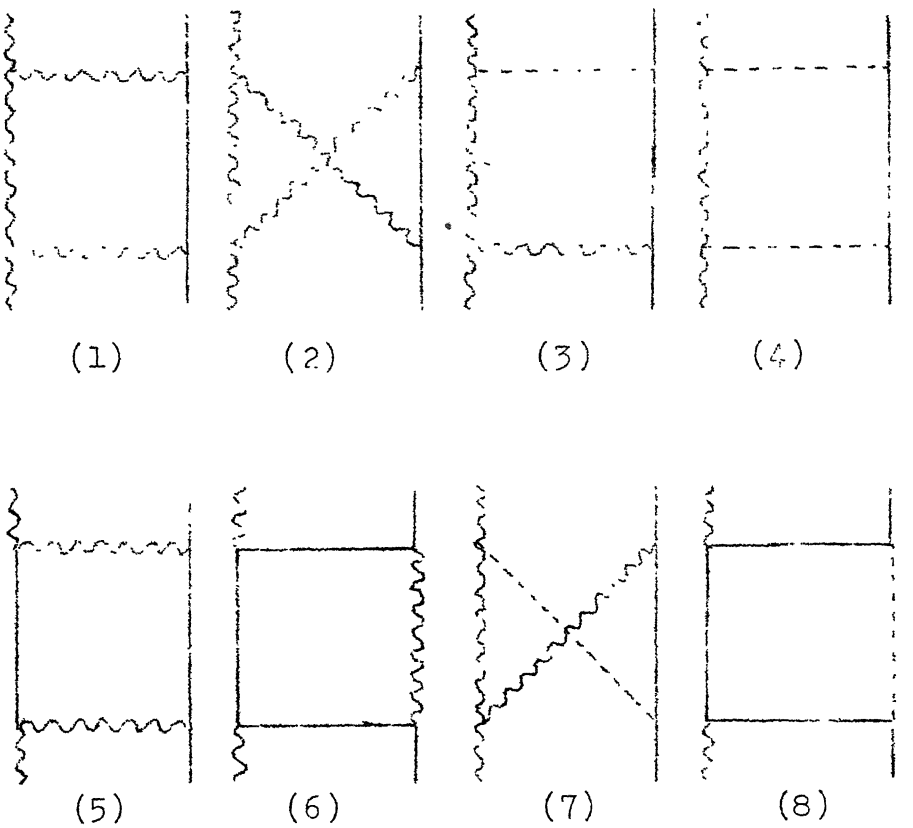

Fig. 17: Some box-diagrams in $p\pi$ scattering. Only the first two contribute to the leading high-energy amplitude.

always do so. The reason is that the numerator is a polynomial of Lorentz invariant dot-products of internal and external momenta, and as,

$$p_i \cdot p_j = \frac{1}{2}(p_i^+ p_j^- + p_i^- p_j^+) - \vec{p}_{i_\perp} \cdot \vec{p}_{j_\perp} \qquad (7.2)$$

We must have contraction of p_i with p_i^+ of $O(\sqrt{s})$ with p_j which has $p_j^- = O(\sqrt{s})$ to get maximum s factors.

This requirement is satisfied only by the diagram (1) and (2) in Fig. 17. Others either do not have four derivative couplings, or they donot contract in the above manner.

For diagram (1) (see Fig. 1' for distribution of momenta), we have

$$\begin{aligned} n &= (-i)^3 (i)(2g)^4 (2\pi)^{-4} (\delta^{i_3 i_1} \delta^{i_4 i_2} + \delta^{i_3 i_4} \delta^{i_1 i_2}) \\ &\quad \times \varepsilon^{\nu *}_{\lambda_3}(p_3)\, \varepsilon^{\nu}_{\lambda_1}(p_1) [(p_3 - p_1 - k)_\nu g_{\nu\sigma} \\ &\quad + (p_1 + 2k - p_2 + p_4)_\nu g_{\sigma\mu} + (-k + p_2 - p_4 \\ &\quad + p_3)_\sigma g_{\mu\nu}] [(-k-2p_1)_{\mu'} g_{\sigma\nu'} + (p_1 - k)_\sigma g_{\mu'\nu'} \\ &\quad + (2k+p_1)_{\nu'} g_{\mu'\sigma}] (p_2 + p_4 - k)^\mu (2p_2 - k)^{\mu'} \cdot \frac{-i}{(2\pi)^6} \\ &= 4i(2\pi)^{-10} (2g)^4 (\delta^{i_3 i_1} \delta^{i_4 i_2} + \delta^{i_3 i_4} \delta^{i_1 i_2}) s^2 \\ &\quad \times \varepsilon^*_{\lambda_3} \cdot \varepsilon_{\lambda_1} + \text{terms of lower powers in s.} \qquad (7.3) \end{aligned}$$

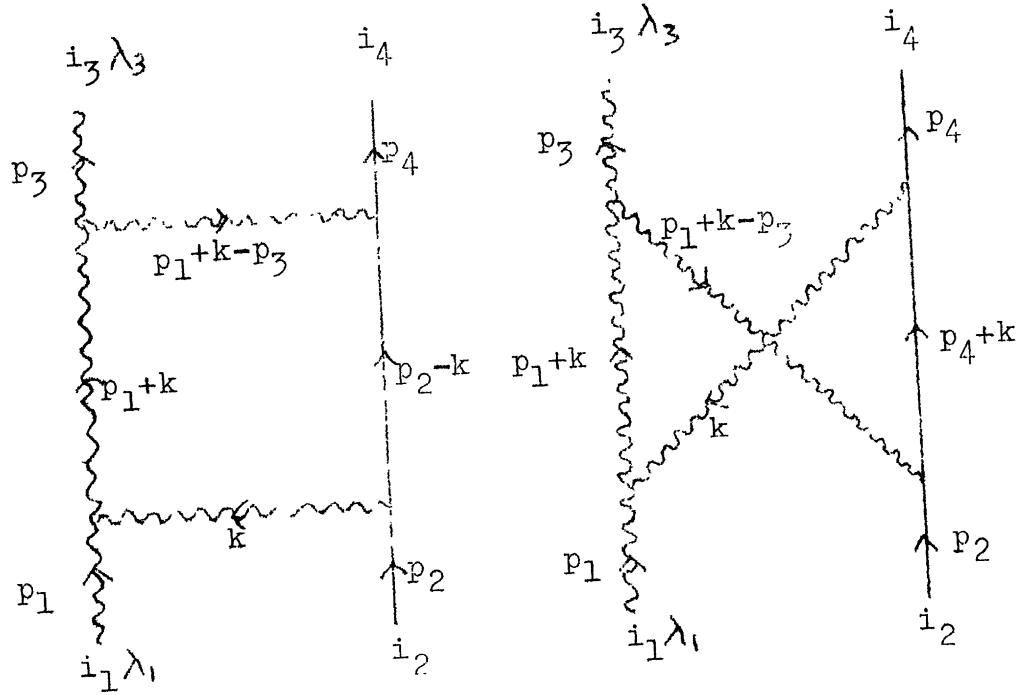

Fig. 18: Distribution of momenta in diagrams (1) and (2) of Fig. 17.

Equation (7.3) corresponds to the expansion (6.4) of the preceding chapter. We notice that with the highest power of s there is no $k_{\pm}$. We have for (7.3),

$$m = 4, \quad m_+ = m_- = 0 \tag{7.4}$$

Also, looking at the distribution of momenta in Fig. 18 we find that, in the notation of Chapter Six,

$$\begin{aligned} \sigma_1 &= 1, \quad \lambda_1^+ = 1, \ \lambda_1^- = 0 \\ \sigma_2 &= 1, \quad \lambda_2^{\pm} = 0 \\ \sigma_3 &= -1, \ \lambda_3^+ = 0, \ \lambda_3^- = 1 \\ \sigma_4 &= 1, \quad \lambda_4^{\pm} = 0 \\ \nu_{13} &= \sigma_1 \lambda_1^+ \cdot \sigma_3 \lambda_3^- = -1 \end{aligned} \tag{7.5}$$

Therefore, the asymptotic behaviour for diagram (1) is given by (6.21).

$$\begin{aligned} M_1 \simeq (\sqrt{s})^{4-2} (\ln s - i\pi) \int d^{2-\epsilon}\vec{k}_\perp \ C^5 \int_0^\infty dy_2 \int_0^\infty dy_4 \\ \times \exp\left[-y_2 \Delta_2^2 - y_4 \Delta_4^2\right] \times \frac{-i}{(2\pi)^6} \end{aligned} \tag{7.6}$$

with,

$$\begin{aligned} C^5 = -i\pi(-1)^4 \times (-4) (2s)^4 (2\pi)^{-4} (\delta^{i_3 i_1} \delta^{i_4 i_2} \\ + \delta^{i_3 i_4} \delta^{i_1 i_2}) \varepsilon^*_{\lambda_3} \cdot \varepsilon_{\lambda_1} \end{aligned} \tag{7.7}$$

$$\Delta_2^2 = (\vec{k}_\perp - \vec{p}_{3\perp})^2 + M^2 \tag{7.8}$$

$$\Delta_4^2 = \vec{k}_\perp^{\,2} + M^2 \tag{7.9}$$

Or, carrying out the y-integrals,

$$M_1 = \frac{1}{\pi(2\pi)^6}(2g)^4 (\delta^{i_3 i_1}\delta^{i_4 i_2} + \delta^{i_3 i_4}\delta^{i_1 i_2})\, \varepsilon_{\lambda_3}\, \varepsilon^*_{\lambda_1 s}$$

$$\times (\ln s - i\pi) \int \frac{d^2\vec{k}_\perp}{(2\pi)^2} \cdot \frac{1}{(\Delta_2^2 - i\varepsilon)(\Delta_4^2 - i\varepsilon)} \tag{7.10}$$

Similarly, for diagram (2) in Fig. 17 , we use formula (6.23) to get,

$$M_2 = -\frac{1}{\pi(2\pi)^6}(2g)^4 (\delta^{i_3 i_1}\delta^{i_4 i_2} + \delta^{i_1 i_4}\delta^{i_3 i_2})$$

$$\times s \ln s\, \varepsilon^*_{\lambda_3} \cdot \varepsilon_{\lambda_1} \int \frac{d^2k_\perp}{(2\pi)^2} \frac{1}{(\Delta_2^2 - i\varepsilon)(\Delta_4^2 - i\varepsilon)} \tag{7.11}$$

As far as other diagrams of Class (A), namely those involving three or less internal lines, are concerned they can be immediately dismissed from our consideration as all of them involve a four point vertex which does not bring any momentum factors into the numerator. The numerator cannot produce any power of $\sqrt{s}$ greater than two, so compared to the diagrams considered above, they are non-leading.

The same holds for diagrams of other classes. The diagrams of (C), (D) and (E) are explicitly down by a factor s (or even s^2 sometimes), because they all involve a common line on $\underline{1} - \underline{3}$ and $\underline{2} - \underline{4}$ paths.

As far class (B), it is known that it will not produce a logarithm. However, looking at a diagram of type (B) (for example the first diagram in Fig. 19) it is not clear that, with a momentum factor on each of the vertices, it will not produce an s^2. It will not as a matter of fact, as can be seen immediately as follows. In order to get maximum $\sqrt{s}$ factors, we must contract a momentum having high p^+ component with another having high p^- component. The contraction takes place through $g^{\mu\nu}$ provided by exchanged vector meson, and the $g^{\mu\sigma}$ of 3-vector meson coupling. Since (in the diagram) the $\underline{1} - \underline{3}$ path has one line in the loop, the two contractions of four momenta will involve two momenta with high p^+ component, one with high p^- and one without any high momentum. Because of (7.2), the structure of the leading term in the numerator is $(\sqrt{s})^3\, k^-$, or, in the language of Chapter Six, $m = 3$, $m_+ = 0$, $m_- = 1$. The asymptotic behaviour of the amplitude is then given by equation (6.30) which means that it is $(\sqrt{s})^{m+m_+-m_-} = s$. The amplitude cannot go as s^2. One can verify that the same holds for other diagrams of Class (B).

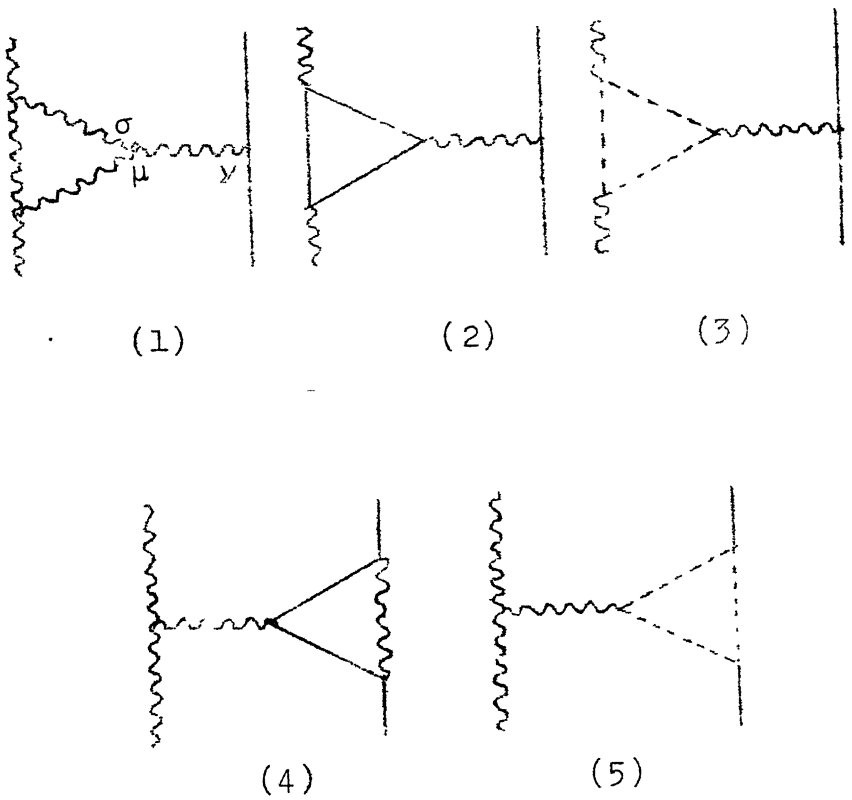

Fig. 19: A few diagrems of Class (3) in $\rho\pi$ scattering which don't contribute to leading asymptotic order.

This completes our analysis of high energy $\rho\pi$ scattering upto one loop level. In the next section we consider the high energy behaviour of the process $\pi\pi \to \rho\pi\pi$.

7.2 HIGH ENERGY BEHAVIOUR OF $\pi\pi \to \rho\pi\pi$ TO ORDER g^5:

The calculation of high-energy behaviour of $\pi\pi \to \rho\pi\pi$ is similar in many respects to $\pi\pi$ scattering.

We shall restrict our attention to the λ-region in the kinematic variables (see Appendix Four, (A 4.16)), and zero helicity production of ρ. The other kinematic region (χ - region; (A4.17)) is symmetric to the first. The zero helicity production amplitude, because of (A1.31), dominates over others at high energy.

The graphs contributing to third and fifth order are shown in Fig. 20. Third order graphs are easily evaluated; the amplitude is,

$$M^{\pi\pi \to \pi\pi\rho}_{Born} = \frac{-i}{(2\pi)^{15/2}} \frac{(2g)^3}{M} \frac{(1-\lambda)s}{t_{24} - M^2} A \qquad (7.12)$$

where,

$$A = (23, 154) - (14, 235) + (12, 354) + (34, 125) \qquad (7.13)$$

and,

$$(i_1 i_2, i_3 i_4 i_5) = \delta^{i_1 i_2} \varepsilon^{i_3 i_4 i_5} \quad \text{etc.}$$

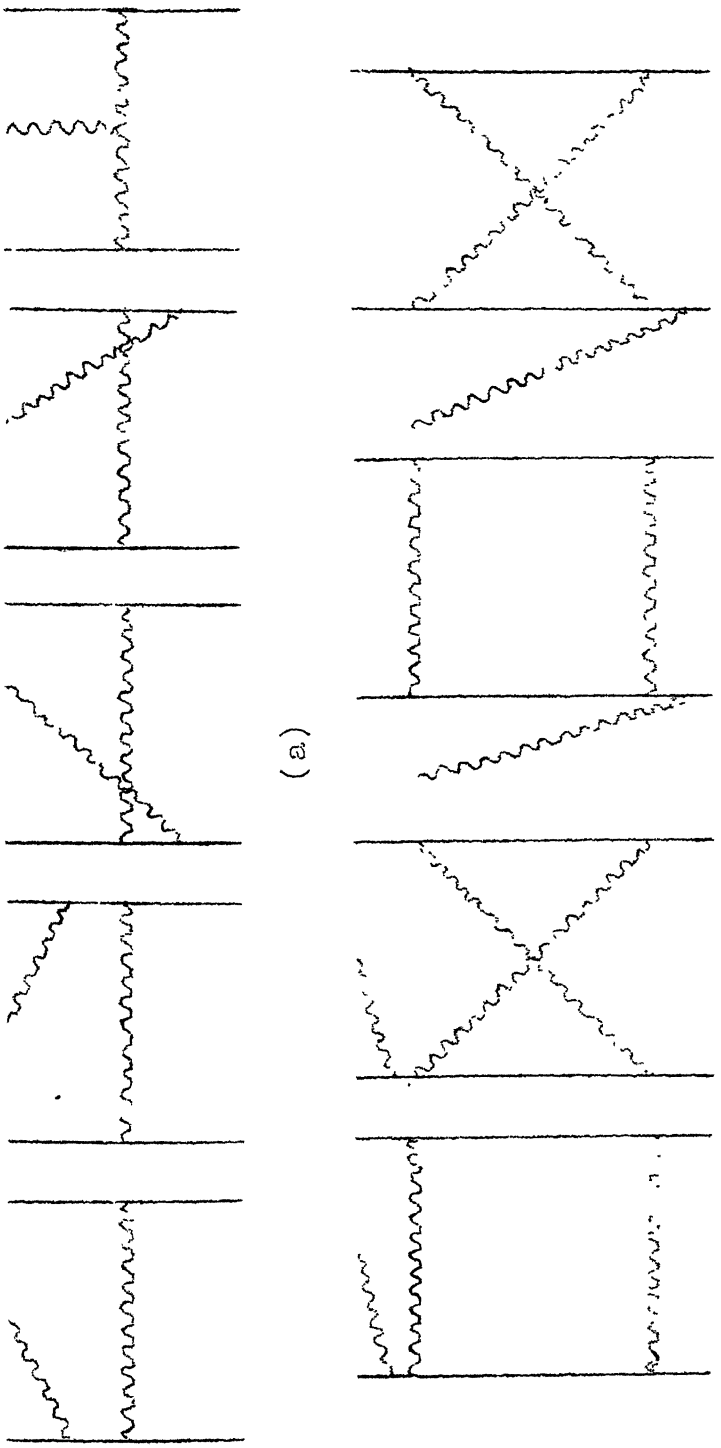

Fig. 20: Diagrams contributing to leading high-energy behaviour in $\pi\pi \longrightarrow \rho\pi\pi$.

Coming to the fifth order graphs, consider B_1 to B_4 in Fig.20. We shall omit the details of this calculation.

$$M_{B_1} = \frac{-i}{(2\pi)^{15/2}} \frac{(2g)^5}{M} [(12,354)+(24,135)]$$

$$x \left(\frac{1}{\pi}\right) s \, (\ln s - i\pi) \, L(\vec{p}_{5\perp}) \qquad (7.14)$$

$$M_{B_2} = - \frac{i}{(2\pi)^{15/2}} \frac{(2g)^5}{M} [(14,235) + (24,135)]$$

$$x \left(- \frac{1}{\pi}\right) s \ln s \, L(\vec{p}_{5\perp}) \qquad (7.15)$$

$$M_{B_3} = - \frac{i}{(2\pi)^{15/2}} \frac{(2g)^5}{M} [(24,135) + (34,125)]$$

$$x \left(- \frac{1}{\pi}\right) \lambda s \, (\ln s - i\pi) \, L(\vec{p}_{5\perp}) \qquad (7.16)$$

$$M_{B_4} = - \frac{i}{(2\pi)^{15/2}} \frac{(2g)^5}{M} [(23,154) - (24,135)]$$

$$x \left(- \frac{1}{\pi}\right) \lambda s \ln s \, L(\vec{p}_{5\perp}) \qquad (7.17)$$

where,

$$L(\vec{p}_{5\perp}) = \int d^2k_\perp (2\pi)^{-2} [(\vec{k}_\perp^2 + M^2 - i\varepsilon)(\vec{k}_\perp + \vec{p}_{5\perp})^2 + M^2 - i\varepsilon)]^{-1} \qquad (7.18).$$

It is important to realise that the diagrams in which the vector meson is emitted from the internal lines of a

$\pi\pi$-scattering graph does not contribute to the leading order as shown in detail in section 6.3.2.

In the next section we shall discuss these results.

7.3 DISCUSSION OF RESULTS AND FURTHER PROBLEMS TO BE STUDIED:

We shall now collect the asymptotic formulas (7.1), (7.10) and (7.11) for the $\rho\pi \to \rho\pi$ scattering. We see that the non-helicity-flip amplitude in the leading order can be written as,

$$M_{\text{one loop}} = M_{\text{Born}}^{\rho\pi\to\rho\pi} \left(1 - \frac{(2g)^2}{\pi} \frac{t-M^2}{2} \text{lns.K}(t)\right) \qquad (7.19),$$

where,

$$K(t) = \int d^2\vec{k}_\perp (2\pi)^{-2} ((\Delta_2^2 - i\varepsilon)(\Delta_4^2 - i\varepsilon))^{-1} \qquad (7.20),$$

and where $M_{\text{Born}}^{\rho\pi\to\rho\pi}$ is given by (7.1) except that we have $\delta_{\lambda_3\lambda_1}$ for $\varepsilon_{\lambda_3}(p_3).\varepsilon_{\lambda_1}(p_1)$ in the case of non-helicity-flip. The expression in the bracket in (7.18) is of the same form as the first two terms obtained by Tyberski[110], Yeung[112] and McCoy and Wu[109] for fermion-fermion and vector-meson-vector-meson scattering. They have calculated upto one or two more terms in the $(2g)^2$ geometric series. Our calculation has been a modest attempt to verify the same for $\rho\pi$ scattering in a model where pions are included. The exact similarity of the expression in (7.18) with that obtained by the authors mentioned, leads us to believe that our results are consistent

with the Reggeization of the vector meson in gauge theories.

For production amplitudes (7.12-17) for $\pi\pi \to \rho\pi\pi$ we do not have similar calculation in gauge theories to compare. However, it is interesting to observe that when we add the fifth order leading logarithms in (7.14) to (7.17) the result is

$$M_5^{\pi\pi \to \rho\pi\pi} = -\frac{i}{(2\pi)^{15/2}} \frac{(2g)^5}{\pi M} s \ln s \, L(\vec{p}_{5\perp})$$

$$\times [(12, 354) - (14, 235) - (34,125)\lambda$$

$$- \lambda(23, 154)]$$

$$= -i \frac{1}{(2\pi)^{15/2}} \frac{(2g)^5}{\pi M} s \ln s \, L(\vec{p}_{5\perp})$$

$$\times \varepsilon^{j42} (\varepsilon^{jkl} \varepsilon^{k35} - \lambda \varepsilon^{jk3} \varepsilon^{k15}) \quad (7.21),$$

where for sake of convenience we have written ε^{123} for $\varepsilon^{i_1 i_2 i_3}$ etc.

Combined with the corresponding isospin component of the Born amplitude (7.12), the one-loop, zero helicity production amplitude is

$$M_{\text{one-loop}}^{\pi\pi \to \rho\pi\pi} = -\frac{i(2g)^3}{(2\pi)^{15/2} M} s \varepsilon^{j42} (\varepsilon^{jkl} \varepsilon^{k35}$$

$$- \lambda \varepsilon^{jk3} \varepsilon^{k15}) \frac{1}{t_{24} - M^2}$$

$$\times \left[1 - \frac{t_{24} - M^2}{\pi} (2g)^2 L(\vec{p}_{5\perp}) \ln s\right] \quad (7.22)$$

a formula, with striking similarity to (7.19). We sense here a similar Regge-type behaviour. In order to confirm it the calculation should be carried to higher orders, a task which in this investigation we have not been able to accomplish because of an overwhelmingly large number of diagrams in the higher orders. Added to the larger number of diagrams in higher orders are the problems due to divergent self-energy and vertex part. These problems do not arise in the lower order diagrams.

We conclude this chapter with a few directions in which the present investigation can be extended.

(i) The above calculations should be extended to two-loop level. The formalism of chapter Six should be generalized, and it should be possible to classify higher order diagrams (which are very many) so that one can base one's studies on all diagrams of a given order than just restricting to special subclasses of them.

(ii) One should study the backward scattering at high-energy. This means that $t \to -\infty$, and u remains fixed.

It is hoped that with the very interesting high energy behaviour shown by gauge theories, such studies may give some insight into the hadronic interactions.

APPENDIX ONE

KINEMATICS OF $\rho\pi$ SCATTERING AND 1^+ PARTIAL WAVE AMPLITUDES

Throughout we shall use the Minkowski metric with $g_{oo} = 1$, $g_{11} = g_{22} = g_{33} = -1$. Pion field is written as

$$\pi^i(x) = \frac{1}{(2\pi)^{3/2}} \int \frac{d^3k}{2k^o} \left(a^i(k)\, e^{-ikx} + a^{i\dagger}(k)\, e^{ikx}\right) \tag{A1.1}$$

where $i = 1,2,3$ is the isospin index.

One particle state $|\vec{p}_i$ is obtained from the vacuum by

$$a^{i\dagger}(p)\ |0\rangle = |\vec{p}^{\,i}\rangle \tag{A1.2}$$

with Lorentz invariant normalizatio ,

$$\langle \vec{p}_i \,|\, \vec{p}'i' \rangle = 2p^o \delta^3 (\vec{p} - \vec{p}')\, \delta_{ii'} \tag{A1.3}$$

Similarly ρ-field is written,

$$\rho^{i\mu}(x) = \frac{1}{(2\pi)^{3/2}} \sum_{\lambda=-1}^{1} \int \frac{d^3k}{2k^o} \left(\varepsilon^\mu_\lambda(k)\, a^i_\lambda(k)\, e^{-ikx} + \varepsilon^\mu_\lambda(k)\, a^{i\dagger}_\lambda(k)\, e^{ikx}\right) \tag{A1.4}$$

The corresponding one particle helicity states are,

$$|\vec{p}\ \lambda i\rangle = a^{i\dagger}_{\lambda}(\vec{p})\ |0\rangle \qquad (A1.5).$$

They have the normalization,

$$\langle \vec{p}\ \lambda i\ |\vec{p}'\ \lambda' i'\rangle = 2p^{o}\delta^{3}(\vec{p}-\vec{p}')\,\delta_{\lambda\lambda'}\,\delta_{ii'} \qquad (A1.6),$$

and transform under a Lorentz transformation Λ as,

$$|p,\lambda i\rangle \xrightarrow{\Lambda} \sum_{\lambda'} |\vec{\Lambda p},\ \lambda' i\rangle\ D^{l}_{\lambda'\lambda}(R(\Lambda,\vec{p})) \qquad (A1.7),$$

where

$$R(\Lambda,\vec{p}) = (H(\vec{\Lambda p}))^{-1}\ \Lambda\, H(\vec{p}) \qquad (A1.8)$$

is the Wigner rotation, D^{l} the rotation matrix corresponding to angular momentum l, and

$$H(p) = R(\phi,\theta,-\phi)\exp[-i K_{3}\zeta] \qquad (A1.9)$$

is the 'helicity boost' corresponding to momentum $\vec{p}$ with polar angles θ and ϕ. Our notation regarding the helicity states is the same as Jacob and Wick.[131]

Consider the ρ-π scattering $\rho(1) + \pi(2) \to \rho(3) + \pi(4)$ S-matrix element can be written in the form,

$$\langle p_3\ \lambda_3\ i_3,\ p_4 i_4 \mid S \mid p_1\ \lambda_1\ i_1,\ p_2\ i_2 \rangle$$

$$= 2p_1^0 \cdot 2p_2^0\ \delta^3(\vec{p}_1 - \vec{p}_3)\ \delta^3(\vec{p}_2 - \vec{p}_4)$$

$$\times \delta_{i_3 i_1}\ \delta_{i_2 i_4}\ \delta_{\lambda_3 \lambda_1} + i(2\pi)^4\ \delta^4(p_1+p_2-p_3-p_4)$$

$$\times\ T^{i_3 i_4, i_1 i_2}(s,t) \qquad (A1.10),$$

where s, t are Mandelstam variables,

$$s = (p_1+p_2)^2$$

$$t = (p_1-p_3)^2 \qquad (A1.11)$$

We shall now analyse the scattering in the centre of mass frame and construct the partial wave amplitudes.

First of all, the over-all center-of-mass motion can be separated from the two particle states;

$$|p_1 \lambda_1\ i_1,\ p_2 i_2\rangle = |P_\mu\rangle \otimes |p\theta\phi,\ \lambda_1 i_1 i_2\rangle \qquad (A1.12)$$

where $\theta\phi$ are the polar angles of $\vec{p}_1 = -\vec{p}_2$ and $p = |\vec{p}_1|$. The normalization of states $|p\,\theta\phi\ ,\ \lambda_1\ i_1 i_2\rangle$ is

$$\langle p'\theta'\phi'\ \lambda' i' j' \mid p\theta\phi\ \lambda i j\rangle = \frac{4\sqrt{s}}{p}\ \delta(\cos\theta'-\cos\theta)$$

$$\times\ \delta(\phi'-\phi)\ \delta_{\lambda'\lambda}\ \delta_{i'i}\ \delta_{j'j}$$

(A1.13)

Total angular momentum states can be constructed from $|p\theta\phi\lambda,\rangle$ as follows

$$|JM,\ \lambda ij\rangle = \left(\frac{2J+1}{4\pi}\right)^{\frac{1}{2}} \left(\frac{p}{4\sqrt{s}}\right)^{\frac{1}{2}} \int d\Omega\ \ D^{J*}_{M\lambda}\ (\phi\ \theta - \phi) \times |p\theta\phi\ \ \lambda ij\rangle \qquad (A1.14).$$

The inverse relationship is,

$$|p\theta\phi\lambda\ ,\ ij\rangle = \left(\frac{4\sqrt{s}}{p}\right)^{\frac{1}{2}} \sum_{JM} \left(\frac{2J+1}{4\pi}\right)^{\frac{1}{2}} D^{J}_{M\lambda}\ (\phi\,\theta-\phi)\,|JM\ \lambda\ ,ij\rangle \qquad (A1.15)$$

As defined, the normalization of $|JM\,\lambda\,,\ ij\rangle$ is

$$\langle JM\ \lambda ij\ |J'M'\lambda'i'j'\rangle = \delta_{JJ'}\ \delta_{MM'}\ \delta_{\lambda\lambda'}\delta_{ii'}\ \delta_{jj'} \qquad (A1.16)$$

and under parity and time reversal these states have simple transformation properties

$$P\ :\quad |JM,\ \lambda ij\rangle \rightarrow \eta_p\eta_\pi\ (-1)^{J-1}\ |J,\ -M,\ -\lambda ij\rangle \qquad (A1.17)$$

$$T\ :\quad |JM,\ \lambda ij\rangle \rightarrow (-1)^{J-M}\ |J,\ -M,\ \lambda ij\rangle \qquad (A1.18).$$

As S-matrix is invariant under rotations,

$$\langle P'|\otimes\langle J'M'\lambda'i'j'\ |S-1|\ JM\ \lambda ij\rangle\otimes|P\rangle = i(2\pi)^4\ \delta^4\ (P'-P)\ \delta_{JJ'}\ \delta_{MM'}\ T^{J\ i'j',ij}_{\lambda\ \lambda}(s) \qquad (A1.$$

Invariance under P and T requires,

$$P: \quad T^{Ji'j',ij}_{\lambda'\lambda} = T^{J\ i'j',ij}_{-\lambda',-\lambda} \tag{A1.20}$$

$$T: \quad T^{Ji'j',ij}_{\lambda'\lambda} = T^{J\ i'j',ij}_{\lambda\lambda'} \tag{A1.21}$$

The amplitudes $T^{Ji_3i_4,i_1i_2}_{\lambda_3\lambda_1}(s)$ are related to $T^{i_3i_4,i_1i_2}_{\lambda_3\lambda_1}(s,t)$ as follows,

$$T^{J\ i_3i_4,i_1i_2}_{\lambda_3\lambda_1}(s) = \frac{\pi p}{2\sqrt{s}} \int_{-1}^{1} d(\cos\theta)\ T^{i_3i_4,i_1i_2}_{\lambda_3\lambda_1}(s,t)\ d^J_{\lambda_1\lambda_3}(\theta) \tag{A1.22}$$

where, in the center-of-mass, t is given by

$$t = -2p^2(1-\cos\theta).$$

Inversely,

$$T^{i_3i_4,i_1i_2}_{\lambda_3\lambda_1}(s,t) = \frac{\sqrt{s}}{p\pi} \sum_J (2J+1)\ d^{J*}_{\lambda_1\lambda_3}(\theta)\ T^{J\ i_3i_4,i_1i_2}_{\lambda_3\lambda_1}(s) \tag{A1.23}$$

We are particularly interested in the amplitudes between states with total angular momentum 1 and even parity. From (A1.17) it follows that the required $J^P = 1^+$ states are

$$\frac{1}{\sqrt{2}}\,|1M,\ 1\ i_1i_2\rangle + \frac{1}{\sqrt{2}}\,|1M,\ -1\ i_1i_2\rangle \tag{A1.24}$$

and $\quad |1M,\ 0\ i_1 i_2\rangle \qquad (A1.25).$

Amplitudes between these states are the so-called 'parity conserving amplitudes'

$$T^{1^+}_{(1,1)} = T^1_{11} + T^1_{1-1}$$

$$T^{1^+}_{(1,0)} = \sqrt{2}\, T^1_{10} = T^{1^+}_{(0,1)}$$

$$T^{1^+}_{(0,0)} = T^1_{00} \qquad (A1.26)$$

where the superscript $i_3 i_4, i_1 i_2$ has been omitted. Also the index 1 within round brackets refers to the state (A1.24) with helicity ± 1 combination of even parity. We remark that because of parity and time reversal constraints (A1.20) and (A1.21), out of nine helicity amplitudes $T^J_{\lambda'\lambda}$ only the above three are independent.

The differential cross-section is given by

$$\frac{d\sigma}{d\Omega} = \frac{(2\pi)^{10}}{16s} |T_{\lambda_3\lambda_1}(s,t)|^2 \qquad (A1.27)$$

and using (A1.25),

$$\sigma_{tot} = \int d\Omega \frac{d\sigma}{d\Omega} = \frac{\pi}{p^2} \sum_J (2J+1) |(2\pi)^4 T^J_{\lambda_3\lambda_1}(s)|^2 \qquad (A1.28)$$

We shall require the expression for $T^{i_3 i_4, i_1 i_2}_{\lambda_3\lambda_1}(s,t)$ and

$T^{1^+}_{(\alpha_\rho)}{}^{i_3 i_4, i_1 i_2}$ as given by perturbation theory. To this end we first notice that $T^{i_3 i_4, i_1 i_2}_{\lambda_3 \lambda_1}(s,t)$ for $\rho\pi$ scattering can be written by Lorentz and parity invariance as,

$$T^{i_3 i_4, i_1 i_2}_{\lambda_3 \lambda_1}(s,t) = \frac{1}{(2\pi)^6}\, \varepsilon^{\nu *}_{\lambda_3}(p_3)\, \varepsilon^{\mu}_{\lambda_1}(p_1)$$

$$\times \left[A^{i_3 i_4, i_1 i_2}(s,t)\, g_{\nu\mu} + B^{i_3 i_4, i_1 i_2}(s,t)\, p_{2\nu} p_{2\mu} \right.$$

$$+ C^{i_3 i_4, i_1 i_2}(s,t)\, p_{1\nu} p_{2\mu} + D^{i_3 i_4, i_1 i_2}(s,t)\, p_{2\nu}\, p_{3\mu}$$

$$\left. + E^{i_3 i_4, i_1 i_2}(s,t)\, p_{1\nu}\, p_{3\mu} \right. \qquad \text{(A1.29)}.$$

Under time-reversal,

$$p \leftrightarrow -p', \quad k \leftrightarrow -k', \quad \varepsilon_\lambda \leftrightarrow -\varepsilon_\lambda$$

and therefore (A1.29) is invariant only if

$$C^{i_3 i_4, i_1 i_2}(s,t) = B^{i_3 i_4, i_1 i_2}(s,t) + D^{i_3 i_4, i_1 i_2}(s,t) \qquad \text{(A1.30)}$$

The explicit expressions of the polarization function are,

$$\varepsilon^{\mu}_{\pm 1}(p) = \left[0, \mp \frac{1}{\sqrt{2}} (1 - \cos\phi\, e^{\mp i\phi} (1-\cos\theta)), \right.$$

$$- \frac{i}{\sqrt{2}} (1 \pm i \sin\phi\, e^{\pm i\phi} (1-\cos\theta)),$$

$$\left. \pm \frac{1}{\sqrt{2}} \sin\theta\, e^{\pm i\phi} \right]$$

$$\varepsilon_o^\mu (p) = \frac{1}{M} [|\vec{p}|, p^o \sin\theta \cos\phi, p^o \sin\theta \sin\phi, p^o \cos\theta] \qquad (A1.31),$$

where $\theta\phi$ are the polar angles of $\vec{p} = (p^1, p^2, p^3)$ and $p^o = (\vec{p}^{\,2} + M^2)^{1/2}$

In the center-of-mass frame defined by,

$$p_1^\mu = (\Omega, 0, 0, p)$$

$$p_2^\mu = (\omega, 0, 0, -p)$$

$$p_3^\mu = (\Omega, p \sin\theta, 0, p \cos\theta)$$

$$p_4^\mu = (\omega, -p \sin\theta, 0, -p \cos\theta)$$

$$\Omega^2 = M^2 + p^2$$

$$\omega^2 = m^2 + p^2 \qquad (A1.32).$$

Substituting (A3.31) in (A1.33) gives,

$$T_{1-1}(s,t) = -\frac{1}{(2\pi)^6} [\tfrac{1}{2}A(1-\cos\theta) + \tfrac{1}{2}(D-E)p^2 \sin^2\theta] \qquad (A1.33)$$

$$T_{11}(s,t) = \frac{1}{(2\pi)^6} [-\tfrac{1}{2}A(1+\cos\theta) + \tfrac{1}{2}(D-E)p^2 \sin^2\theta] \qquad (A1.34$$

$$T_{10}(s,t) = \frac{1}{(2\pi)^6}\,\frac{\Omega}{M\sqrt{2}}\sin\theta\,\Big[-A + (B-C)\,\frac{p^2\sqrt{s}}{\Omega} + (D-E)\,p^2\,(1-\cos\theta)\Big] \qquad (A1.35)$$

$$T_{00}(s,t) = \frac{1}{(2\pi)^6}\,\frac{\Omega^2}{M^2}\Big[A\Big(\frac{p^2}{\Omega^2} - \cos\theta\Big) + \frac{p^2\sqrt{s}}{\Omega}\Big(\frac{B\omega + C\Omega}{\Omega} + (B-C)\cos\theta\Big) + p^2\,(1-\cos\theta)\Big(\frac{D\omega + E\Omega}{\Omega} + (D-E)\cos\theta\Big)\Big] \qquad (A1.36).$$

These expressions when substituted in (A1.22) give for $T^{1^+}_{(\alpha\beta)}(s)$ defined in (A1.26),

$$T^{1^+}_{(11)} = \frac{\pi p}{2\sqrt{s}}\,\frac{1}{(2\pi)^6}\int_{-1}^{+1} dx\,\Big[-\frac{A}{2}(1+x^2) + \frac{D-E}{2}\,p^2 x\,(1-x^2)\Big]$$

$$T^{1^+}_{(10)} = \frac{\pi p}{\sqrt{2s}\,M}\,\frac{1}{(2\pi)^6}\int_{-1}^{+1} dx\,\frac{1-x^2}{2}\Big[-A + (B-C)\,\frac{p^2\sqrt{s}}{\Omega} + (D-E)\,p^2\,(1-x)\Big]$$

$$T^{1^+}_{(0,0)} = \frac{\pi p}{2\sqrt{s}}\,\frac{\Omega^2}{M^2}\cdot\frac{1}{(2\pi)^6}\int_{-1}^{+1} dx.x\Big[A\Big(\frac{p^2}{\Omega^2} - x\Big) + \frac{p^2\sqrt{s}}{\Omega}\Big(\frac{B\omega + C\Omega}{\Omega} + x(B-C)\Big) + p^2(1-x)\,x\Big(\frac{D\omega + E\Omega}{\Omega} + x(D-E)\Big)\Big] \qquad (A1.3$$

where we have omitted isospin indices for convenience of writing, and used the standard $d^{J}_{mm'}$ matrices, which, for our case of J = 1, are given by,

$$d^{1}_{-1-1}(\theta) = d^{1}_{11}(\theta) = \frac{1}{2}(1+\cos\theta)$$

$$d^{1}_{-10}(\theta) = -d^{1}_{0-1}(\theta) = d^{1}_{01}(\theta) = -d^{1}_{10}(\theta) = \frac{1}{\sqrt{2}}\sin\theta$$

$$d^{1}_{-11}(\theta) = d^{1}_{1-1}(\theta) = \frac{1}{2}(1-\cos\theta)$$

$$d^{1}_{00}(\theta) = \cos\theta \qquad \text{(A1.38).}$$

Finally, the amplitudes $T^{i_3 i_4, i_1 i_2}_{\lambda_3 \lambda_1}(s,t)$, $T^{J\, i_3 i_4, i_1 i_2}_{\lambda_3 \lambda_1}(s)$ $A^{i_3 i_4, i_1 i_2}(s,t)$ etc. can be projected to definite total isospin amplitudes by using appropriate Clebsch-Gordon coefficients. As we are interested in projecting them to I = 1, we give the transformation matrix for this case below. Let

$$|II_3\rangle = \sum_{ij=1}^{3} S^{II_3}{}_{ij}\,|ij\rangle \qquad \text{(A1.39)}$$

Then $S^{II_3}{}_{ij}$ for I = 1 is given by,

$$S^{1\pm1}{}_{11} = S^{1\pm1}{}_{12} = S^{1\pm1}{}_{21} = S^{1\pm1}{}_{22} = S^{1\pm1}{}_{33} =$$

$$S^{1-1}{}_{31} = -i\,S^{1-1}{}_{23} = +i\,S^{1-1}{}_{32} = -S^{1-1}{}_{13}$$

$$= S^{11}{}_{13} = -i\,S^{11}{}_{23} = +i\,S^{11}{}_{32}$$

$$= -S^{11}{}_{31} = \frac{1}{2}$$

$$S^{10}{}_{ij} = 0 \quad \text{for} \quad ij = 11,\ 12,\ 13,\ 22,\ 23,\ 31,\ 32,\ 33$$

$$S^{10}{}_{21} = -S^{10}{}_{12} = i/\sqrt{2} \tag{A1.40}$$

The amplitude $T^{I}_{\lambda_3\lambda_1}(s,t)$ (and other quantities of the same type) are given by,

$$T^{I}_{\lambda_3\lambda_1}(s,t) = \sum_{i_3 i_4 i_1 i_2} S^{II_2 *}{}_{i_3 i_4}\, S^{II_3}{}_{i_1 i_2} \times T^{i_3 i_4, i_1 i_2}_{\lambda_3\lambda_1}(s,t) \tag{A1.41}$$

Note that as isospin is conserved, the above expression is independent of I_3. Specifically if,

$$T^{i_3 i_4, i_1 i_2} = \varepsilon^{i_1 i_3 k}\, \varepsilon^{i_2 i_4 k},\ \varepsilon^{i_1 i_4 k}\, \varepsilon^{i_3 i_2 k},\ \varepsilon^{i_1 i_2 k}\, \varepsilon^{i_3 i_4 k}$$
$$\delta^{i_1 i_3}\, \delta^{i_2 i_4}$$

with sum over k, then

$$T^{I} = 1,\ 1,\ 2,\ 1 \tag{A1.42}$$

respectively.

APPENDIX TWO

BARDAKCI MODEL AND CALCULATION OF DISCONTINUITIES

Bardakci Model[7] is in one sense the simplest model which incorporates the idea of spontaneously broken gauge symmetries in strong interactions. The essential idea in this model is to maintain a global SU(2) invariance although the vector meson masses are obtained by breaking the symmetry spontaneously. This is achieved through an ingenious device[6] of breaking the symmetry of an original group which is a direct product of a local SU(2) X SU(2) and a global SU(2) X SU(2). The vacuum expectation values of Higgs scalars are so chosen that although each of the SU(2) X SU(2) is broken, a global SU(2) X SU(2) remains intact. Vector and axial vector meson masses are obtained, and are equal. One can next break the chiral symmetry spontaneously to obtain different masses for vector and axial vector mesons, and pion is obtained as a Goldstone boson. To obtain pion mass one breaks the chiral symmetry explicitly in the Lagrangian.

In solving the N/D equations for $1^+(1)$ channel in $\rho\pi$ scattering, and to look for an A_1 resonance, we need some physical information to be fed in as input. This we take to be the discontinuity across the left hand cut of $J^P(I) = 1^+(1)$ partial wave amplitudes of lowest order $\rho\pi$ scattering. These amplitudes can be calculated from couplings of Bardakci Model which we now write.

We take a vector isotriplet V_μ, an axial vector isotriplet A_μ, psuedo-scalar triplets M_1 and N_2, scalar triplet N_1, scalar singlets M_2 and N_3, and psuedo-scalar singlet N_4.

Define

$$W_\mu \equiv (\vec{V}_\mu \cdot \vec{\tau} + \gamma_5 \vec{A}_\mu \cdot \vec{\tau})\, \pi_+ \qquad (A2.1)$$

$$M \equiv (\vec{M}_1 \cdot \vec{\tau}\, i\gamma_5\gamma_0 + M_2\gamma_0)\, \pi_+ \qquad (A2.2)$$

$$N \equiv (\vec{N}_1 \cdot \vec{\tau} + \vec{N}_2 \cdot \vec{\tau}\, \gamma_5)\, \sigma_1 + (N_3 + N_4 \gamma_5)\, \sigma_2 \qquad (A2.3)$$

where γ_0, γ_5 are usual Dirac matrices, σ, τ are usual Pauli matrices and $\pi_\pm = 1 \pm \sigma_3/2$. The local SU(2) X SU(2) transformations act according as,

$$W_\mu \to S_\pm^L\, W_\mu\, S_\pm^{L\,-1} + \frac{i}{g} S_\pm^L\, (\partial_\mu\, S_\pm^{L\,-1})$$

$$M \to S_\pm^L\, M\, S_\pm^{L\,-1}$$

$$N \to S_\pm^L\, N\, S_\pm^{L\,-1} \qquad (A2.4)$$

where,

$$S_{\pm}^{L}(s) = \exp\left(i\,\vec{\theta}_{\pm}(x).\vec{\tau}\,\pi_{+}\,\gamma_{\pm}\right) \qquad (A2.4).$$

The global SU(2) X SU(2) transformations act as follows,

$$\begin{aligned} W_{\mu} &\rightarrow W_{\mu} \\ M &\rightarrow M \\ N &\rightarrow S_{\pm}^{G}\, N\, S_{\pm}^{G^{-1}} \end{aligned} \qquad (A2.5)$$

where,

$$S_{\pm}^{G} = \exp\left(i\vec{\theta}_{\pm} \cdot \vec{\tau}\,\pi_{-}\,\gamma_{\pm}\right) \qquad (A2.6)$$

With this the invariant Lagrangian can be written as,

$$\begin{aligned} \mathcal{L} = & -\frac{1}{32}\,\mathrm{tr}\left[\left(\partial_{\mu}W - \partial_{\nu}W_{\mu} + \frac{g}{i}\left[W_{\mu}, W_{\nu}\right]\right)^{2}\right] \\ & + \frac{1}{16}\,\mathrm{tr}\left[\left(\partial_{\mu}M + \frac{g}{i}\left[W_{\mu}, M\right]\right)^{2}\right] \\ & + \frac{1}{32}\,\mathrm{tr}\left[\left(\partial_{\mu}N + \frac{g}{i}\left[W_{\mu}, N\right]\right)^{2}\right] \\ & + \frac{1}{8}\lambda_{1}\,\mathrm{tr}\left[M^{2}\right] + \frac{1}{16}\lambda_{2}\,\mathrm{tr}\left[N^{2}\right] \\ & - \frac{1}{8}\lambda_{3}\,\mathrm{tr}\left[M^{4}\right] - \frac{1}{64}\lambda_{4}\left(\mathrm{tr}\left[M^{2}\right]\right)^{2} \\ & - \frac{1}{16}\lambda_{5}\,\mathrm{tr}\left[N^{4}\right] - \frac{1}{256}\lambda_{6}\left(\mathrm{tr}\left[N^{2}\right]\right)^{2} \\ & - \frac{1}{128}\lambda_{7}\,\mathrm{tr}\left[N^{2}\right].\,\mathrm{tr}\left[M^{2}\right] \\ & - \frac{1}{8}\lambda_{8}\,\mathrm{tr}\left[N^{2}M^{2}\right] \end{aligned} \qquad (A2.7$$

We break the symmetry spontaneously by non-zero vacuum expectation value to M_2 and N_3. Let,

$$\langle 0|M_2|\ 0\rangle \ = \ \alpha\ , \quad \text{and}$$
$$\langle 0|N_3|\ 0\rangle \ = \ \beta. \tag{A2.8}$$

Shifting the fields to $M_2' = M_2-\alpha$ and $N_3' = N_3-\beta$, using the stability conditions,

$$\lambda_1 - (\lambda_3 + \lambda_4)\ 2\alpha^2 - (\lambda_7 + \lambda_8)\ \beta^2 = 0 \quad \text{and}$$
$$\lambda_2 - (\lambda_5 + \lambda_6)\ 2\beta^2 - (\lambda_7 + \lambda_8)\ \alpha^2 = 0\ , \tag{A2.9}$$

and choosing the gauge to be such that

$$\vec{N}_1 \ = \ 0$$
$$\beta\,\vec{N}_2 + 2\alpha\,\vec{M}_1 \ = \ 0 \tag{A2.10}$$

We obtain,

$$\mathcal{L} = -\tfrac{1}{4}(\partial_\mu \vec{V} - \partial_\nu \vec{V}_\mu)^2 - \tfrac{1}{4}(\partial_\mu \vec{A}_\nu - \partial_\nu \vec{A}_\mu)^2$$
$$+ \tfrac{1}{2} g^2\beta^2 \vec{V}_\mu^{\,2} + \tfrac{1}{2} g^2(\beta^2+4\alpha^2)\ \vec{A}_\mu^{\,2} + \tfrac{1}{2}(\partial_\mu \vec{\phi})^2$$
$$+ \tfrac{1}{2}(\partial_\mu M_2')^2 - 4\alpha^2(\lambda_3+\lambda_4)\ M_2'^{\,2} + \tfrac{1}{2}(\partial_\mu N_3')^2$$
$$- 4\beta^2(\lambda_5+\lambda_6)\ N_3'^{\,2} + \tfrac{1}{2}(\partial_\mu N_4)^2 - 4\beta^2\lambda_5 N_4^{\,2}$$

$$-2g\,(\partial_\mu \vec{V}_\nu).(\vec{V}^\mu \times \vec{V}_\nu) - 2g\,(\partial_\mu \vec{V}_\nu).(\vec{A}^\mu \times \vec{A}^\nu)$$

$$-2g\,(\partial_\mu \vec{A}_\nu).(\vec{V}^\mu \times \vec{A}^\nu) - 2g\,(\partial_\mu \vec{A}_\nu).(\vec{A}^\mu \times \vec{V}^\nu) \cdot$$

$$-g^2\,(\vec{V}_\mu)^4 - g^2(\vec{A}_\mu)^4 - 2g^2\,(\vec{V}_\mu)^2(\vec{A}_\mu)^2$$

$$+ g^2\,(\vec{V}_\mu \cdot \vec{V}_\nu)^2 + g^2(\vec{A}_\mu \cdot \vec{A}_\nu)^2 + 2g^2(\vec{V}_\mu \cdot \vec{A}_\nu)^2$$

$$- 4g^2\,(\vec{V}_\mu \cdot \vec{A}^\mu)^2 + 2g^2\,(\vec{V}_\mu \cdot \vec{V}_\nu)\,(\vec{A}^\mu \cdot \vec{A}^\nu)$$

$$+ 2g^2\,(\vec{V}_\mu \cdot \vec{V}_\nu)(\vec{A}^\mu \cdot \vec{A}^\nu)$$

$$+ 2g\,\frac{\beta^2 + 2\alpha^2}{\beta^2 + 4\alpha^2}\,(\partial^\mu \vec{\phi}).(\vec{V}_\mu \times \vec{\phi})$$

$$- \frac{4g^2\alpha\beta}{(\beta^2 + 4\alpha^2)^{1/2}}\,\vec{A}^\mu.(\vec{V}_\mu \times \vec{\phi}) + \frac{2g^2\,(\alpha^2+\beta^2)}{\beta^2+4\alpha^2}\,\vec{V}_\mu{}^2\,\vec{\phi}^2$$

$$+ \frac{2g^2\alpha^2}{\beta^2 + 4\alpha^2}\,\vec{A}_\mu{}^2\,\vec{\phi}^2 - \frac{2g^2\beta^2}{\beta^2 + 4\alpha^2}\,(\vec{V}_\mu \cdot \vec{\phi})^2$$

$$+ \frac{2g^2\beta^2}{\beta^2 + 4\alpha^2}\,(\vec{A}_\mu \cdot \vec{\phi})^2 + \frac{2g\alpha}{(\beta^2 + 4\alpha^2)^{1/2}} \times$$

$$\times\,(N_4\,\partial^\mu \vec{\phi} - \partial^\mu N_4\,\vec{\phi}).\,\vec{V}_\mu$$

$$+ \frac{2g\alpha}{(\beta^2 + 4\alpha^2)^{1/2}}\,(N_3'\,\partial^\mu \vec{\phi} - \partial^\mu N_3'\,\vec{\phi}).\vec{A}_\mu$$

$$+ \frac{2g\beta}{(\beta^2 + 4\alpha^2)^{1/2}}\,(\vec{\phi}\,\partial^\mu M_2' - M_2'\,\partial^\mu \vec{\phi}).\vec{A}_\mu$$

$$+ 4g^2\alpha\vec{A}_\mu{}^2 M_2' + 2g^2 A_\mu{}^2 M_2'^2 + \frac{4g^2\beta}{(\beta^2+4\alpha^2)^{1/2}} (\vec{V}_\mu \times \vec{A}^\mu)\cdot\vec{\phi} M_2'$$

$$+ g^2\beta (\vec{V}_\mu{}^2+\vec{A}_\mu{}^2) N_3' + 2g^2\beta(\vec{V}_\mu\cdot\vec{A}^\mu) N_4$$

$$+ \tfrac{1}{2} g^2 \vec{V}_\mu{}^2 N_3'^2 + \tfrac{1}{2} g^2 \vec{A}_\mu{}^2 N_3'^2 + \tfrac{1}{2} g^2 \vec{V}_\mu{}^2 N_4{}^2$$

$$+ \tfrac{1}{2} g^2 \vec{A}_\mu{}^2 N_4{}^2 + 2g^2 \vec{V}_\mu\cdot\vec{A}^\mu N_3' N_4$$

$$- \frac{1}{(\beta^2+4\alpha^2)^2} (\beta^4(\lambda_3+\lambda_4) + 16\alpha^4(\lambda_5+\lambda_6)$$

$$+ 4\beta^2\alpha^2(\lambda_7+\lambda_8))\vec{\phi}^4 - \frac{1}{(\beta^2+4\alpha^2)} (2\beta^2(\lambda_3+\lambda_4)$$

$$+ 4\alpha^2(\lambda_7+\lambda_8))\vec{\phi}^2 M_2' - \frac{1}{(\beta^2+4\alpha^2)} (4\beta^2\alpha(\lambda_3+\lambda_4)$$

$$+ 8\alpha^3(\lambda_7+\lambda_8))\vec{\phi}^2 M_2'^2 - \frac{1}{(\beta^2+4\alpha^2)} (8\alpha^2(\lambda_5+\lambda_6)$$

$$+ \beta^2(\lambda_7+\lambda_8))\vec{\phi}^2 N_3'^2 - \frac{1}{(\beta^2+4\alpha^2)} (16\alpha^2\beta(\lambda_5+\lambda_6)$$

$$+ 2\beta^3(\lambda_7+\lambda_8))\vec{\phi}^2 N_3' - \frac{1}{(\beta^2+4\alpha^2)} (8\alpha^2(\lambda_5+\lambda_6)$$

$$+ \beta^2(\lambda_7+\lambda_8))\vec{\phi}^2 N_4{}^2 - (\lambda_3+\lambda_4) M_2'^4 - 4\alpha(\lambda_3+\lambda_4) M_2$$

$$- (\lambda_5+\lambda_6) N_3'^4 - 4\beta(\lambda_5+\lambda_6) N_3'^3 - (\lambda_5+\lambda_6) N_4{}^4$$

$$- 2(3\lambda_5+\lambda_6) N_3'^2 N_4{}^2 - 4\beta(3\lambda_5+\lambda_6) N_3' N_4{}^2$$

$$- (\lambda_7+\lambda_8) M_2'^2 N_3'^2 - 2\beta(\lambda_7+\lambda_8) M_2'^2 N_3'$$

$$- (\lambda_7+\lambda_8) M_2'^2 N_4{}^2 - 2\alpha(\lambda_7+\lambda_8) M_2' N_3'^2$$

$$-4\alpha\beta\,(\lambda_7+\lambda_8)\,M_2'N_3' - 2\alpha\,(\lambda_7+\lambda_8)\,M_2'\,N_4^2$$
$$+ (\lambda_1\alpha^2 + \lambda_2\beta^2 - (\lambda_3+\lambda_4)\,\alpha^4 - (\lambda_5+\lambda_6)\,\beta^4$$
$$- (\lambda_7+\lambda_8)\,\alpha^2\beta^2). \qquad \text{(A2.11)}$$

where we have defined the pion field $\vec{\phi}$ as $(\beta + 4\alpha^2)^{1/2}\,\vec{M}_1/\beta$.

The above Lagrangian is global SU(2) X SU(2) invariant and the pion mass is still zero. In order to give mass to pion we have to break the chiral symmetry explicitly by introducing a term,

$$\frac{1}{8}\,\lambda_9\,\mathrm{tr}\,[MN\pi_-\,\gamma_0 N] \qquad \text{(A2.12)}.$$

With this term, the stability conditions become

$$2\alpha\,[\lambda_1 - (\lambda_3+\lambda_4)\,2\alpha_1^2 - (\lambda_7+\lambda_8)\,\beta^2] + \lambda_9\beta^2 = 0$$

and

$$\lambda_2 - (\lambda_5+\lambda_6)\,2\beta^2 - (\lambda_7+\lambda_8)\,\alpha^2 + \lambda_9\alpha = 0 \qquad \text{(A2.13)},$$

pion gets a mass term,

$$-\frac{1}{2}\,\frac{\lambda_9}{\alpha}\,(\beta^2+4\alpha^2) \qquad \text{(A2.14)}$$

mass-squares of M_2' and N_4 change respectively to,

$$8\alpha^2\,(\lambda_3+\lambda_4) + \frac{\lambda_9\beta^2}{\alpha} \qquad \text{(A2.15)}$$

and

$$8\lambda_5\,\beta^2 + 4\lambda_9\alpha \qquad \text{(A2.16}$$

and the following terms get added to the interaction Lagrangian,

$$-\frac{4\lambda_9\,\alpha^2}{\beta^2+4\alpha^2}\,M_2'\,\vec{\phi}^2-\frac{4\lambda_9\,\alpha\beta}{\beta^2+4\alpha^2}\,N_3'\,\vec{\phi}^2+\lambda_9\,M_2'N_3'^2$$

$$-\lambda_9 M_2' N_4^2+2\beta\lambda_9\,M_2'\,N_3' \qquad \text{(A2.17)}.$$

The parameters g, α^2, β^2 can be estimated from the masses of ρ, A_1 and $\rho \to 2\pi$ decay width to first order. We find,

$$\begin{aligned} g &= 4.69 \\ \alpha^2 &= 7.1 \times 10^3\ (\text{MeV})^2 \\ \beta^2 &= 2.66 \times 10^4\ (\text{MeV})^2 \end{aligned} \qquad \text{(A2.18)}$$

We shall now calculate the discontinuity across the left hand cut of $J^P = 1^+$ partial wave amplitudes of the diagrams shown in Figs. 3,4 and 6. Vertices are shown in Fig. 21.

For ρ exchange the invariant amplitudes $A^1(s,t)$ are,

$$\begin{aligned} A_\rho^1(s,t) &= -4g^2\,\frac{s-u}{t-M^2} \\ B_\rho^1(s,t) &= 0 \\ C_\rho^1(s,t) &= 16g^2\,\frac{1}{t-M^2} = D^1(s,t) \\ E_\rho^1(s,t) &= 0 \end{aligned} \qquad \text{(A2.19}$$

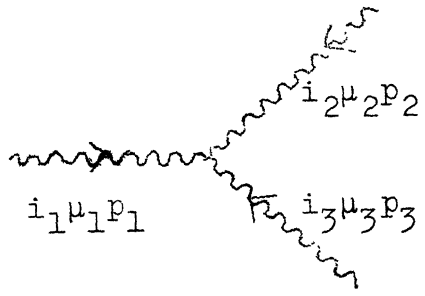

$$2g\varepsilon^{i_1 i_2 i_3}\,[(p_2-p_3)^{\mu_1} g^{\mu_2\mu_3} + \text{ + cyclic terms}]$$

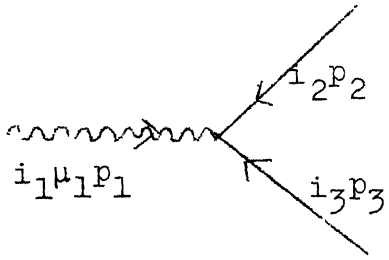

$$2g\varepsilon^{i_1 i_2 i_3}(p_2-p_3)^{\mu_1}$$

[to be multiplied by a factor $\frac{\beta^2+2\alpha^2}{\beta^2+4\alpha^2}$ in Bardakci Model]

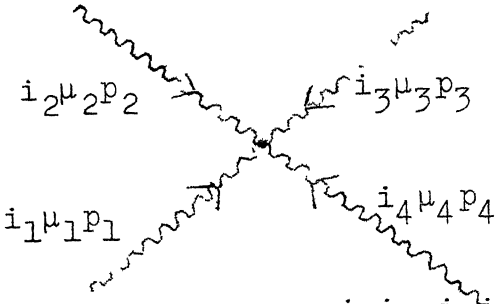

$$\begin{aligned}-4ig^2[\, & g^{\mu_1\mu_2} g^{\mu_3\mu_4}(2\delta^{i_1 i_2}\delta^{i_3 i_4} - \delta^{i_1 i_3}\delta^{i_2 i_4} - \delta^{i_1 i_4}\delta^{i_2 i_3}) \\ & + g^{\mu_1\mu_3} g^{\mu_2\mu_4}(2\delta^{i_1 i_3}\delta^{i_2 i_4} - \delta^{i_1 i_2}\delta^{i_3 i_4} \\ & - \delta^{i_1 i_4}\delta^{i_2 i_3}) + g^{\mu_1\mu_4} g^{\mu_2\mu_3}(2\delta^{i_1 i_4}\delta^{i_2 i_3} \\ & - \delta^{i_1 i_2}\delta^{i_3 i_4} - \delta^{i_1 i_3}\delta^{i_2 i_4})]\end{aligned}$$

Fig. 21: Principal couplings in gauge models.

For π exchange we have similarly,

$$A_\pi^1(s,t) = 0$$

$$B_\pi^1(s,t) = -16g^2\gamma^2 \frac{1}{u-m^2}$$

$$C_\pi^1(s,t) = 0$$

$$D_\pi^1(s,t) = -B_\pi^1(s,t)$$

$$E_\pi^1(s,t) = 0 \qquad \text{(A2.20)}$$

where,

$$\gamma = \frac{\beta^2 + 2\alpha^2}{\beta^2 + 4\alpha^2} \qquad \text{(A2.21)}$$

A_1 exchange in the u-channel gives,

$$A_A^1(s,t) = \frac{16g^4\alpha^2\beta^2}{\beta^2+4\alpha^2} \cdot \frac{1}{u-m_A^2}$$

$$B_A^1(s,t) = C_A^1(s,t) = D_A^1(s,t) = E_A^1(s,t) = 0 \qquad \text{(A2.22}$$

In order to calculate the position of the left hand cuts and discontinuities of partial wave amplitudes it suffices to observe that the t-channel exchange partial wave amplitude involves, from equation (A1.37) an integral of the form,

$$\int_{-1}^{+1} dx \; \frac{F(x)}{x - (1 + \frac{\mu^2}{2p^2})} \qquad \text{(A2.23}$$

where μ is the mass of the particle exchanged. As

$$p^2 = \frac{1}{4s}(s - (M+m)^2)(s-(M-m)^2),$$

points in the s-plane for which $1 + \frac{\mu^2}{2p^2}$ becomes equal to a real number between -1 and +1, correspond to singularities of the partial wave amplitude. For $\mu^2 < 4m^2$ the singularities are located on the real line and the circle $|s| = M^2-m^2$. For $\mu^2 > 4m^2$ but $< 4M^2$ the singularities form part of the circle and the real line $(-\infty, 0)$. For $\mu^2 > 4M^2$, the singularities lies entirely on the real negative s, truncated in two cuts, one stretching from zero to a value $> -(M^2-m^2)$ the other stretching from $-\infty$ to a value $< -(M^2-m^2)$. The singularities for ρ exchange in the t-channel are shown in Fig. 3 and for scalar exchange in Fig. 5.

Similarly the exchange of a particle of mass μ in the u-channel involves partial wave amplitudes of the form

$$\int_{-1}^{1} dx \left[F(x)/(x-(1+\frac{2M^2+2m^2-\mu^2-s}{2p^2}))\right] \qquad (A2.24)$$

The expression,

$$1 + \frac{2M^2 + 2m^2 - \mu^2 - s}{2p^2}$$

takes values between -1 to +1 for s xranging from $-\infty$ to 0 and from $2M^2 + 2m^2 - \mu^2$ to $(M^2 - m^2)^2/\mu^2$. Therefore the region of singularity for u-channel exchanges is the whole of

negative real axis, and the 'small cut' from $2M^2+2m^2-\mu^2$ to $(M^2-m^2)^2/\mu^2$. For small enough μ this part of the cut may lie well within the unitarity cut. In that case the s- and u- channel regions overlap. This actually happens for π exchange in the u-channel for our case. We show these singularities for u channel pion and A_1 exchange in Figs. 4 and 10 respectively.

The discontinuities across the unphysical cuts mentioned above can be found very simply from the expressions (A2.23) and (A2.24) by using the well known formula,

$$\frac{1}{x \pm i\varepsilon} = P\frac{1}{x} \mp i\pi\,\delta(x) \qquad \text{(A2.25)}.$$

As is clear from the above discussion, the discontinuity across the cut follows directly from (A1.37), and formula (A2.25). We give the expressions below.

Exchange in t-channel:

The cuts are shown in Fig. 3. We define,

$$y_\rho = 1 + \frac{M^2}{2p^2} \qquad \text{(A2.26)}$$

$$u' = 2M^2 + 2m^2 - s + 2p^2\,(1-y_\rho) \qquad \text{(A2.27)}$$

$$\Delta^\rho_{00}(s) = \frac{g^2\Omega^2m^2\,(\beta^2+2\alpha^2)}{4M^2s(\beta^2+4\alpha^2)}\; y_\rho\; \left[-\frac{s-u'}{p^2}\left(\frac{p^2}{\Omega^2}-y_\rho\right)\right.$$

$$\left. + 4\left(y_\rho + \frac{2\omega}{\Omega} + 1\right)(1-y_\rho)\right]$$

$$\Delta^{\rho}_{10}(s) = \frac{g^2\,\Omega m\,(\beta^2+2\alpha^2)}{4\sqrt{2}\,M\sqrt{s}\,(\beta^2+4\alpha^2)}\left[\frac{s-u'}{p^2} - \frac{4\omega}{\Omega} - 4y_\rho\right](1-y_\rho^2)$$

$$\Delta^{\rho}_{01}(s) = \Delta^{\rho}_{10}(s)$$

$$\Delta^{\rho}_{11}(s) = \frac{g^2(\beta^2+2\alpha^2)}{8(\beta^2+4\alpha^2)}\left[\frac{s-u'}{p^2}(1+y_\rho^2) + 4y\,(1-y_\rho^2)\right]$$

(A2.28)

On the real negative axis, we find,

$$\tilde{T}_{\alpha\beta}(s+i\varepsilon) - \tilde{T}_{\alpha\beta}(s-i\varepsilon) = \mp 2\pi i\ \Delta^{\rho}_{\alpha\beta}(s)$$

where - sign is to be taken for s lying in $(-\infty, -(M^2-m^2))$ and + for s in $(-(M^2-m^2), 0)$. On the circle $s = (M^2-m^2)e^{i\phi}$, and

$$\tilde{T}_{\alpha\beta}((M^2-m^2+\varepsilon)\,e^{i\phi}) - \tilde{T}_{\alpha\beta}((M^2-m^2-\varepsilon)\,e^{i\phi})$$

$$= \mp 2\pi i\ \Delta^{\rho}_{\alpha\beta}((M^2-m^2)\,e^{i\phi})$$

where - sign is taken for ϕ ranging from

$$\phi_o \equiv \cos^{-1}((m^2+M^2/2)/(M^2-m^2))$$

to π, and + for π to $2\pi-\phi_o$. These signs are conveniently summarized in the Fig. 3. where $\tilde{T}_{\alpha\beta}$ lying just a little on the + side of the cut minus $\tilde{T}_{\alpha\beta}$ just a little on the - side is $2\pi i\ \Delta^{\rho}_{\alpha\beta}$.

π exchange in u-channel:

As in the previous case we define,

$$y_\pi = 1 + \frac{2M^2+m^2-s}{2p^2} \qquad (A2.29)$$

$$\Delta^\pi_{00} = \frac{g^2 m^2 \Omega^2 \gamma^2}{s M^2} y_\pi \left(y_\pi + \frac{\omega}{\Omega}\right)^2$$

$$\Delta^\pi_{10} = \frac{g^2 m \Omega \gamma^2}{\sqrt{2s}\ M} (1-y_\pi^2) \left(y_\pi + \frac{\omega}{\Omega}\right)$$

$$\Delta^\pi_{01} = \Delta^\pi_{10}$$

$$\Delta^\pi_{11} = -g^2\gamma^2 y_\pi (1-y_\pi^2) \qquad (A2.30)$$

and the discontinuities in $\tilde{T}_{\alpha\beta}(s)$ are $\pm 2\pi i\, \Delta^\pi_{\alpha\beta}$ with the sign convention shown in Fig. 4.

A_1 exchange in u-channel:

In this case, define,

$$y_A = 1 + \frac{2M^2 + 2m^2 - m_A^2 - s}{2p^2} \qquad (A2.31)$$

$$\Delta^A_{00} = -\frac{g^4 \alpha^2 \beta^2 m^2 \Omega^2}{(\beta^2+4\alpha^2) M^2 s p^2} y_A \left(\frac{p^2}{2\Omega^2} - y_A\right)$$

$$\Delta^A_{01} = \frac{g^4 \alpha^2 \beta^2 m \Omega}{2\sqrt{2}\,(\beta^2+4\alpha^2)\, M \sqrt{s}\, p^2} (1-y_A^2)$$

$$\Delta_{10}^{L} = \Delta_{01}^{L}$$

$$\Delta_{11}^{A} = -\frac{g^4 \alpha^2 \beta^2}{2(\beta^2+4\alpha^2)p^2}(1+y_A^2). \qquad \text{(A2.32)}$$

The signs of discontinuities are shown in Fig. 10.

APPENDIX THREE

In this appendix we shall briefly outline the procedure for solving the N/D equations (4.22) and (4.23) numerically.

As explained in Chapter Four, we can write one integral equation for D, (see (4.24) and (4.25))

$$D(s) = 1 - \frac{s-s_o}{2\pi} \int_U ds'' \; R(s, s'') \Delta(s'') D(s'') \quad (A3.1)$$

$$R(s,s'') = \int_P ds' \; \frac{\rho(s')}{(s' - s_o)(s'-s)(s''-s)} \quad (A3.2).$$

One can regard the first equation as an integral equation for D(s) with s ranging over the unphysical values of s; i.e. values of s lying on the unphysical cuts U. Choosing n points S_j on U, we can write (A3.1) as a pair of matrix equations,

$$\sum_{\substack{\alpha'=0,1 \\ j'=0,..,n}} A_{\alpha j, \alpha' j'} \; D_{\alpha' o j'} = u^{o}{}_{\alpha j} \quad (A3.3),$$

and,

$$\sum_{\substack{\alpha'=0,1 \\ j'=0,..,n}} A_{\alpha j, \alpha' j'} \; D_{\alpha' 1 j'} = u^{1}{}_{\alpha j} \quad (A3.4),$$

where,

$$u^{o}{}_{\alpha j} = 1 \text{ for } \alpha = 0, \; 0 \text{ for } \alpha = 1 \text{ for all } j. \quad (A3.5)$$

$$u^{1}_{\alpha j} = 0 \text{ for } \alpha = 0, \; 1 \text{ for } \alpha = 1 \text{ for all } j. \qquad (A3.6)$$

$$D_{\alpha\beta j} = D_{\alpha\beta}(s_j), \quad \alpha, \beta = 0, 1 \qquad (A3.7)$$

$$A_{\alpha j, \alpha' j'} = \delta_{\alpha\alpha'} \delta_{jj'} + \frac{s_j - s_o}{2\pi} w_{j'} \sum_{\beta=0,1} R_{\alpha\beta}(s_j, s_{j'}) \times \Delta_{\beta\alpha'}(s_{j'}) \qquad (A3.8)$$

and $w_{j'}$ is the weight factor at the point $s_{j'}$ when the integral,

$$\sum_{\beta, \beta'} \int_U ds'' \; R_{\alpha\beta}(s, s'') \; \Delta_{\beta\beta'}(s'') \; D_{\beta'\alpha'}(s'') \qquad (A3.9)$$

is changed to a sum,

$$\sum_{\beta\beta'} \sum_{j'=1}^{n} w_{j'} \; R_{\alpha\beta}(s, s_{j'}) \; \Delta_{\beta\beta'}(s_{j'}) \; D_{\beta'\alpha'}(s_{j'}) \qquad (A3.10)$$

We calculate $R_{\alpha\beta}(s_j, s_{j'})$ and (A3.9) with the help of Gaussian quadrature formulas. A is then calculated using Δ from (4.28-40). Equations (A3.3) and (A3.4) are then solved for D by inverting A. After D is found for points s_j, the calculation of D and N on right hand side proceeds as follows. N is calculated for s in the physical region by (4.23),

$$N(s) = \int_U ds'' \; \frac{\Delta(s'') \; D(s'')}{(s'' - s)} \qquad (A3.11)$$

again, using the Gaussian quadrature. The knowledge of N on right hand side gives,

$$\mathrm{Re}\ D(s) = 1 - \frac{s-s_0}{2\pi} P \int_{(M+m)^2}^{\infty} ds' \frac{\rho(s')\, N(s')}{(s'-s_0)(s'-s)} \qquad (A3.12)$$

$$\mathrm{Im}\ D(s) = -\frac{1}{2}\, \rho(s)\, N(s) \qquad (A3.13).$$

The principal value integral is evaluated using,

$$P \int_{(M+m)^2}^{\infty} ds' \frac{\rho(s')\, N(s')}{(s'-s_0)(s'-s)}$$

$$= \int_{M^2}^{\Lambda} ds' \left(\frac{\rho(s')N(s')}{s'-s_0} - \frac{\rho(s)\, N(s)}{s-s_0} \right) \frac{1}{s'-s}$$

$$+ \frac{\rho(s)\, N(s)}{s-s_0} \ln \left(\frac{\Lambda - s}{s-M_+^2} \right)$$

$$+ \int_{\Lambda}^{\infty} ds' \frac{\rho(s')\, N(s')}{(s'-s_0)(s'-s)} \qquad (A3.14)$$

for $s < \Lambda$, where Λ is a big number. We neglect the last integral on the right hand side, and evaluate the first by simply evaluating the area under the polygon formed by joining values of the integrand at discrete points by straight lines. The values s are chosen always to be different from s'. By choosing the points closer and closer and Λ big enough, one can obtain a good approximation to the principal part (A3.14).

This gives us $\tilde{T}(s)$ for the physical values of s.

APPENDIX FOUR

In this Appendix certain kinematical details pertaining to high energy behaviour are discussed.

A4.1 SCATTERING $\underline{1} + \underline{2} \to \underline{3} + \underline{4}$:

We consider the scattering $\underline{1} + \underline{2} \to \underline{3} + \underline{4}$.

We shall assume that the variable $s = (p_1+p_2)^2 = (p_3+p_4)^2$ tends to infinity while $t = (p_1-p_3)^2$ is kept fixed and finite.

We can always choose p_1 to be in the +z direction, and p_2 in -z direction in the center of mass frame. Then

$$p_1^{\mu} = (\sqrt{(p^2+m_1^2)},\ 0,\ 0,\ p) \qquad (A4.1)$$

$$p_2^{\mu} = (\sqrt{(p^2+m_2^2)},\ 0,\ 0,\ -p) \qquad (A4.2)$$

For any four-vector p^{μ} we define,

$$p^{\pm} = p^0 \pm p^3 \qquad (A4.3)$$

$$\vec{p}_{\perp} = (p^1,\ p^2) \qquad (A4.4),$$

so that

$$p.k \equiv p^{\mu} k_{\mu} = \tfrac{1}{2}(p^+k^- + p^-k^+) - \vec{p}_{\perp}.\vec{k}_{\perp} \qquad (A4.5).$$

With this definition, we get, using the condition that t is finite,

$$p_1^+ = \sqrt{s} + O(\frac{1}{\sqrt{s}}),\ p_1^- = O(\frac{1}{\sqrt{s}}),\ \vec{p}_{1\perp} = 0 \qquad (A4.6)$$

$$p_2^+ = O(\frac{1}{\sqrt{s}}),\ p_2^- = \sqrt{s} + O(\frac{1}{\sqrt{s}}),\ \vec{p}_{2\perp} = 0 \qquad (A4.7)$$

$$p_3^+ = \sqrt{s} + O(\frac{1}{\sqrt{s}}),\ p_3^- = O(\frac{1}{\sqrt{s}}) \qquad (A4.8)$$

$$p_4^+ = O(\frac{1}{\sqrt{s}}) \quad p_4^- = \sqrt{s} + O(\frac{1}{\sqrt{s}}) \qquad (A4.9)$$

$$\vec{p}_{3\perp} = -\vec{p}_{4\perp}. \qquad (A4.10).$$

The coefficients of the above asymptotic formulas are not required. Suffice is to say that any linear combination p of external momenta p_1 to p_4 will have,

$$p^{\pm} = \lambda^{\pm}\sqrt{s} + \mu^{\pm}(p_1, \ldots, p_4)\frac{1}{\sqrt{s}} \qquad (A4.11),$$

where $\lambda^{\pm}$ are constants, and $\mu^{\pm}$ are functions of $p_1, \ldots, p_4$ which tend to constants as $s \to \infty$.

A4.2 ONE PARTICLE PRODUCTION:

Consider $\underline{1} + \underline{2} \to \underline{3} + \underline{4} + \underline{5}$ with mass of $\underline{1}$, $\underline{2}$, $\underline{3}$, $\underline{4}$ to be m and that of $\underline{5}$ to be M. To describe such a process, five invariants are sufficient. They are

$$s_{34} = (p_3 + p_4)^2$$

$$s_{35} = (p_3 + p_5)^2$$

$$s_{45} = (p_4 + p_5)^2$$

$$t_{13} = (p_1 - p_3)^2$$

$$t_{24} = (p_2 - p_4)^2 \qquad (A4.12).$$

The square of center of mass energy, s, is given by,

$$s = s_{34} + s_{35} + s_{45} - 2m^2 - M^2 \qquad (A4.13).$$

Inversely,

$$2p_1 \cdot p_2 = s - 2m^2$$

$$2p_1 \cdot p_3 = 2m^2 - t_{13}$$

$$2p_1 \cdot p_4 = s - s_{35} + t_{24} - m^2$$

$$2p_1 \cdot p_5 = s_{35} - t_{24} + t_{13} - m^2$$

$$2p_2 \cdot p_3 = s - s_{45} + t_{13} - m^2$$

$$2p_2 \cdot p_4 = 2m^2 - t_{24}$$

$$2p_2 \cdot p_5 = s_{45} + t_{24} - t_{13} - m^2$$

$$2p_3 \cdot p_4 = s_{34} - 2m^2$$

$$2p_3 \cdot p_5 = s_{35} - M^2 - m^2$$

$$2p_4 \cdot p_5 = s^{45} - M^2 - m^2 \qquad (A4.14$$

We are interested in the case when $s \to \infty$, but t_{13} and t_{24} are kept fixed.

As $s \to \infty$ we get five different kinematic regions according as,

(i) $s_{35} = o(s)$, $s_{34}, s_{45} = O(s)$

(ii) $s_{45} = o(s)$, $s_{34}, s_{35} = O(s)$

(iii) $s_{34}, s_{35} = o(s)$, $s_{45} = O(s)$

(iv) $s_{35}, s_{45} = o(s)$, $s_{34} = O(s)$

(v) $s_{34}, s_{45} = o(s)$, $s_{35} = O(s)$ (A4.15),

where $x = o(s)$ means that $x/s \to 0$ as $s \to \infty$.

Note that we cannot have both s_{35} and s_{45} of $O(s)$ as t_{13} and t_{25} are fixed, and the sum of 3-momenta of particles 3, 4, 5 have to be finite in any frame, in particular, equal to zero in the center of mass frame.

We shall use only the first two kinematical regions which are characterized by the fact that all the particles have their energies of the order of $\sqrt{s}$, i.e., they move with high velocities. The analysis of high-energy behaviour is specially simple in these cases.

In case (i) listed above in (A4.15) we have in the center of mass frame the following asymptotic values for momenta,

$$p_1^+ = \sqrt{s} + O(\tfrac{1}{\sqrt{s}}),\ p_1^- = O(\tfrac{1}{\sqrt{s}}),\ \vec{p}_{1\perp} = 0,$$

$$p_2^+ = O(\tfrac{1}{\sqrt{s}}),\ p_2^- = \sqrt{s} + O(\tfrac{1}{\sqrt{s}}),\ \vec{p}_{2\perp} = 0$$

$$p_3^+ = \lambda\sqrt{s} + O(\tfrac{1}{\sqrt{s}}),\ p_3^- = O(\tfrac{1}{\sqrt{s}}),\ \vec{p}_{3\perp} = O(1)$$

$$p_4^+ = O(\tfrac{1}{\sqrt{s}}),\ p_4^- = \sqrt{s} + O(\tfrac{1}{\sqrt{s}}),\ \vec{p}_{4\perp} = O(1)$$

$$p_5^+ = (1-\lambda)\sqrt{s} + O(\tfrac{1}{\sqrt{s}}),\ p_5^- = O(\tfrac{1}{\sqrt{s}}),\ \vec{p}_{5\perp} = O(1)$$

$$\vec{p}_{3\perp} + \vec{p}_{4\perp} + \vec{p}_{5\perp} = 0 \qquad \text{(A4.16)}$$

In case (ii)

$$p_3^+ = \sqrt{s} + O(\tfrac{1}{\sqrt{s}}),\ p_3^- = O(\tfrac{1}{\sqrt{s}}),\ \vec{p}_{3\perp} = O(1)$$

$$p_4^+ = O(\tfrac{1}{\sqrt{s}}),\ p_4^- = x\sqrt{s} + O(\tfrac{1}{\sqrt{s}}),\ \vec{p}_{4\perp} = O(1)$$

$$p_5^+ = O(\tfrac{1}{\sqrt{s}}),\ p_5^- = (1-x)\sqrt{s} + O(\tfrac{1}{\sqrt{s}}),\ \vec{p}_{5\perp} = O(1) \qquad \text{(A4.17)}$$

We shall call these two regions λ and x regions.

Note that $0 < (\lambda\ ,\ x) < 1$.

APPENDIX FIVE

USE OF MELLIN TRANSFORMS IN EVALUATING THE ASYMPTOTIC BEHAVIOUR OF FUNCTIONS

For the sake of completeness and reference we shall quote a result [132], especially useful in extracting the high-energy behaviour of integrals encountered in Chapter Six.

Definition: Mellin transform of a function $f(s)$ is defined to be the function

$$\Phi(z) = \int_0^\infty s^{z-1} f(s)\, ds \qquad (A5.1)$$

of a complex variable z, when this integral exists.

The result whose use we shall make often is the following.

Let $\Phi(z)$ be analytic in a right half plane $\mathrm{Re}\ z \geq a > 0$ except for singular points of one-valued character (i.e. poles or essential singularities) $\lambda_0, \lambda_1, \ldots$ with $a < \mathrm{Re}\ \lambda_0 < \mathrm{Re}\ \lambda_1, \ldots$. Let the principal part of the Laurent expansion of $\Phi(z)$ at $z = \lambda_\nu$ be

$$b_1^{(\nu)} (z - \lambda_\nu)^{-1} + b_2^{(\nu)} (z - \lambda_\nu)^{-2} + \ldots + b_{r_\nu}^{(\nu)} (z-\lambda_\nu)$$

(A5.2)

then provided

(i) In every finite width $a \leq \mathrm{Re}\ z \leq a_0$ $\Phi(\sigma + i\tau) \to 0$ as $|\tau| \to \infty$ uniformly in σ and

(ii) between two singularities λ_ν and $\lambda_{\nu+1}$ there exists a real number β_ν with

$$\mathrm{Re}\ \lambda_\nu < \beta_\nu < \mathrm{Re}\ \lambda_{\nu+1}$$

such that the integral

$$\int_{-\infty}^{\infty} s^{-i\tau}\ \Phi(\beta_\nu + i\tau)\, d\tau$$

converges uniformly for $s \geq S_\nu$ for some $S_\nu > 0$,

the inverse Mellin transform exists and has the asymptotic expansion,

$$f(s) = -\sum_{\nu=0}^{n} \Big[b_1^{(\nu)} - \frac{b_2^{(\nu)}}{1} \ln s + \cdots + (-1)^{r_\nu - 1} \frac{b_{r_\nu}^{(\nu)}}{(r_\nu - 1)} (\ln s)^{r_\nu - 1} \Big] s^{-\lambda_\nu} + (2\pi i)^{-1} \int_{\beta_n - i\infty}^{\beta_n + i\infty} s^{-z}\ \Phi(z)\, dz \qquad \text{(A5.)}$$

as $s \to \infty$, and the last term is of order $o(s^{-\beta_n})$.

REFERENCES

Following abbreviations for names of journals are used:

PR, PRL, PL, NC, NP, JMP

for Physical Review, Physical Review Letters, Physics Letter, Nuovo Cimento, Nuclear Physics and Journal of Mathematical Physics respectively.

1. For an excellent review see E.S. Abers and B.W.Lee, Physics Reports, 9C, 1 (1973).

2. See ref. 6 and 7. and
J. Pati and A. Salam, PR D8, 1240 (1973),
J.Pati and A. Salam, PRL 31, 851 (1973).
B. deWit, NP B51, 237 (1973),
I.Bars, M.B.Halpern and M. Yoshimura, PRL, 969 (1972),
I.Bars, M.B. Halpern, M. Yoshimura, L7 1233 (1973),
B. deWit, PR D9, 3399 (1974).

3. S. Weinberg, PRL 18, 507 (1967).

4. G.F. Chew and S. Mandelstam, PR 119, 476 (1960),
G.F. Chew and S.Mandelstam, NC 19, 753 (1961).
P.D.B. Collins and V.L. Teplitz, PR 140, B 663 (1965).

5. S.C. Frautchi and J.D. Walecka, PR 120, 1486 (1960),
E. Abers, C. Zemach, PR 131, 2305 (1963),
J. Hamilton; High Energy Physics, Vol. I, ed. E.H. Burhop (Interscience, London 1967).

6. K. Bardakci and M.B. Halpern, PR D6, 696 (1972).

7. K. Bardakci, NP B51, 174 (1972).

8. This method is discussed in section 5.2.

9. J. Goldstone, NC 19, 154 (1961).

10. J. Goldstone, A. Salam, S. Weinberg, PR 127, 965 (1962).

11. P.W. Higgs, PL 12, 132 (1964).

12. P.W. Higgs, PRL 13, 508 (1964).

13. P.W. Higgs, PR 145, 1156 (1966).

14. G. Goldhaber et al, PRL, 12, 336 (1964).

15. G. Bellini et al, NC 29, 896 (1963).

16. F.R. Huson and W.B. Fretter, Bull. Am.Phys. Soc. 8, 325 (1963).

17. M. Aderholz et al, PL 10, 226 (1964).

18. S.U.Chung et al. PRL 12, 621 (1964).

19. M.J. Emms et al, NP B93, 1(1976) and references therein.

20. M. Deutschmann et al, PL 20, 82 (1966).

21. G. Ascoli et al, PRL 21, 113 (1968).

22. J. Ballam et al, PRL 21, 934 (1968).

23. C. Caso et al, NC 51A, 983 (1968).

24. K. Boesebeck et al, NP B4, 501 (1968).

25. S.U. Chung et al, PR 165, 1491 (1968).

26. B. Junkmann et al, NP 138, 471 (1968).

27. A.W. Key et al, PR 166, 1430 (1968).

28. G. Ascoli,et al, PR D7, 669 (1973).

28. G. Ascoli, in Proceedings of the XVI International Conference on High Energy Physics, Chicago-Batavia, Ill., 1972, Edited by J.D. Jackson and A. Roberts (NAL, Batavia, Ill. 1973), Vol. 1, p. 3.

29. G.L. Kane, University of Michigan preprint UM HE-75-3 (1975).

30. E.W. Anderson et al. PRL 22, 1390 (1969).

31. M.J. Emms et al, PL 60B, 109 (1975).

32. J.A. Danyasz et al, NC 51A, 801 (1967).

33. A. Fridman et al, PR 167, 1268 (1968).

34. G. Alexander et al, PR 183, 1168 (1969).

35. R.E. Juhala et al, PRL 19, 1355 (1967).

36. J.C. Berlinghieri et al, PRL 23, 42 (1969).

37. W.W.M. Allison et al, PL 25B, 619 (1967).

38. See footnote 5 in reference 36.

39. F. Wagner, M. Tabak, D.M. Chew, PL 58B, 201 (1975).

40. M. Nauenberg and A. Pais, PRL 8, 82 (1962).

41. R.F. Pierls, PRL 6, 641 (1961).

42. R.T. Deck, PRL 13, 169 (1964).

43. U. Maor and T.A. O'Halloran Jr., PL 15, 281 (1965).

44. U. Maor, Ann. Phys. (N.Y.) 41, 456 (1967).

45. L. Stodolsky, PRL 18, 973 (1967).

46. M. Ross and Y. Yam, PRL 19, 545 (1967).

47. E.L. Berger, PR 166, 1525 (1968).

48. H. M.Chan, K. Kajantie and G. Ranft, NC 49A, 157 (1967).

49. G. Ascoli, PR D9, 1963 (1974),
G. Ascoli et.al., PR D8, 3894 (1973).

50. G.F. Chew and A. Pignotti, PRL 20, 1078 (1968).

51. D.D. Brayshaw, PRL 36, 73 (1976).

52. D.D. Brayshaw, PR D11, 2583 (1975).

53. M.G. Bowler, M.A.V. Game, I.J.R. Aitchison, J.B.Dainton, NP B97, 227 (1975).

54. See for example A.D. Martin and T.D. Spearman, Elementary Particle Theory, (North-Holland, 1970), p. 363.

55. Ref. 54. p. 383.

56. E.Abers and V.L. Teplitz, PR 158, 1365 (1967), Specially section IIIc.

57. J.D. Bjorken and M.Nauemberg, PR 121, 1250 (1961).

58. L. Castillejo, R.H. Dalitz, F.J. Dyson, PR 101, 453 (1956).

59. S. Mandelstam, Ann. Phys. (N.Y.) 21, 302 (1963) P.D.B. Collins and E.J. Squires, Regge Poles in Particle Physics, Springer Tracts in Modern Physics, Vol. 45 (Springer-Verlag, 1968) p. 145.

60. J.S. Ball, W.R. Frazer and M. Nauemberg, PR 128, 478 (1962).

61. M. Yamazaki, N. Masuda, J. Otokozawa, Progr. Theo.Phys. 31, 679 (1964).

62. G.F. Chew and S.C. Frautchi, PRL 7, 394 (1961).

63. G.F. Chew and S.C. Frautchi, PRL 8, 4 (1962).

64. G.F. Chew and S.C. Frautchi, PR 123, 1478 (1961).

65. S.C. Frautchi, M. Gell-Mann, F. Zachariasen, PR 126, 2204 (1962).

66. T. Regge, NC 14, 951 (1959).

67. T. Regge, NC 18, 947 (1960).

68. M. Gell-Mann and M.L. Goldberger, PRL 9, 275 (1962).

69. R. Blankenbecler, L.F. Cook, M.L. Goldberger, PRL 8, 463 (1962).

70. M. Gell-Mann, M.L. Goldberger, F.E.Low and F.Zachariasen, PL 4, 265 (1963).

71. M.Levy, PRL 9, 235 (1962).

72. F. Zachariasen, PL 4, 265 (1963).

73. M.Gell-Mann, M.L. Goldberger, F.E.Low, E.Marx and F.Zachariasen, PR 133B, 145 (1964).

74. M.Gell-Mann, M.L. Goldberger, F.L.Low, V.Singh and F.Zachariasen, PR 133B, 161 (1964).

75. S. Mandelstam, PR 137, B 949 (1965).

76. E. Abers and V.L. Teplitz, PR 158; 1365 (1967).

77. H. Cheng and T.T. Wu, PR 140 B465 (1965).

78. B.W. Lee and R.F. Sawyer, PR 127, 2266 (1962).

79. P.G. Federbush and M.T. Grisaru, Ann. Phys. (N.Y.), 22, 263 (1963).

80. G. Tiktopoulos, PR 131, 480 (1962).
G. Tiktopoulos, PR 131, 2373 (1963).

81. J.C. Polkinghorne, JMP 4, 503 (1963).

82. J.C. Polkinghorne, JMP 4, 1393 (1963).

83. I.G. Halliday, NC 30, 177 (1963).

84. J.D. Bjorken and T.T. Wu, PR 130, 2566 (1963).

85. T.L. Trueman and T. Yao, PR 132, 2741 (1963).

86. J.C. Polkinghorne, JMP 5, 431 (1964) for a detailed discussion.

87. N. Byers and C.N. Yang, PR 142, 976 (1966).

88. T.T. Chou and C.N. Yang, PR 170, 1591 (1968).

89. T.T. Chou and C.N. Yang, PRL 20, 1213 (1968).

90. R.J. Glauber, in Lectures in Theoretical Physics, W.E. Brittin and L.G. Dunham (eds.), Interscience, New York, 1959, Vol. 1.

91. H. Cheng and T.T. Wu, PRL 22, 666 (1969).

92. H. Cheng and T.T. Wu, PR 182, 1852 (1969).

93. H. Cheng and T.T. Wu, PR 182, 1868 (1969).

94. H. Cheng and T.T. Wu, PR 182, 1873 (1969).

95. H. Cheng and T.T. Wu, PR 182, 1899 (1969).

96. S.-J.Chang and S.Ma, PRL 22, 1334 (1969).

97. S.-J.Chang and S.Ma, PR 188, 2375 (1969).

98. H.Cheng and T.T.Wu, PR 186, 1611 (1969).

99. H.D.I.Abarbanel and C.Itzykson, PRL 23, 53 (1969).

100. F.Englert et.al., NC 64A, 561 (1969).

101. M.Levy and J. Sucher, PR 186, 1656 (1969).

102. R.Torgerson, PR 143, 1194 (1966).

103. G.Tiktopoulos and S.B.Trieman, PR D2, 805 (1970).

104. S.-J.Chang and P.M. Fishbane, PR D2, 1104 (1970).

105. H.Cheng and T.T.Wu, PR D1, 1069 (1970).

106. H.Cheng and T.T.Wu, PR D1, 2775 (1970).

107. H.T.Nieh and Y.P.Yao, PRL 32, 1074 (1974).

108. B.M.McCoy and T.T.Wu, PRL 35, 1074 (1974).

109. B.M. McCoy and T.T. Wu, PR D12, 3257 (1975).

110. L.Tyburski, PR D13, 1107 (1976).

111. C.Y.Lo and H.Cheng, PR D13, 1131 (1976).

112. P.S. Yeung, PR D13, 2306 (1976).

113. M.T. Grisaru, H.J. Schmitzer, H.S. Tsao, PR D8, 4498 (1973).

114. R.Chisholm, Proc. Comb. Phil. Soc. 48, 300 (1952).

115. R.J. Eden, PR 119, 1763 (1960).

116. J.V.Greenman, JMP 7, 1782 (1966).

117. J.V.Greenman, JMP 8, 26 (1967).

118. C.S.Lam and J.P. Lebrun, NC 59A, 397 (1969).

119. C.S.Lam, N.C. 62A, 97 (1969).

120. C.S. Lam, N.C. 59A, 422 (1969).

121. However the revised calculation by Nich and Yao, PR D13, 1082 (1976) done by Feynman parameter method does not agree with McCoy and Wu[109] who calculated using the momentum space technique or with Tyburski[110] who uses a mixture of both. McCoy and Wu and Tyburski agree, however. We donot know the reason for this discrepancy.

122. B.M.McCoy and T.T.Wu, PR D13, 369-512 (1976).

123. S.Weinberg, PR 118, 838 (1960).

124. Fink, JMP 9, 1389 (1968).

125. M.C.Bergere and Y.-M.P.Lam, Comm. Math. Phys. 39, 1 (1974).

126. K.Pohlmeyer, in International Symposium on Mathematical Problems in Theoretical Physics, Lecture Notes in Physics No. 39 (Springer-Verlag 1975), p. 59.

127. J.M. Cornwall, D.NiLevin, G.Tiktopoulos PR D10, 1145 (1975), G. Tiktopeulos, PR D11, 2252 (1975).

128. I.G.Halliday and J.C.Polkinghorne, PR 132, 852 (1963).

129. H.Cheng and T.T.Wu, PR D1, 456 (1970).

130. See for example Gradshteyn,I.S. and I.M. Ryzhik, Table of Integrals, Series and Products. (Academic Press, 1965) Section (8.353) formula 5.

131. M. Jacob and G.C. Wick, Ann. Phys. (N.Y.) 7, 404 (1959).

132. F. Oberhettinger, Table of Mellin Transforms (Springer-Verlag 1974), see Introduction.